

**Impact of glycation and
advanced glycation end products (AGEs)
on macrophage activation**

Dissertation

zur Erlangung des
Doktorgrades der Naturwissenschaften
(Dr. rer. nat.)

der

Naturwissenschaftlichen Fakultät I
– Biowissenschaften –
der Martin-Luther-Universität Halle-Wittenberg

vorgelegt

von Frau Veronika Bezold
geb. am 04.06.1991 in Amberg

Gutacher:

PD Dr. Ralph Golbik

Prof. Dr. Rüdiger Horstkorte

Prof. Dr. Otmar Huber

(Friedrich-Schiller-Universität Jena)

Datum der Verteidigung:

17.02.2020

Contents

Abstract	IV
Inhaltsangabe	V
Abbreviations	VI
Table of figures	VIII
1 Introduction.....	1
1.1 Glycation and advanced glycation end products (AGEs)	1
1.1.1 Receptors for AGEs.....	2
1.1.1.1 Structure and function of RAGE	3
1.1.1.2 AGE-mediated RAGE signalling	4
1.1.2 MGO induced glycation	6
1.1.2.1 The physiological role of MGO induced glycation.....	7
1.1.2.2 MGO detoxification by the glyoxalase system	7
1.1.3 Degradation of AGEs.....	9
1.1.4 Disease relevance of glycation and AGEs.....	10
1.2 Macrophages	12
1.2.1 Macrophage polarization	12
1.2.1.1 Classically activated M1 macrophages.....	14
1.2.1.2 Alternatively activated M2 macrophages	16
1.2.2 Macrophages in wound healing.....	17
1.2.2.1 Macrophage involvement in regeneration and tissue repair	17
1.2.2.2 Macrophage dysfunction in diabetic wounds	18
1.3 Aim of work	19
2 Materials and Methods	20
2.1 Materials.....	20
2.1.1 Chemicals and reagents.....	20
2.1.2 Buffers and solutions	22
2.1.3 Equipment	23
2.1.4 Oligonucleotides	24
2.1.5 Antibodies and staining reagents	25
2.1.6 Cells and culture media	26
2.1.7 Software	26
2.2 Methods	27
2.2.1 Cell culture methods.....	27
2.2.1.1 Cultivation of THP-1 cells	27

2.2.1.2	Differentiation and polarization	27
2.2.1.3	Preparation of glycated FCS.....	28
2.2.1.4	Stimulation of macrophages	28
2.2.1.5	Immunofluorescence staining.....	28
2.2.1.6	Metabolic activity assay	29
2.2.1.7	Intracellular ROS measurement	29
2.2.1.8	Flow cytometry	30
2.2.1.8.1	Phagocytosis assay	30
2.2.1.8.2	Apoptosis assay	30
2.2.1.8.3	Cell surface staining for polarization	31
2.2.1.8.4	Analysis of RAGE expression via flow cytometry	32
2.2.1.9	Preparation of cell lysates.....	32
2.2.2	DNA analysis techniques.....	32
2.2.2.1	Total RNA isolation.....	32
2.2.2.2	cDNA synthesis & quantitative real-time PCR	33
2.2.3	Protein analysis techniques.....	34
2.2.3.1	Determination of protein concentration.....	34
2.2.3.2	Immunoprecipitation	34
2.2.3.3	SDS-PAGE	34
2.2.3.4	Immunoblotting.....	35
2.2.3.5	Dot blot analysis	36
2.2.3.6	Cytokine quantification	36
2.2.4	Statistical analysis	36
3	Results	37
3.1	Glycation of macrophages.....	37
3.1.1	Consequences of MGO treatment.....	39
3.1.1.1	Metabolic activity of macrophages after glycation	40
3.1.1.2	Cell viability of macrophages after glycation.....	41
3.1.2	Comparison between glycation of cellular proteins and treatment with AGE-modified proteins	43
3.1.3	Glycation does not interfere with ROS production	44
3.2	Glycation and RAGE activation	45
3.2.1	RAGE expression after glycation.....	45
3.2.2	Analysis of NF- κ B expression after glycation	47
3.3	Glycation interferes with cytokine expression.....	48

3.3.1	Expression of IL-1 β and involvement of the inflammasome	48
3.3.2	Expression of IL-6.....	51
3.3.3	Expression of IL-8.....	52
3.3.4	Expression of TNF- α	53
3.3.5	Expression of IL-10.....	54
3.4	Effect of glycation on phagocytosis	55
3.4.1	Phagocytic efficiency	55
3.4.2	Glycation of phagocytosis associated surface receptors	56
3.5	Influence of glycation on macrophage polarization.....	57
3.5.1	Flow cytometry analysis of surface marker.....	57
3.5.2	qPCR analysis of expression marker.....	60
4	Discussion	62
4.1	MGO induces glycation of macrophages.....	62
4.2	RAGE is only activated upon treatment with soluble AGEs.....	64
4.3	Glycation has an influence on cytokine expression	66
4.4	Phagocytic efficiency is reduced upon glycation	69
4.5	Glycation has no influence on macrophage polarization	70
5	Summary	72
	References	IX
	Acknowledgements	XXI
	List of Publications.....	XXII
	Curriculum vitae.....	XXIII
	Eidesstattliche Erklärung	XXV

Abstract

Glycation is the non-enzymatic reaction that leads to the formation of so called advanced glycation end products (AGEs). Glycation and the accumulation of AGEs are known to occur during normal aging, but also in the progression of diseases, such as diabetes, Alzheimer's disease, atherosclerosis and Parkinson's disease. Methylglyoxal (MGO), a reactive dicarbonyl compound and by-product of glycolysis, potently induces glycation. The plasma concentration of MGO was found to be elevated in several diseases. In diabetic patients, almost five-fold higher MGO concentrations could be found due to permanently higher blood glucose levels and glycolysis rates.

Impaired wound healing and the development of foot ulcers are well known complications in diabetes. However, the underlying mechanisms of impaired wound healing in diabetic or elder patients are still unknown. In general, macrophages are known to play an important role in impaired wound healing. Under normal conditions, macrophages are able to polarize into M1 or M2 phenotypes when recruited into wounds. M1 macrophages display pro-inflammatory functions, whereas the population later switches to M2 phenotypes, which reduce inflammation and induce tissue remodelling. In diabetic wounds macrophages tend to remain predominantly in the M1 activation state, but defined mechanisms remain unknown. Elevated blood glucose levels as well as elevated MGO levels in diabetic patients result in glycation and an increase of AGEs. In this work, the effects of glycation and AGEs on macrophage activation were investigated. It could be shown that glycation, but not treatment with AGE-modified serum proteins, increased expression of pro-inflammatory cytokines interleukin (IL)-1 β , IL-6, IL-8 and tumour necrosis factor (TNF)- α , resulting in increased inflammation. In addition, the expression of anti-inflammatory cytokine IL-10 was affected. At the same time, glycation reduced phagocytic efficiency and led to impaired clearance rates of invading microbes and cellular debris. It could also be demonstrated that the inflammatory effects caused by glycation of the cells do not result from activation of the receptor for AGEs (RAGE). This work demonstrates that glycation contributes to changes of macrophage activity and cytokine expression and therefore could support the understanding of disturbed wound healing during aging and diabetes.

Inhaltsangabe

Die Glykierung ist eine nicht-enzymatische Reaktion, die zur Bildung der sogenannten *advanced glycation end products* (AGEs) führt. Glykierung und die Akkumulierung von AGEs treten während des Alterungsprozesses auf, können aber im Verlauf bestimmter Krankheitsbilder, wie zum Beispiel Diabetes, Atherosklerose, der Alzheimer oder der Parkinson Krankheit, verstärkt sein. Methylglyoxal (MGO), ein reaktives Nebenprodukt der Glykolyse, führt zur vermehrten Glykierung. In diversen Krankheiten konnten erhöhte MGO-Konzentrationen im Plasma nachgewiesen werden, beispielsweise wurden bei Diabetikern bis zu fünffach erhöhte MGO-Konzentrationen gemessen auf Grund von erhöhtem Blutzucker und Glykolyseraten.

Eine gestörte Wundheilung, einhergehend mit der Entstehung von Fußulzera, ist eine bekannte Komplikation im Diabetes. Allerdings sind die genauen Mechanismen der Wundstörung in älteren und Diabetespatienten weitgehend unbekannt. Generell spielen Makrophagen eine wichtige Rolle im Kontext dieser gestörten Wundheilung. Unter normalen Begebenheiten polarisieren Makrophagen in den M1 oder M2 Phänotyp nach ihrer Rekrutierung in Wunden. Zuerst fördern die M1 Makrophagen die Entzündung, während sich die Population später in M2 Makrophagen umwandelt, um die Entzündung zu reduzieren und die Gewebeneubildung zu fördern. In diabetischen Wunden konnten hauptsächlich M1 und kaum M2 Makrophagen nachgewiesen werden, aber genauere Ursachen sind noch unbekannt. Erhöhte Blutzuckerwerte und erhöhte MGO-Konzentrationen können bei Diabetikern zu vermehrter Glykierung und der Bildung von AGEs führen. In der vorliegenden Arbeit wurden diese Einflüsse auf die Aktivität von Makrophagen untersucht. Es konnte nachgewiesen werden, dass Glykierung, aber nicht die Behandlung mit AGE-modifizierten Proteinen, die Expression von pro-inflammatorischen Zytokinen wie Interleukin (IL)-1 β , IL-6, IL-8 und des Tumornekrosefaktors (TNF)- α fördert, was zu verstärkten Entzündungsreaktionen führt. Auch die Expression vom anti-inflammatorischen Zytokin IL-10 ist verändert. Zeitgleich verringert Glykierung die Phagozytoserate der Makrophagen, was wiederum zu verringerter Aufnahme und Abbau von Mikroben und Zellschrott führt. Es konnte weiterhin gezeigt werden, dass diese Effekte, die durch Glykierung der Zellen hervorgerufen wurden, nicht auf eine Aktivierung des Rezeptors für AGEs (RAGE) zurückzuführen sind. Diese Arbeit demonstriert, dass Glykierung zu einer Veränderung der Aktivität der Makrophagen und der Zytokinsekretion beiträgt und daher dabei helfen kann, die Mechanismen der gestörten Wundheilung während des Alterns und Diabeteserkrankungen zu verstehen.

Abbreviations

AD	Alzheimer's disease
AGEs	advanced glycation end products
AGE-FCS	glycated fetal calf serum
AGE-R	advanced glycation end products receptor complex
APC	allophycocyanin
APS	ammonium persulfate
ASC	apoptosis-associated speck-like protein containing a C-terminal caspase-recruitment domain
BCA	bicinchoninic acid
BSA	bovine serum albumin
CaCl ₂	calcium chloride
CBA	cytometric bead array
CD	cluster of differentiation
cDNA	complementary DNA
CEL	carboxyethyllysine
CML	carboxymethyllysine
CSF	colony stimulating factor
Ctrl	control
DAMPs	danger- associated molecular patterns
DMSO	dimethylsulfoxid
DTT	dithiothreitol
EDTA	ethylenediaminetetraacetic acid
FCS	fetal calf serum
FITC	fluorescein isothiocyanate
GLO	glyoxalase
GM-CSF	granulocyte-macrophage colony-stimulating factor
GOLD	glyoxal-lysine dimer
H ₂ DCFDA	2',7'-dichlorodihydrofluorescein diacetate
HCl	hydrochloric acid
HRP	horseradish peroxidase
IF	immunofluorescence
IFN	interferon
IL	interleukin
IP	immunoprecipitation
JNK	c-Jun N-terminal kinase
KCl	potassium chloride
LCIS	live cell imaging solution
LPS	lipopolysaccharide
MAPK	mitogen activated protein kinase
MD-2	lymphocyte antigen 96
MgCl ₂	magnesium chloride
MG-H	hydroimidazolone derivate
MGO	methylglyoxal
MOLD	methylglyoxal-lysine dimer

MTT	thiazolyl blue tetrazolium bromide
MyD88	myeloid differentiation primary response 88
NaCl	sodium chloride
Na ₂ HPO ₄	sodium hydrogen phosphate
NaN ₃	sodium azide
NF-κB	nuclear factor kappa B
NLRP	nucleotide-binding oligomerization domain, leucine rich repeat and pyrin domain containing
NOD	nucleotide-binding oligomerization domain
qPCR	quantitative real-time polymerase chain reaction
PAGE	polyacrylamide gel electrophoresis
PAMPs	pathogen- associated molecular patterns
PBS	phosphate buffered saline
PFA	paraformaldehyde
PIC	protease inhibitor cocktail
PMA	phorbol 12-myristate 13-acetate
PMSF	phenylmethylsulfonyl fluoride
P/S	penicillin-streptomycin
RAGE	receptor for advanced glycation end products
ROS	reactive oxygen species
RPL32	ribosomal protein L32
RPMI	Roswell Park Memorial Institute medium
SD	standard deviation
SDS	sodium dodecyl sulfate
SDS-PAGE	sodium dodecyl sulfate polyacrylamide gel electrophoresis
SR	scavenger receptor
SSA	sulfosalicylic acid
TBS	tris-buffered saline
TCA	trichloroacetic acid
TEMED	tetramethylethylenediamine
TGF	transforming growth factor
THP	tetrahydropyrimidine
THP-1	Tohoku Hospital Pediatrics-1
TLR	toll-like receptor
TNF	tumour necrosis factor
TRIS	tris(hydroxymethyl)aminomethane
7-AAD	7-aminoactinomycin

Table of figures

Figure 1: The pathway of AGE formation.	1
Figure 2: Chemical structures of different AGEs.....	2
Figure 3: Structure of receptors for AGEs.....	3
Figure 4: RAGE signalling pathways.	5
Figure 5: MGO derived AGE-structures.....	6
Figure 6: The glyoxalase system.	8
Figure 7: Macrophage differentiation and polarization.....	13
Figure 8: The NLRP3-inflammasome.	15
Figure 9: Immunoblot of glycated THP-1 macrophages.	38
Figure 10: IF staining of surface glycation of THP-1 macrophages.	39
Figure 11: Micrographs of THP-1 macrophages after MGO incubation.....	40
Figure 12: Metabolic activity of THP-1 macrophages after glycation.	41
Figure 13: Cell viability of THP-1 macrophages after glycation.	42
Figure 14: Dot blot analysis of AGE-FCS	43
Figure 15: Intracellular ROS production after glycation.	44
Figure 16: RAGE protein expression after glycation.....	46
Figure 17: Detection of RAGE after glycation via flow cytometry.....	47
Figure 18: NF- κ B protein expression after glycation.....	48
Figure 19: Expression of IL-1 β after glycation.	49
Figure 20: Expression of caspase-1 after glycation.....	50
Figure 21: Expression of IL-6 after glycation.	51
Figure 22: Expression of IL-8 after glycation.	52
Figure 23: Expression of TNF- α after glycation.	53
Figure 24: Expression of IL-10 after glycation.	54
Figure 25: Phagocytic efficiency after glycation.....	55
Figure 26: Detection of glycation of TLR4.	57
Figure 27: Analysis of CD16 in M1 and M2 macrophages.....	58
Figure 28: Analysis of polarization marker in M1 and M2 macrophages.	59
Figure 29: Analysis of polarization related cytokine expression.....	61
Figure 30: Table of analysed cytokines.	66

1 Introduction

1.1 Glycation and advanced glycation end products (AGEs)

In 1912, Louis Camille Maillard was the first scientist to describe a non-enzymatic browning reaction that could be observed when sugars and amino acids were heated. This reaction was named Maillard reaction according to its discoverer and was termed as a non-enzymatic glycosylation reaction (Maillard, 1912). Nowadays, this reaction is called glycation and the visible browning products are called advanced glycation end products (AGEs). A free amino group of a protein, mostly an arginine or lysine residue, reacts with the free carbonyl group of a reducing sugar, e.g. glucose or fructose, in a nucleophilic addition reaction. The formed product is known as a Schiff base and is not very stable. The amount of Schiff bases can directly be correlated with the glucose concentration available in the reaction system (Cerami, 1985; Ulrich and Cerami, 2001). Further rearrangement of this Schiff base leads to formation of a so-called Amadori product. Although the Amadori product is more stable than the Schiff base, it also gets further processed and undergoes several chemical modifications, such as oxidation, condensation or dehydration, finally resulting in a protein with an AGE-structure or AGE-crosslinks (Vistoli et al., 2013). A schematic overview of the glycation reaction is shown in figure 1. Besides sugars, reactive dicarbonyl compounds like methylglyoxal (MGO), glyoxal or 3-deoxyglucosone can also lead to glycation. These compounds are generated during rearrangement of the Amadori product as proteins are glycated by glucose (Thornalley et al., 1999).

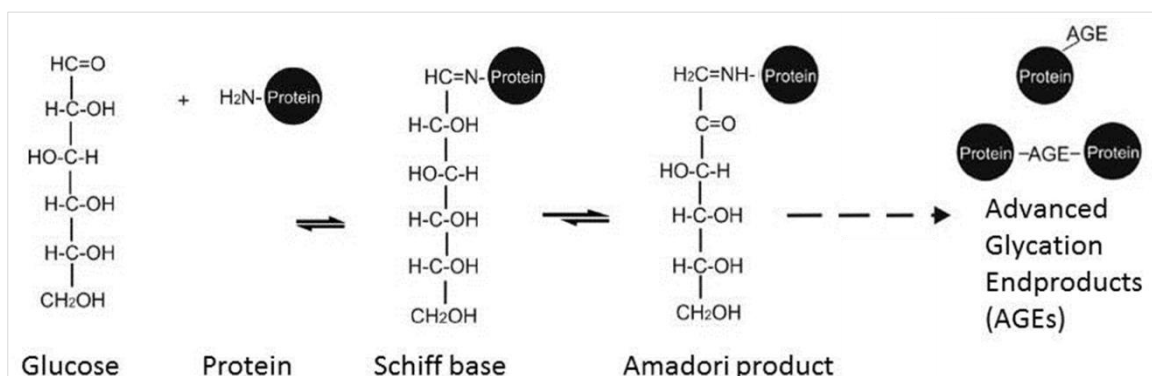


Figure 1: The pathway of AGE formation.

Glycation reaction based on the example of glucose is schematically shown. Single AGE-modification and AGE-crosslinks of the protein is demonstrated. Figure modified from Salahuddin et al. (2014).

Due to the variety of different proteins that can react with different glycating agents in glycation reactions, there exist many different AGE structures. Several examples of dietary AGEs are shown in figure 2. Some of these structures, for example pentosidine, have been first described by their yellow-brown fluorescent colour and their ability to form protein crosslinks (Vlassara et al., 1984). Other AGE-structures, like carboxymethyllysine (CML), carboxyethyllysine (CEL) and pyrraline, do neither show any colour or fluorescence, nor form crosslinks (Reddy et al., 1995). Glyoxal-lysine dimer (GOLD) and methylglyoxal-lysine dimer (MOLD) are prominent dietary AGEs, they have been identified in the hydrolysates of bakery products (Henle, 2005).

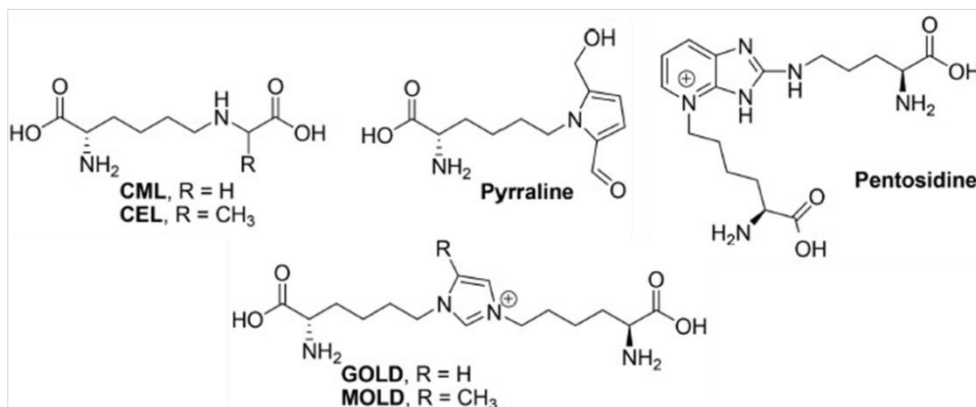


Figure 2: Chemical structures of different AGEs.

The image illustrates different dietary AGE-structures, from shorter carbonyl structures like CML or CEL to long-chained structures with fluorescent rings like pentosidine. CML = carboxymethyllysine; CEL = carboxyethyllysine; GOLD = glyoxal-lysine dimer; MOLD = methylglyoxal-lysine dimer. Figure modified from Zhu et al. (2018).

1.1.1 Receptors for AGEs

AGEs can be recognised by several cell surface receptors, mediating the activation of different signalling pathways (Ott et al., 2014). One of the best characterised pathways is the receptor for advanced glycation end products (RAGE), a multi-ligand receptor of the immunoglobulin superfamily (Ramasamy et al., 2008). Besides RAGE, there are several other receptors known, for example the AGE-receptor complex (AGE-R). AGE-R consists of three components, namely AGE-R1 (OST-48), AGE-R2 (80K-H) and AGE-R3 (galectin-3), and is involved in endocytic uptake of AGEs (Li et al., 1996; Vlassara et al., 1995). Some members of the scavenger receptor (SR) family have also been reported to bind AGEs, for example SR-A (Araki et al., 1995), CD36 (Ohgami et al., 2001a) and SR-BI (Ohgami et al., 2001b) from the SR-B subfamily, LOX-1 (Jono

et al., 2002) from the SR-E subfamily, and FEEL-1 and FEEL-2 (Tamura et al., 2003) from the SR-H subfamily. All known receptors for AGEs are depicted in figure 3.

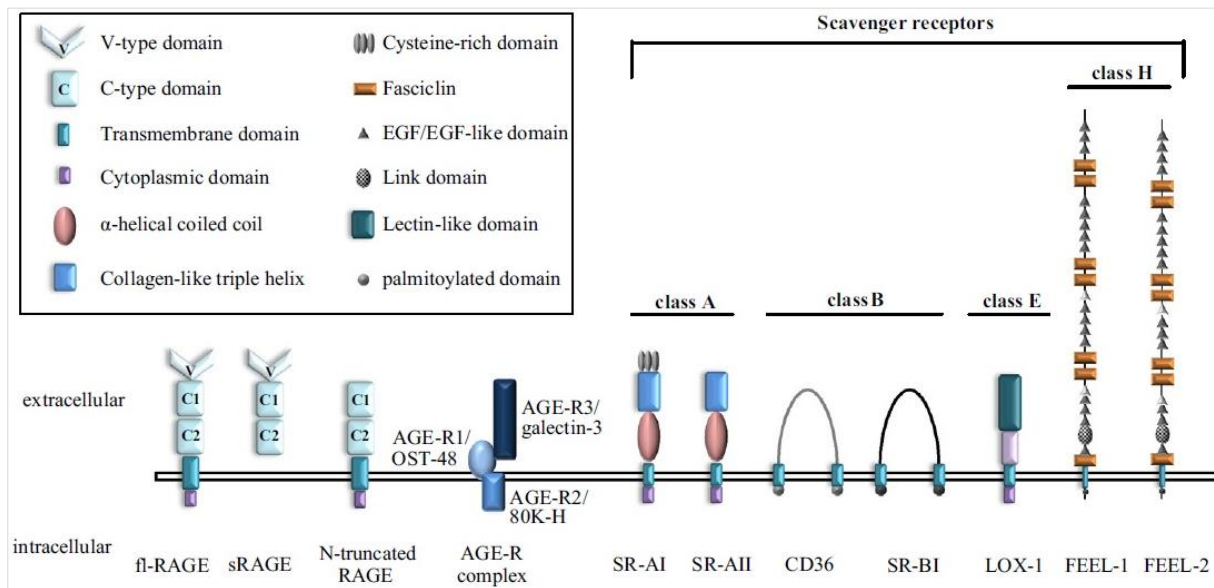


Figure 3: Structure of receptors for AGEs.

Different surface receptors are shown that can recognise AGEs. RAGE and the AGE-R complex (AGE-R1/OST-48, AGE-R2/80K-H and AGE-R3/galectin-3) do not belong to the scavenger receptor family, but also recognise AGEs. Adapted from Ott et al. (2014).

1.1.1.1 Structure and function of RAGE

RAGE was first described in 1992 as a pattern recognition receptor of the immunoglobulin superfamily that recognises AGE-structures. RAGE has an approximate molecular mass of 35 kDa, however, due to posttranslational modification (e.g. glycosylation) higher molecular masses can be detected in immunoblots between 45 kDa and 50 kDa (Neeper et al., 1992). Mature RAGE consists of an extracellular, a transmembrane and a cytosolic domain. The extracellular domain in turn is also composed of three subdomains, one V-type domain (variable) and two C-type domains (constant; as illustrated in figure 3). The V-type domain has multi-ligand binding sites and is responsible for signalling. The transmembrane domain functions as an anchor in the plasma membrane, while signals into the cell are transduced via the cytosolic domain (Lee and Park, 2013). More than 20 different alternative splicing forms of full-length RAGE are known (Falcone et al., 2013). Two major splice variants are well-characterised, the soluble RAGE and the N-truncated RAGE. Soluble RAGE lacks the C-terminal domain, but contains all C-type and V-type domains. It can be secreted

extracellularly or released by proteolytic cleavage of the full length version. Instead, N-truncated RAGE is only lacking the N-terminal V-type domain and is still anchored in the cell membrane like the full-length version. However, these splice variants are not able to transduce signals into the cell (Yonekura et al., 2003).

RAGE is expressed in different cell types, among them immune cells like monocytes and macrophages (Ohashi et al., 2010; Wang et al., 2010b) or T-lymphocytes (Akirav et al., 2012; Ohashi et al., 2010), but also endothelial cells (Pollreisz et al., 2010) or fibroblasts (Liu et al., 2010). Besides AGEs, RAGE is also able to bind to β -amyloid, phosphatidylserine, S-100 proteins and high-mobility group box protein 1 (Ramasamy et al., 2012). High expression of RAGE can be observed during embryonic development and is associated with neurite outgrowth (Hori et al., 1995). However, in adult tissue RAGE-expression is very low (Brett et al., 1993). RAGE is also known to be involved in inflammation processes and immune response, bone metabolism, lung homeostasis and neuronal differentiation (Chuah et al., 2013; Ott et al., 2014). It has also been demonstrated that RAGE is important for microbe recognition by interaction with lipopolysaccharides (LPS; Yamamoto et al., 2011). Other functions can be the mediation of cell migration and proliferation (Rai et al., 2012). Besides all these findings and theories, the entire physiological functions of RAGE are still not completely understood (Ott et al., 2014).

1.1.1.2 AGE-mediated RAGE signalling

Binding of AGEs to RAGE induces a wide range of signalling cascades, resulting in enhanced generation of reactive oxygen species (ROS) and finally in the activation of nuclear factor kappa-light-chain-enhancer of activated B cells (NF- κ B; Herold et al., 2007; Negre-Salvayre et al., 2009; Vazzana et al., 2009). A detailed overview of RAGE-signalling is depicted in figure 4. RAGE stimulates the activation of mitogen activated protein kinases (MAPK), like p38, extracellular signal-regulated kinase (ERK) 1/2 and c-Jun N-terminal kinase (JNK), the activation of JAK-STAT pathway, phosphoinositol 3-kinase (PI3K) as well as members of the Rho GTPase signalling pathway (Cdc42/ Rac-1). Through the activation of NAD(P)H oxidase among others, generation of intracellular ROS is also induced (Vazzana et al., 2009). Ultimately, NF- κ B is activated, dislocates into the nucleus and induces the expression of several target genes like cytokines and adhesion molecules (shown in figure 4) as well as its own

expression and the expression of RAGE as a positive feedback loop (Bierhaus et al., 2005). Hence, accumulation of AGEs could also be correlated to higher RAGE expression in the respective tissue (Sun et al., 1998; Tanji et al., 2000).

However, the network of RAGE signalling is diverse and very complex. Considering the fact that every ligand bound to RAGE can induce different signalling and activate or suppress different pathways, the mechanisms can be different for every cell type that expresses RAGE (Bierhaus et al., 2005). Therefore, the whole function of RAGE and its signalling are still not completely understood.

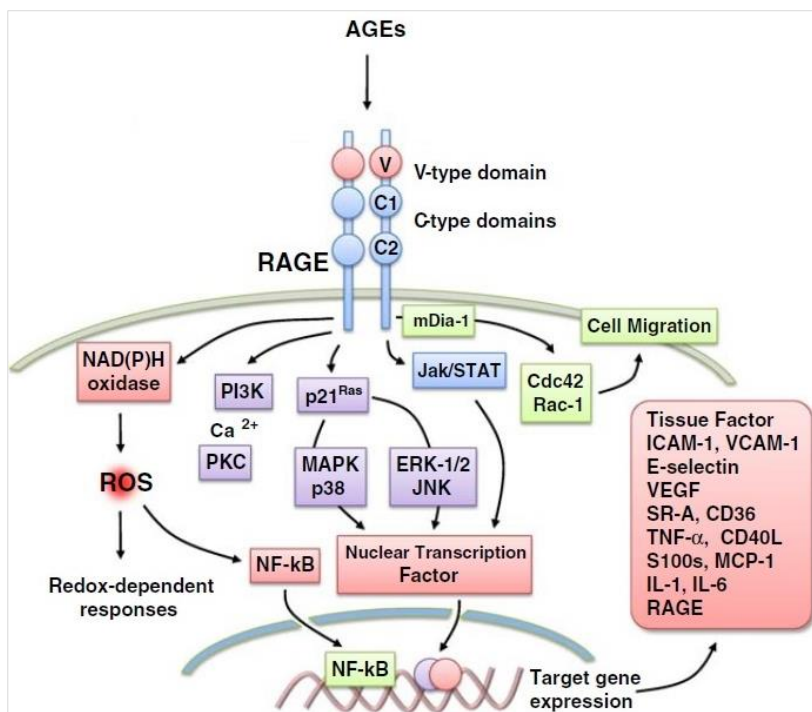


Figure 4: RAGE signalling pathways.

The figure illustrates the AGE-mediated signalling pathway of RAGE. Binding of AGEs to RAGE activates several MAPK (p38, ERK-1/2, JNK), JAK-STAT pathway, PI3K and Rho GTPase signalling pathway (Cdc42/ Rac-1). Activation of NAD(P)H oxidase also triggers intracellular ROS production. Ultimately, NF- κ B is activated and induces the gene expression of several target genes as well as its own expression and the expression of RAGE. Figure modified from Vazzana et al. (2009).

1.1.2 MGO induced glycation

MGO is one of the most potent glycating agents. It is a naturally occurring side product of glycolysis but evolves also during threonine catabolism and lipid peroxidation. During glycolysis, up to 0.4 % of glycolytic intermediates are metabolised to MGO (Kalapos, 2008a; Thornalley, 1988). MGO is a highly reactive α -oxoaldehyde and is mostly formed by the spontaneous, non-enzymatic degradation of triose phosphate intermediates, dihydroxyacetone phosphate or glyceraldehyde-3-phosphate (Phillips and Thornalley, 1993b; Richard, 1993). Under normal conditions, approx. 120 μmol MGO per kg of cell mass are formed daily in the human body (Phillips and Thornalley, 1993a; Thornalley, 1988). MGO is much more reactive than glucose but has a short half-life time. Most of the MGO molecules *in vivo* are therefore bound to macromolecules (Kalapos, 2008a; Sousa Silva et al., 2013). MGO-derived glycation is mainly directed to arginine or lysine residues of proteins. Figure 5 shows exemplary some of the AGEs that can be formed by MGO. The reaction of MGO with arginine residues of proteins results mainly in hydroimidazolone derivatives (MG-H, three related isoforms, only MG-H1 is depicted), but can also form argpyrimidine or tetrahydropyrimidine (THP) derivatives, while reaction with lysine residues leads to formation of CEL or MOLD.

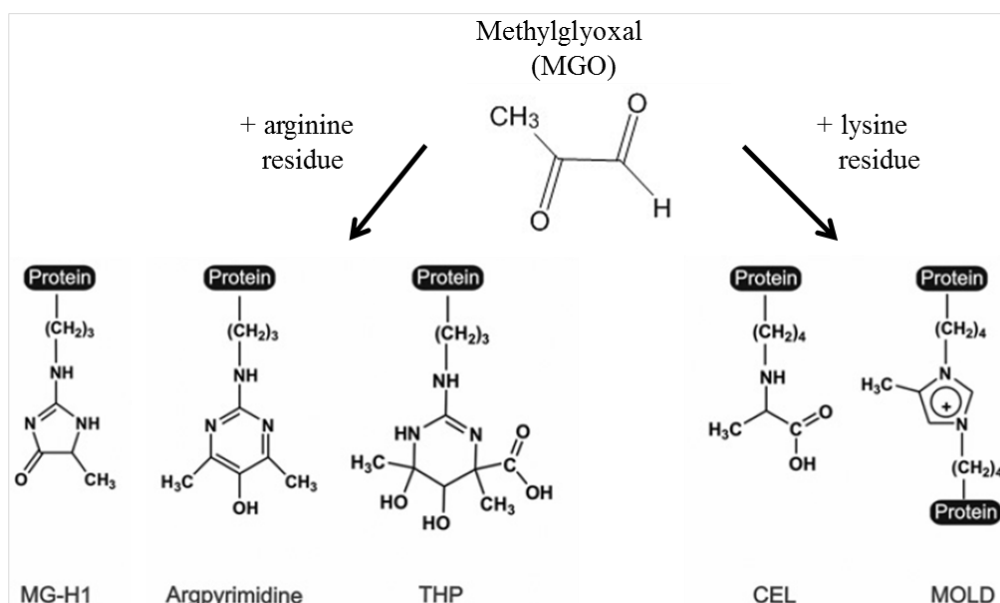


Figure 5: MGO derived AGE-structures.

AGEs can be derived from the reaction of MGO with either arginine or lysine residues of proteins. MG-H1: hydroimidazolone derivative 1; THP: tetrahydropyrimidine derivative; CEL: carboxyethyllysine; MOLD: methylglyoxal-lysine dimer; Figure modified from Sousa Silva et al. (2013).

1.1.2.1 The physiological role of MGO induced glycation

Elevated MGO levels can be observed during ageing but also during the progression of several diseases, such as obesity, diabetes mellitus, cardiovascular diseases, Alzheimer's disease and chronic renal disease. The accumulation of such reactive carbonyl species like MGO or glyoxal is also referred to as carbonyl stress, which can lead to apoptosis of cells and ROS generation (Rabbani and Thornalley, 2015). Especially in tumour cells, changes in the metabolic activity, e.g. higher rates of glucose uptake and therefore of glycolysis, can lead to an increase of MGO synthesis and likewise of glycation (Shinohara et al., 1998). Heat Shock Protein 27 was identified as major MGO-modified protein in cancer cells, being beneficial for the evasion of apoptosis (van Heijst et al., 2006). Besides modification of proteins, MGO is also able to modify nucleic acids and DNA, which can have severe biological complications such as in tumorigenesis. Glycation of DNA may result in DNA crosslinks with other DNA or protein molecules, strand breaks, mutagenesis or even glycation of nucleosomal proteins such as histones (Vaca et al., 1994). However, diabetes and diabetic complications are still the most prominent disorders in case of increased MGO concentrations in plasma and blood (Beisswenger et al., 2005; McLellan et al., 1994). MGO levels in plasma of diabetic patients tend to be increased two- to fivefold compared to healthy individuals (McLellan et al., 1994). Hence, new strategies discuss the use of MGO and MGO-derived AGEs as a highly stable chemically reactive biomarker for the detection of both diabetes type I and type II and even prediabetes (Beisswenger, 2014; Ramachandra Bhat et al., 2019). Nevertheless, high concentrations of MGO can be cytotoxic for many cells, resulting in inhibition of proliferation, DNA-, RNA- and protein synthesis and finally induction of apoptosis (Kang et al., 1996).

1.1.2.2 MGO detoxification by the glyoxalase system

Due to its high reactivity and cytotoxicity, most of the endogenously formed MGO is directly metabolised by the glyoxalase system, which involves enzymes as glyoxalase-I and glyoxalase-II, as well as catalytic amounts of reduced glutathione (Schmoch et al., 2017). These enzymes metabolise MGO into D-lactate by using NADPH and glutathione (Thornalley, 2003), as shown in figure 6. MGO reacts spontaneously and non-enzymatically with reduced glutathione and forms a hemithioacetal. Next,

glyoxalase-I catalyses the isomerisation of the hemithioacetal into S-D-lactoylglutathione. S-D-lactoylglutathione is then further hydrolysed into D-lactate via catalysis of glyoxalase-II. In this step also the reduced glutathione, which was consumed by glyoxalase-I, is regenerated. The glyoxalase system is located in the cytosol as well as in the mitochondria, and it protects the cells against cellular damage or apoptosis caused by MGO or glyoxal (Sousa Silva et al., 2013; Thornalley, 1990). Since MGO is the major physiological substrate of glyoxalase-I, its activity prevents the accumulation of MGO and can prevent glycation reactions in the cells (Rabbani and Thornalley, 2012; Shinohara et al., 1998). Interestingly, expression of glyoxalase-I can be negatively regulated by RAGE activation, although the exact mechanism remains unclear (Rabbani et al., 2014).

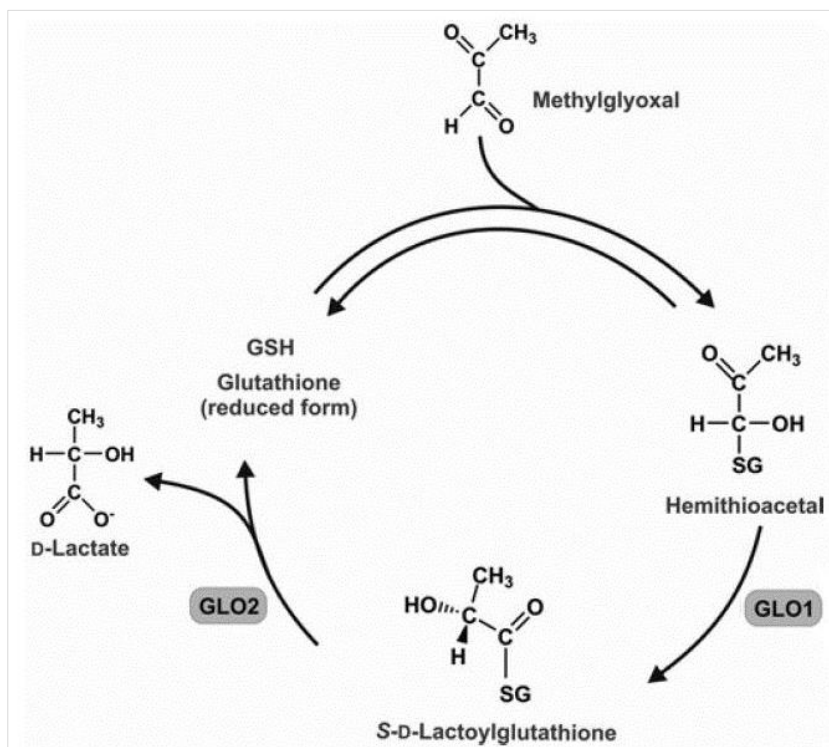


Figure 6: The glyoxalase system.

MGO is glutathione-dependent metabolised into D-lactate by two enzymes, glyoxalase-I (GLO1) and glyoxalase-II (GLO2). Figure modified from Sousa Silva et al. (2013).

1.1.3 Degradation of AGEs

Besides endogenous production inside the human body, AGEs can also be exogenously produced and ingested via food consumption or uptake by smoking (Cerami et al., 1997; Zhu et al., 2018). The intake is estimated to be around 25 - 75 mg of AGEs per day, mainly consisting of pyrraline and CML (Henle, 2003). Since AGEs do not undergo metabolic degradation, they accumulate over time in the body. AGE-structures could be identified extracellularly circulating in the plasma and serum or excreted in the urine and faeces, but also intracellularly in various tissues including lens and skin collagens, as well as in blood cells (Henning and Glomb, 2016). Most of the modified proteins are stable and long-lived proteins, although modification of short-lived proteins cannot be excluded. In general, there are two main proteolytic systems in the cells that are able to degrade macromolecules: the membrane-enclosed lysosome and the ubiquitin-proteasome-system. Extracellular material targeted for lysosomal degradation can be incorporated through endocytosis while intracellular objects are sequestered by autophagy (Saftig and Klumperman, 2009). Receptors for AGEs are generally known to endocytose AGE-structures; however, RAGE receptor only recognises AGEs in the extracellular environment but is not responsible for endocytosis of AGEs (Grimm et al., 2012). Scavenger receptors, in contrast, are capable to endocytose AGEs, especially CD36 and SR-A in macrophages or macrophage-derived cells (Horiuchi et al., 2003). An accumulation of AGEs in phagocytes could be demonstrated under conditions of reduced lysosomal activity, suggesting that lysosomal enzymes are crucial for the proteolysis of AGE-structures (Miyata et al., 1997). Aggregates of AGE-modified proteins might be packed in aggresomes and targeted for autophagy (Kueper et al., 2007). However, uptake of AGEs or AGE-aggregates into the lysosome does not imply that lysosomal enzymes are able to degrade the material completely (Yamamoto and Simonsen, 2011). Mostly, this process mediates the filtration and excretion of AGEs by the kidney (Gugliucci and Bendayan, 1996), though not all AGEs can be excreted (Makita et al., 1994). Consequently, a stronger accumulation of AGEs could be observed by patients with renal dysfunction (Miyata et al., 1998; Sell and Monnier, 1990). For proteasomal degradation, proteins are first targeted with ubiquitin moieties by ubiquitin ligases. The proteasome, a multimeric protease complex, then recognises ubiquitin-labelled proteins, deubiquitylates, unfolds and finally degrades them (Tomko and Hochstrasser, 2013). It has already been demonstrated that the 20S proteasome is not able to

degrade AGE-modified albumin (Grimm et al., 2010) and CML-structures (Bulteau et al., 2001). In contrast, some cells, e.g. microglial cells, seem to be able to degrade AGE-modified BSA through proteasomal and lysosomal degradation (Stolzing et al., 2006). Additionally, AGEs have been shown to inhibit the activity of proteasomes but induce the expression of immunoproteasomes (Grimm et al., 2012). Although it has not been demonstrated whether this leads to an elevated clearance of AGEs, it can be assumed that the immunoproteasome may degrade AGEs in a very slow and inefficient manner.

1.1.4 Disease relevance of glycation and AGEs

The accumulation of AGEs throughout the human body can be observed during normal ageing (Wu, 1993). Nevertheless, there are some disease models that are directly linked to an increased production and accumulation of AGEs. As already mentioned diabetes is strongly associated with glycation and AGE-accumulation due to hyperglycaemia and elevated MGO levels. Glycation may contribute to diabetic complications including nephropathy, retinopathy, neuropathy and atherosclerosis (Jakus and Rietbrock, 2004; Yamagishi, 2011). Especially CML-modified proteins seem to accumulate in diabetic patients; they could be detected in collagens of skin tissue (Baynes, 1991), in the lens (Dunn et al., 1989) and also in urine (Knecht et al., 1991). In atherosclerosis, which is often linked to obesity and diabetes, AGEs play an important role in the onset of pathogenesis. AGEs were reported to contribute to the increase of ROS production within adipocytes, which can also affect their ability to clear oxidized and damaged proteins (Boyer et al., 2015; Diez et al., 2016). In Alzheimer's disease (AD), glycation of β -amyloid alter its toxicity and contribute to neurodegeneration (Vicente Miranda et al., 2016). AGE-modified proteins have also been identified in the neurofibrillary tangles and the cerebrospinal fluid of AD patients (Angeloni et al., 2014). Increased levels of AGEs could be detected in the plasma and brain in patients suffering from multiple sclerosis. These AGEs are mostly derived from MGO, due to elevated intracellular glycolysis rates and impairments of the glyoxalase system, and contribute to the pathogenesis of multiple sclerosis (Wetzels et al., 2017).

Besides endogenous production of AGEs and MGO, also dietary ingested AGEs are known to contribute to the progression of several diseases. Since exogenous AGEs conduce to the pool of endogenous AGEs, they promote the increase of inflammation

reactions and oxidative stress. Therefore, they contribute especially to the onset of chronic diseases, including diabetes, neurodegenerative diseases, chronic kidney disease or cardiovascular diseases (Uribarri et al., 2015). These findings suggest that AGE-low diets could be a beneficial tool in several disease models and should not be neglected in the overall pattern of glycation and AGEs in disease relevance.

1.2 Macrophages

Macrophages are myeloid cells of the immune system and the major differentiated cells of the mononuclear phagocyte system. They originate from the bone marrow, which contains resting macrophages (M0 phenotype), as well as their precursors monoblasts, promonocytes and monocytes (Lewis and McGee, 1992). In the past, blood monocytes were believed to be the only macrophage progenitors, being recruited to several tissues where they then differentiate into macrophages. Nowadays it is known that resident macrophages are widely distributed in the body, being present in many organs and in the connective tissue (Gordon, 2007). They participate in a wide range of physiological processes, e.g. immune responses, homeostasis and wound healing. Macrophages provide the first line of defence against pathogens and microbes (Kloc, 2017; Mosser and Edwards, 2008). One of their major functions is to clear blood, lymph and tissues of particles – for example microbes, dead cells or debris – that are ingested via phagocytosis (Lewis and McGee, 1992; van Furth et al., 1972). Additionally, macrophages adapt their phenotype according to their environment and selectively release cytokines and growth factors in order to encourage or decrease inflammation (Gordon, 2003). This activation process is termed macrophage polarization. *In vivo*, macrophages also need special survival cytokines including the colony stimulating factor 1 (CSF-1) and granulocyte-macrophage colony-stimulating factor (GM-CSF) in order to regulate their population numbers and maintain proliferation by suppressing apoptosis (Hamilton and Achuthan, 2013; Lavin et al., 2015). *In vitro*, differentiation of monocytes into macrophages using for example phorbol 12-myristate 13-acetate (PMA) inhibits their proliferation, unless the cultures are not fed with GM-CSF and CSF-1 (Murray, 2017).

1.2.1 Macrophage polarization

Macrophage polarization was originally discovered by the observation, that stimulation of macrophages with interleukin (IL)-4 induced different gene expression in comparison to the classical activation with interferon (IFN)- γ and LPS (Nathan et al., 1983). The activation with IL-4 was therefore termed alternative activation (Stein et al., 1992). Later on, a new classification was proposed, separating the macrophages in M1 or M2 phenotype (Mills et al., 2000). This classification was based on findings in

mouse models with different T helper type background. T helper type 1 mouse strains with T cells that produced mostly IFN- γ generated nitric oxide (NO) from arginine upon activation. In contrary, T cells of T helper type 2 mouse strains produced mostly IL-4 and transforming growth factor (TGF)- β resulting in ornithine production (Mills et al., 2000). This resulted in the correlation that M1 (classically activated) macrophages exhibit pro-inflammatory, while M2 (alternatively activated) macrophages exhibit anti-inflammatory properties. Later on, M2 macrophages were even further divided into M2a, M2b, M2c and M2d phenotypes, depending on their activation stimuli (Mantovani et al., 2004; R szer, 2015). The classification in M1 and M2 is still in use, while some claim that this is an oversimplified classification, thus it helps to understand the differences in macrophage activation mechanisms. Figure 7 illustrates the differentiation and polarization process from monocyte to M1 or M2 phenotype under *in vitro* conditions.

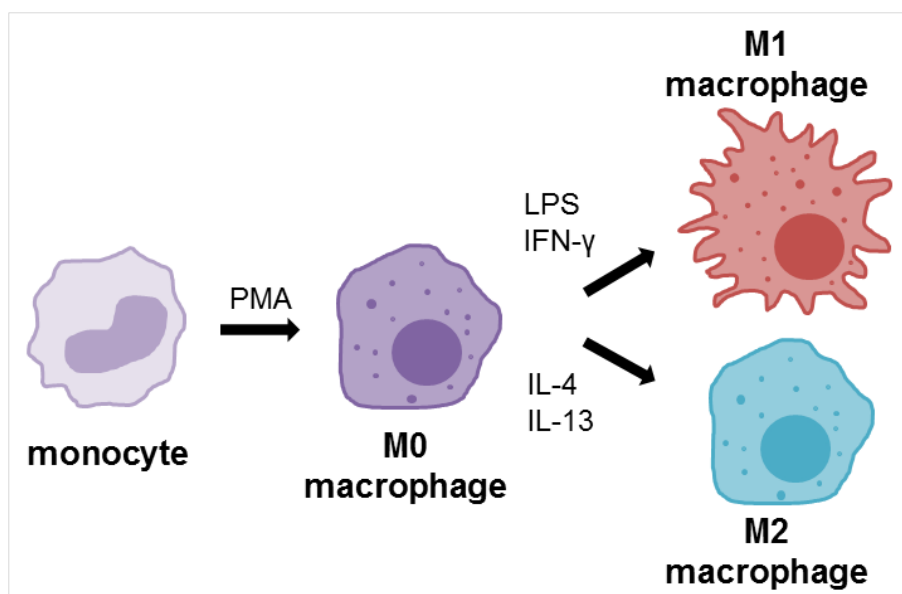


Figure 7: Macrophage differentiation and polarization.

Monocytes can be differentiated into macrophages (resting, M0) using the differentiation agent 12-myristate 13-acetate (PMA). M0 macrophages can be further polarized into M1 (pro-inflammatory, classically activated) phenotype using LPS and IFN- γ or into M2 (anti-inflammatory, alternatively activated) using IL-4 and IL-13 treatment. Adapted from Bezold et al. (2019).

1.2.1.1 Classically activated M1 macrophages

M1 or classically activated macrophages are defined as cells displaying a pro-inflammatory phenotype. They produce high amounts of pro-inflammatory cytokines like IL-1 β , IL-6, IL-8, IL-12, IL-18, IL-23 and tumour necrosis factor (TNF)- α , reactive oxygen and nitrogen intermediates, while they only secrete low amounts of anti-inflammatory cytokine IL-10 and TGF- β . Also, they interfere with pathogens and show high phagocytic efficiency. M1 macrophages can be defined by cell surface markers histocompatibility complex class II (MHC II) molecules, CD68, CD80 and CD86 (Duluc et al., 2007; Rószler, 2015). MHC II molecules are expressed on the cell surface of antigen presenting cells. They are presented after phagocytosis and initiate the immune response via T cell activation (Jones et al., 2006). CD68 (or macrosialin) is a glycoprotein which is heavily glycosylated and is expressed by macrophages in response to inflammatory stimuli and chronic stimuli with for example LPS (Barros et al., 2013; Chistiakov et al., 2017). CD80 (or B7 type I) and CD86 (or B7 type II) are closely related membrane proteins of the immunoglobulin superfamily that are also extensively glycosylated and important for T cell activation (Peach et al., 1995).

For the maturation and secretion of pro-inflammatory cytokines IL-1 β and IL-18, a protein complex termed the inflammasome needs to be activated (Martinon et al., 2002; Tschopp et al., 2003). The inflammasome involves different enzymes, proteins and receptors, depending on its activator, and typically consists of the proteolytic enzyme caspase-1, apoptosis-associated speck-like protein containing a C-terminal caspase-recruitment domains (ASC) and nucleotide-binding oligomerization domain-like (NOD-like) receptors (Kanneganti, 2015). Inflammasomes assemble in the cytosol after activation of pattern recognition receptors by pathogen-associated molecular patterns (PAMPs) or danger-associated molecular patterns (DAMPs; Martinon et al., 2002). Specifically, nucleotide-binding oligomerization domain, leucine rich repeat and pyrin domain containing (NLRP) proteins, which belong to the NOD-like receptor family, are important for the assembly of the inflammasome. ASC acts as an adaptor, it then recruits and activates caspase-1 by its polymerization to so called ASC specks (Franklin et al., 2014). Caspase-1 cleaves pro-IL-1 β and pro-IL-18, as well as gasdermin D, into their mature active protein forms (Cerretti et al., 1992; Mariathasan et al., 2004; Thornberry et al., 1992). Caspase-1 is also known to promote a form of inflammation induced cell death called pyroptosis (Lamkanfi and Dixit, 2014). Figure 8

depicts the formation of NLRP3-inflammasome, which is one of the most characterised inflammasomes.

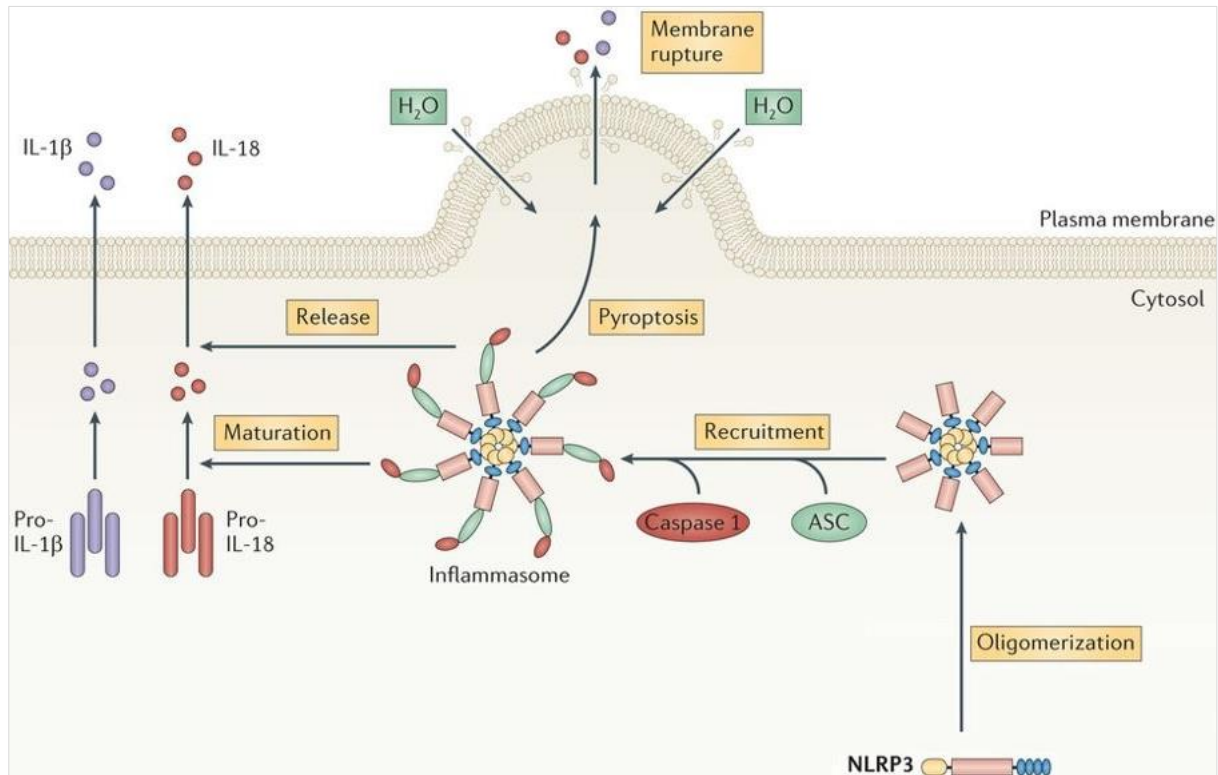


Figure 8: The NLRP3-inflammasome.

After activation of NLRP3 and ASC, caspase-1 is activated and assembles to the inflammasome. The inflammasome then mediates the maturation of pro-IL-1 β and pro-IL-18 to IL-1 β and IL-18, which are released through the plasma membrane. Also, pyroptosis is induced which leads to inflammation induced cell death. NLRP: nucleotide-binding oligomerization domain, leucine rich repeat and pyrin domain containing protein; ASC: apoptosis-associated speck-like protein containing a C-terminal caspase-recruitment domain. Figure modified from Walsh et al. (2014).

The LPS mediated activation of toll-like receptor (TLR) 4 plays a pivotal role in M1 polarization. TLRs are a family of type I membrane proteins that belong to a group of pattern recognition receptors and TLR4 is one of the most studied among them (Vaure and Liu, 2014). After LPS mediated activation, TLR4 activates the STAT1 signalling pathway dependent on the TLR-adaptor proteins myeloid differentiation primary response 88 (MyD88) and lymphocyte antigen 96 (MD-2) (Toshchakov et al., 2002). This leads to the activation of NF- κ B and MAPK pathways, finally resulting in release of pro-inflammatory cytokines (Pålsson-McDermott and O'Neill, 2004). Besides, TLRs

are known to be assistant receptors in phagocytosis (Fitzgerald et al., 2004; Qureshi and Medzhitov, 2003). In macrophages, especially TLR4 regulates phagocytosis, modulating the clearance of invading microbes (Anand et al., 2007).

1.2.1.2 Alternatively activated M2 macrophages

M2 or alternatively activated macrophages are cells displaying an anti-inflammatory phenotype. They produce mainly anti-inflammatory cytokines and growth factors, like IL-10, TGF- β , IL-1 receptor antagonist and arginase 1, while they only secrete low amounts of IL-1 β , IL-12 and IL-23. M2 macrophages can be defined among others by cell surface markers CD163, CD206 and CD209 (Duluc et al., 2007; R szer, 2015). CD163 is a macrophage-specific scavenger receptor with high affinity to the haemoglobin-haptoglobin complex. Upregulated expression of CD163 contributes to the anti-inflammatory response and is known as one of the major switches during alternative macrophage activation (Kristiansen et al., 2001; Onofre et al., 2009). CD206, or mannose receptor 1, is a C-type lectin on the macrophage surface, which is important for the binding and internalization of different glycoproteins (Porcheray et al., 2005; R szer, 2015). It is upregulated upon IL-4 activation and mediates phagocytosis of pathogens (Goerdts and Orfanos, 1999). CD209, or dendritic cell-specific intercellular adhesion molecule-3-grabbing non-integrin, is also a C-type lectin that plays an important role in the recognition of pathogens and viruses via binding of mannose type carbohydrates (Tassaneetrihetp et al., 2003).

The M2 phenotype can be further subdivided into M2a, M2b, M2c and M2d. The M2a phenotype is induced by IL-4 and IL-13, M2b is induced by immune complexes, TLR ligands or IL-1 receptor, while M2c is induced by IL-10 stimulation and glucocorticoid hormones (Mantovani et al., 2004). M2d activation is related to IL-6 activation and adenosines, and their appearance is associated with the promotion of tumour progression (Wang et al., 2010a). All four subtypes are said to have distinct gene expression profiles, which overlap more or less (Mantovani et al., 2004; R szer, 2015). Still, the division in these four subtypes is not yet believed to be adequate enough to describe the whole diversity of different macrophage populations *in vivo*.

1.2.2 Macrophages in wound healing

As described before, macrophages are key regulators in wound healing processes. They adapt their phenotype accordingly to the stages of wound healing (Mosser and Edwards, 2008). Their dynamic plasticity allows them to support destructive as well as reparative processes in tissues. Generally, wound healing can be divided into haemostasis (blood clotting), inflammation, proliferation and remodelling or maturation (Wang et al., 2018). During haemostasis, a fibrin clot is formed in order to arrest bleeding, together with the recruitment of inflammatory cells into the wound bed. Next, inflammatory cells secrete pro-inflammatory cytokines, among them for example IL-1 β , IL-8, TNF- α , and clear up the site of inflammation by phagocytosis of invading microbes, damaged cells and debris. During proliferation phase, keratinocytes start to migrate between the cloth and the epidermis. They proliferate in order to re-establish the stratified epidermis. This restores the epithelial barrier and remodelling of the tissue occurs. Collagen is realigned and remaining inflammatory cells are removed via apoptosis or cell death (Lindley et al., 2016).

1.2.2.1 Macrophage involvement in regeneration and tissue repair

Macrophages are involved in all phases of wound healing except haemostasis. They are important for inflammation as well as clearance of the cell debris and the coordination of tissue repair (Kim and Nair, 2019). During the beginning of the inflammation phase, polymorphonuclear leukocytes invade into the wound. Their arrival leads to successive infiltration of monocytes, which differentiate into macrophages within the wound tissue (Boniakowski et al., 2017). Tissue-resident macrophages are recruited to the inflammation site, but the main macrophage population is derived from differentiating blood monocytes (Thuraisingam et al., 2010). The differentiated macrophages, as well as the tissue-resident macrophages, switch to the M1 phenotype and promote inflammation. Besides secretion of pro-inflammatory cytokines, invading pathogens are engulfed (Gundra et al., 2014). When the phase of proliferation is initiated, macrophages switch to the M2 phenotype. They phagocytose surrounding dead cells and cell debris, but also secrete vascular endothelial growth factors, TGF- β and IL-10. The growth factors promote proliferation of endothelial cells, skeletal myoblasts, and fibroblasts and also support neo-angiogenesis, while IL-10 suppresses further invasion of macrophages (Kotwal and Chien, 2017; Minutti et al.,

2017; Novak and Koh, 2013). This continues during the remodelling phase. Macrophages are also known to be important for the breakdown and degradation of matrix fragments (Madsen et al., 2013). After completion of remodelling, macrophage numbers decline rapidly, when wound healing is completed (Martin and Leibovich, 2005).

1.2.2.2 Macrophage dysfunction in diabetic wounds

In diabetes, one of the major complications is impaired and delayed wound healing, followed by the persistence of chronic wounds. Up to 10 % of diabetic patients develop foot ulcers which can lead to non-traumatic limb amputations (Lavery et al., 2003; Singh et al., 2005). Almost 40,000 amputations per year are the result of diabetic complications in Germany (Kröger et al., 2017). There are many different factors which contribute to delayed wound healing in diabetes, among them hyperglycaemia, macro- and microcirculatory dysfunction, chronic inflammation, hypoxia and neuropathy (Baltzis et al., 2014). It has already been shown that macrophages play an important role in diabetic wound healing. They remain predominantly in the pro-inflammatory M1 phenotype, resulting in chronic inflammations (Baltzis et al., 2014; Falanga, 2005; Loots et al., 1998). During the remodelling phase of diabetic wounds, increased numbers of the M1 phenotype could be found, whereas the M2 population was decreased (Yan et al., 2018). Increased concentrations of the pro-inflammatory cytokine IL-1 β were detected in diabetic wounds, indicating a positive feedback loop that sustains the chronic pro-inflammatory profile of the wounds. In addition, by blocking the IL-1 β pathway, it has been shown that macrophages switch to a more healing associated, reparative phenotype, which was beneficial for proper wound healing (Mirza et al., 2013). In general, the phenotype switch of macrophages during wound healing from M1 to M2 phenotype seems to be affected in diabetes (Yan et al., 2018). However, the underlying mechanisms of impaired wound healing in diabetic as well as in elder patients are still not completely understood, though recently AGEs and glycation were also discussed to have an impact in this dysfunction (Basu Mallik et al., 2018).

1.3 Aim of work

Glycation and the accumulation of AGEs are known to occur during normal aging but also in the progression of several diseases, such as diabetes. In older patients as well as in diabetic patients, a dysfunction in wound healing can be observed. This raises the question, whether there is a connection between impaired wound healing and glycation or AGE-formation. The healing process tends to be much slower compared to healthy patients, while prolonged and chronic infections occur more often and tissue remodelling seems to be drastically decelerated. For diabetic wounds, it is known that macrophages play a critical role in the dysfunction of proper wound healing. There is a strong correlation between increased concentrations of glucose and MGO in blood and tissues of diabetic and elderly patients and increased levels of glycation and AGE-formation. However, not much is known about the impact of glycation on impaired wound healing. This thesis demonstrates the role of glycation and AGEs on macrophage activation, which could be beneficial for understanding the influence of glycation on macrophage dysfunction in impaired wound healing. The human macrophage cell line THP-1 was used as a model for the analyses of glycation and AGE-treatment on macrophages. Besides investigations of MGO induced glycation on cell behaviour, also some functional properties of macrophages ought to be analysed, among them cytokine expression and phagocytic efficiency.

2 Materials and Methods

2.1 Materials

2.1.1 Chemicals and reagents

General laboratory chemicals	
acrylamide / bisacrylamid solution	Carl Roth GmbH
albumin fraction V from bovine serum (BSA)	Carl Roth GmbH
ammonium persulfate (APS)	Carl Roth GmbH
bromphenol blue	SERVA
calcium chloride (CaCl ₂)	Merck KGaA
dimethylsulfoxid (DMSO)	Sigma Aldrich
dithiothreitol (DTT)	AppliChem GmbH
ethanol, absolute	Sigma Aldrich
ethylenediaminetetraacetic acid (EDTA)	Carl Roth GmbH
glycerol, 99,8 %	Carl Roth GmbH
glycine	Carl Roth GmbH
hydrochloric acid (HCl)	Carl Roth GmbH
isopropanol	Carl Roth GmbH
interferon- γ (IFN- γ ; human recombinant)	ImmunoTools
interleukin 4 (IL-4; human recombinant)	ImmunoTools
interleukin 13 (IL-13; human recombinant)	ImmunoTools
lipopolysaccharide (LPS) from <i>E.coli</i> O111:B4	Sigma Aldrich
magnesium chloride (MgCl ₂)	Merck KGaA
methylglyoxal (MGO), 40 % aqueous solution	Sigma Aldrich
non-fat milk powder	Carl Roth GmbH
paraformaldehyde (PFA)	Carl Roth GmbH
phenylmethylsulfonyl fluoride (PMSF)	Boehringer Mannheim
phorbol 12-myristate 13-acetate (PMA)	Sigma Aldrich
Ponceau-S	Carl Roth GmbH
potassium chloride (KCl)	Sigma Aldrich
sodium azide (NaN ₃)	SERVA
sodium chloride (NaCl)	Carl Roth GmbH
sodium dodecyl sulfate (SDS)	Carl Roth GmbH
sodium hydrogen phosphate (Na ₂ HPO ₄)	Carl Roth GmbH
sulfosalicylic acid (SSA)	Carl Roth GmbH
tetramethylethylenediamine (TEMED)	Carl Roth GmbH
trichloroacetic acid (TCA)	Carl Roth GmbH
thiazolyl blue tetrazolium bromide (MTT)	Sigma Aldrich
tris(hydroxymethyl)aminomethane (TRIS)	SERVA
Triton X-100	Carl Roth GmbH
Tween-20	Carl Roth GmbH
2',7'-dichlorodihydrofluorescein diacetate (H ₂ DCFDA)	Thermo Scientific

Cell culture reagents	
accutase cell detachment solution	PAN-Biotech
fetal calf serum (FCS)	Gibco / Thermo Scientific
Live Cell Imaging Solution (LCIS)	Thermo Scientific
Roswell Park Memorial Institute medium (RPMI 1640)	Gibco / Thermo Scientific
RPMI 1640 without phenol red	Gibco / Thermo Scientific
penicillin-streptomycin (P/S; 10,000 U/mL, 10,000 µg/mL)	Gibco / Thermo Scientific
β-mercaptoethanol	Gibco / Thermo Scientific
Composite reagents and kits	
Amersham ECL select	GE Healthcare
Amersham protran nitrocellulose membrane	GE Healthcare
APC annexin V apoptosis detection kit	Biologend
CBA Human IL-1β Flex Set	BD Biosciences
CBA Human IL-6 Flex Set	BD Biosciences
CBA Human IL-8 Flex Set	BD Biosciences
CBA Human IL-10 Flex Set	BD Biosciences
CBA Human TNF Flex Set	BD Biosciences
CBA Human Soluble Protein Master Buffer Kit	BD Biosciences
<i>ClearMount</i> [™] mounting solution	Thermo Scientific
oligo (dT) ₁₂₋₁₈	Thermo Scientific
PageRuler Plus prestained protein ladder	Thermo Scientific
pHrodo® Green E. coli BioParticles	Thermo Scientific
protease inhibitor cocktail (PIC)	Sigma Aldrich
<i>Pierce</i> BCA protein assay kit	Thermo Scientific
qPCR GreenMaster	Jena Bioscience
Quick-RNA MiniPrep kit	Zymo Research
RiboLock RNase inhibitor	Thermo Scientific
SuperScript II reverse transcriptase	Thermo Scientific
µMACS columns	Miltenyi Biotec
µMACS Protein G MicroBeads	Miltenyi Biotec
7-AAD viability staining solution	Biologend

2.1.2 Buffers and solutions

PBS (1 x) pH 7.4	PBS-EDTA pH 7.4	TBS buffer (1 x) pH 7.6
137 mM NaCl 2.7 mM KCl 10 mM Na ₂ HPO ₄ 1.8 mM KH ₂ PO ₄	137 mM NaCl 2.7 mM KCl 10 mM Na ₂ HPO ₄ 1.8 mM KH ₂ PO ₄ 0.25 % EDTA	137 mM NaCl 7.7 mM TRIS
TBS-T buffer (1 x) pH 7.6	blocking solution (IF)	blocking solution (PAGE)
137 mM NaCl 7.7 mM TRIS 0.05 % (v/v) Tween-20	0.3 % (v/v) FCS in TBS-T	5 % non-fat milk or 5 % BSA in TBS-T
fixation solution (Flow Cyt)	fixation solution (IF)	loading buffer (5 x, PAGE) pH 6.8
2 % PFA 0.1 % (v/v) Triton X-100 in PBS	4 % PFA in PBS	12.5 % (v/v) SDS 0.3 M TRIS 50 % (v/v) glycerol 50 mM DTT bromphenol blue
low-salt wash buffer (IP) pH 7.5	lysis buffer (PAGE) pH 7.5	Ponceau-S solution (PAGE)
20 mM TRIS	10 mM TRIS 150 mM NaCl 1 mM CaCl ₂ 1 mM MgCl ₂ 1 % (v/v) Triton X-100 0.2 % (v/v) PIC 1 mM PMSF	0.2 % Ponceau-S 3 % TCA 3 % SSA
running buffer (PAGE) pH 8.5	separating gel (PAGE) pH 8.8	stacking gel (PAGE) pH 6.8
25 mM TRIS 192 mM glycine 0.1 % (v/v) SDS	10 – 12 % acrylamide 377 mM TRIS 0.05 % (v/v) SDS 0.08 % APS 0.08 % (v/v) TEMED	4 % acrylamide 124 mM TRIS 0.05 % (v/v) SDS 0.04 % APS 0.1 % (v/v) TEMED
staining buffer (Flow Cyt) pH 7.4	transfer buffer (PAGE) pH 8.5	wash buffer (IF) pH 7.4
1 % (v/v) FCS 0.09 % NaN ₃ in PBS	20 mM TRIS 150 mM glycine 10 % (v/v) ethanol	0.1 % (v/v) Tween-20 in PBS

2.1.3 Equipment

Purpose	Model	Manufacturer
balances	MXX-2001 MC1	Denver instruments Sartorius
cell culture equipment	aura 2000 M.A.C. Countess™ Automated Cell Counter HeraCELL waterbath 1003	Bio Air Invitrogen Heraeus GFL
centrifuges	Biofuge fresco Biofuge pico Sprout Universal 320	Heraeus Heraeus Biozym Hettich
flow cytometer	BD Accuri™ C6 BD FACSVerser™	BD Biosciences BD Biosciences
microplate reader	Clariostar	BMG Labtech
microscopes	Axio Observer 7 Axiovert 100 Telaval 31	Carl Zeiss Carl Zeiss Carl Zeiss
mixing	heating magnetic stirrer FB15001 L29 Test-tube rotator minishaker MS2 MyLab SLRM-3 rocking platform RS-TR5 roll incubator	Thermo Scientific Labinco IKA NanoEnTek Biometra Phoenix instrument
PAGE equipment	Dual Cool DCX-700 mini-vertikal system EBX-700 universal heat sealer ES 300 Gel Doc XR+ system	C.B.S. Scientific C.B.S. Scientific GEHO Bio-Rad
PCR equipment	iQ5	Bio-Rad
pH meter	HI2210	HANNA instruments
power supply	Power Pac 300	Bio-Rad
spectrophotometer	NanoDrop 2000	Thermo Scientific

2.1.4 Oligonucleotides

Amplicon		Sequence (5' – 3')	Size [bp]	Source
IL-1 β	forward	GTGGCAATGAGGATGACTTGTTTC	124	(Chanput et al., 2010)
	reverse	TAGTGGTGGTTCGGAGATTCGTA		
IL-6	forward	AGCCACTCACCTCTTCAGAAC	118	(Chanput et al., 2010)
	reverse	GCCTCTTTGCTGCTTTCACAC		
IL-8	forward	CTGATTTCTGCAGCTCTGTG	98	(Chanput et al., 2010)
	reverse	GGGTGGAAAGTTTGGAGTATG		
IL-10	forward	GTGATGCCCAAGCTGAGA	138	(Chanput et al., 2010)
	reverse	CACGGCCTTGCTCTTGTTTT		
IL-12	forward	CACATTCCTACTTCTCCCTGAC	93	(Ali et al., 2015)
	reverse	CTGAGGTCTTGCCGTGAAG		
IL-23	forward	CGTCTCCTTCTCCGCTTCAA	65	(Lin et al., 2012)
	reverse	ACCCGGGCGGCTACAG		
RPL-32	forward	CAACATTGGTTATGGAAGCAACA	80	(Forero et al., 2013)
	reverse	TGACGTTGTGGACCAGGAACT		
TGF- β	forward	CTCTCCGACCTGCCACAGA	95	(Lin et al., 2012)
	reverse	AACCTAGATGGGCGCGATCT		
TNF- α	forward	CTGCTGCACTTTGGAGTGAT	93	(Chanput et al., 2010)
	reverse	AGATGATCTGACTGCCTGGG		

2.1.5 Antibodies and staining reagents

Primary reagent	Specificity	Company	Used in
anti-actin (AB-5)	mouse monoclonal IgG ₁ , clone C4/actin	BD Biosciences	WB 1:5,000
anti-AGE (CML26)	mouse monoclonal IgG ₁ , clone CML26	abcam	IF 1:100 WB 1:1,000
anti-caspase-1 (2225)	rabbit polyclonal	Cell Signalling	WV 1:1,000
anti-CD16 Alexa Fluor® 647	mouse monoclonal IgG _{1,κ}	BD Biosciences	Flow Cyt 1:20
anti-CD68 FITC	mouse monoclonal IgG _{2b,κ}	BD Biosciences	Flow Cyt 1:20
anti-CD163 Alexa Fluor® 647	mouse monoclonal IgG _{1,κ}	BD Biosciences	Flow Cyt 1:20
anti-CD209 FITC	mouse monoclonal IgG _{2b,κ}	BD Biosciences	Flow Cyt 1:5
anti-NF-κB p65	mouse monoclonal IgG _{2b,κ}	BD Biosciences	WB 1:1,000
anti-RAGE (ab3611)	rabbit polyclonal	abcam	Flow Cyt 1:25 WB 1:1,000
anti-TLR4 (25)	mouse monoclonal IgG ₁	Santa Cruz Biotechnology	WB 1:200 IP 4 μg
Hoechst H33258	10 mg/mL	Sigma-Aldrich	IF 1:2,000
IgG _{2b,κ} Isotype Control FITC	mouse monoclonal IgG _{2b,κ}	BD Biosciences	Flow Cyt 1:5
IgG _{1,κ} Isotype Control Alexa Fluor® 647	mouse monoclonal IgG _{1,κ}	BD Biosciences	Flow Cyt 1:20

Secondary reagent	Company	Used in
FITC goat anti-mouse IgG	Thermo Scientific	IF 1:50
FITC goat anti-rabbit IgG	Thermo Scientific	Flow Cyt 1:100
HRP goat anti-mouse IgG	abcam	WB 1:10,000
HRP goat anti-rabbit IgG	abcam	WB 1:20,000

2.1.6 Cells and culture media

Cell line	Description	Source
THP-1	human acute monocytic leukemia cell line (Tsuchiya et al., 1980) (abbreviation stands for Tohoku Hospital Pediatrics-1)	Dr. J. Lehmann Fraunhofer Institute for Cell Therapy and Immunology (Leipzig)

Medium		Supplements
culture medium	RPMI 1640	10 % (v/v) FCS 1 % P/S
freezing medium	-	90 % (v/v) FCS 10 % (v/v) DMSO
differentiation medium	RPMI 1640	10 % (v/v) FCS 1 % P/S 100 ng/mL PMA 50 μ M β -mercaptoethanol
polarization medium (M1 phenotype)	RPMI 1640	10 % (v/v) FCS 1 % P/S 100 ng/mL LPS 20 ng/mL IFN- γ
polarization medium (M2 phenotype)	RPMI 1640	10 % (v/v) FCS 1 % P/S 20 ng/mL IL-4 20 ng/mL IL-13

2.1.7 Software

Software	Company
Adobe Photoshop CS2	Adobe Systems
AxioVision Rel. 4.8.1	Carl Zeiss
BD Accuri C6 Analysis Software, version 1.0.264.21	BD Biosciences
Bio-Rad iQ5, version 2.0	Bio-Rad
Citavi 5, version 5.7.1.0.	Swiss Academic Software
FCAP Array™ Software	BD Biosciences
ImageJ, 1.52n	NIH
Image Lab, version 6.0.1	Bio-Rad
MARS Analysis Software, version 3.20 R2	BMG Labtech
Microsoft Office 2010 (Excel, PowerPoint, Word)	Microsoft
NanoDrop 2000c, version 1.6.198	Thermo Scientific
OriginPro 2018b	OriginLab
Quantity One, version 4.6.2	Bio-Rad

2.2 Methods

2.2.1 Cell culture methods

2.2.1.1 Cultivation of THP-1 cells

THP-1 monocytic cells were grown in suspension in culture medium (see 2.1.6) at approx. 5×10^5 cells/mL density at 37 °C and 5 % CO₂ in a humidified incubator. Cultures were maintained by replacement of medium or by centrifugation (160 g, 3 min) with subsequent resuspension in fresh culture medium every two to three days. Cells were discarded and replaced by frozen stocks after a maximum of 30 passages. Cell numbers were counted using *Countess™ Automated Cell Counter* (Invitrogen) according to manufacturer's instructions. Cell counting and viability measurements are performed using trypan blue staining technique. For longtime storage, 1×10^6 cells were re-suspended in 1 mL freezing medium in cryo vials and stored at -80 °C in an isopropanol filled freezing container for 24 h. Cells were transferred to -150 °C for long time storage periods.

2.2.1.2 Differentiation and polarization

THP-1 monocytes can be differentiated into macrophages. Defined numbers of cells (depending on the size of the culture dishes or plates) were centrifuged (160 g, 3 min), seeded in differentiation medium (see 2.1.6) and incubated for 48 h. The differentiated macrophages (M0 phenotype) are adherent and do not proliferate any more. The consumed differentiation medium was removed via aspiration and replaced with normal growth medium. For polarization in M1 or M2 phenotype, differentiated M0 macrophages were further incubated for 24 h with the respective polarization medium, depending on the desired phenotype. For harvesting, medium was removed via aspiration and cells were incubated with accutase cell detachment solution or PBS-EDTA for 30 min. Cell scrapers were carefully used for total detachment. Cells were then pelleted via centrifugation (160 g, 3 min).

2.2.1.3 Preparation of glycated FCS

FCS with or without addition of 1 mM MGO was incubated at 37 °C for 24 h. FCS was stored at -20 °C until use. FCS without MGO addition was used as a control in order to exclude effects of the incubation temperature. Glycated FCS is further stated to as AGE-FCS. Glycation of AGE-FCS was confirmed via dot blot with an anti-AGE antibody.

2.2.1.4 Stimulation of macrophages

Macrophages were treated with MGO in order to induce glycation of the cells or with AGE-FCS in order to see if soluble AGEs have an influence on the cells. Therefore, culture medium was supplemented with 10 % FCS or 10 % AGE-FCS as prepared under 2.2.1.3. M0 macrophages were either incubated in culture medium containing 1 mM MGO or in medium supplemented with 10 % AGE-FCS for 24 h. For some experiments, cells were analysed directly after this incubation step. For other experiments, cells were polarized into M1 or M2 phenotype afterwards.

2.2.1.5 Immunofluorescence staining

Immunofluorescence (IF) staining uses the specificity of antibodies to their antigens and visualizes their binding in the microscope with fluorescent dyes. 5×10^4 cells were directly seeded in differentiation medium into 8-well chamber slides. After treatment, cells were washed with 200 μ L PBS and fixed with 100 μ L prewarmed fixation solution for 15 min, washed again 3 times with 200 μ L wash buffer and blocked for 15 min with 200 μ L blocking buffer. After 3 washing steps with 200 μ L blocking buffer, cells were stained for 1 h with 100 μ L anti-AGE antibody in blocking solution. The previous washing step was repeated, followed by staining with 100 μ L FITC goat anti-mouse antibody and Hoechst staining in blocking solution for 30 min. Cells were washed 3 times with 200 μ L wash buffer and coverslips were applied using *ClearMount™ mounting solution*. Images were taken with a 20x objective.

2.2.1.6 Metabolic activity assay

The metabolic activity of cells can be measured using an MTT assay. This colorimetric assay is based on the reduction of the yellow, water-soluble dye MTT into a blue-violet, water insoluble formazan by NAD(P)H-dependent cellular enzymes. Macrophages were seeded into 96-well microtiter plates at a density of 5×10^4 cells per well. After treatment, cells were washed with 200 μ L PBS per well. MTT was diluted to a final concentration of 0.5 mg/mL in RPMI without phenol red and cells were incubated for 4 h with 100 μ L MTT solution per well. After removal of the MTT containing medium, remaining formazan crystals were dissolved in 150 μ L DMSO. Absorption values were measured at a wavelength of 570 nm (background 630 nm) in a microplate reader. Untreated control cells were then set to 100 % of metabolic activity and changes in metabolic activity of treated cells were calculated.

2.2.1.7 Intracellular ROS measurement

One of the most important biomarkers for oxidative stress is the intracellular level of ROS. Changes in the production of intracellular ROS can be demonstrated using the fluorescent probe 2',7'-dichlorodihydrofluorescein diacetate (H₂DCFDA; Royall and Ischiropoulos, 1993). H₂DCFDA is converted into a membrane permeable derivative by cellular esterases and gets oxidized into the highly fluorescent 2',7'-dichlorofluorescein in presence of intracellular ROS. For ROS measurement, macrophages were used at a density of 1×10^5 cells per well in 96-well microtiter plates. Cells were loaded with 100 μ L H₂DCFDA (diluted to 10 μ M in PBS) and incubated for 10 min. H₂DCFDA was removed and replaced by 100 μ L culture medium. Basic fluorescence intensity was measured in a plate reader at 495 nm excitation and 525 nm emission. Medium was removed and different treatments in culture medium were applied (100 μ L / well). Different concentrations of H₂O₂ were used as positive controls for ROS induction. Fluorescence intensity was measured as mentioned above after 10, 20, 30 and 60 min of incubation.

2.2.1.8 Flow cytometry

Flow cytometry is a laser-based technology for the analysis cells or particles based on their structure, size or special labels. Cells in suspension are scanned by a laser beam in a single cell stream of fluid. The scattered light is characteristic for the size and morphology of the analysed cells. For further specification or separation of populations, labelling of the cells with special dyes or fluorescent-labelled antibodies can be used.

2.2.1.8.1 Phagocytosis assay

Phagocytosis of pathogens or cell debris is one of the most important functions of macrophages. Particles are engulfed by the macrophages and incorporated into phagosomes, which then fuse with lysosomes in order to destroy and digest the particles. For analysis of the phagocytic efficiency, macrophages were used at a density of 1×10^5 cells per well in 96-well microtiter plates. Macrophages were washed twice with 200 μ L PBS after stimulation and polarization, followed by incubation with 100 μ L *pHrodo*[™] *Green E. coli BioParticles*[™] solution (diluted to 60 μ g/mL) for 1 h. This special dye is non-fluorescent outside the cell at neutral pH, but fluoresces brightly green at acidic pH, such as in phagosomes. After removal of the *E. coli BioParticles*, cells were incubated with 150 μ L accutase for 30 min and harvested. Five wells per sample were united and centrifuged. Cell pellets were then re-suspended in 200 μ L LCIS. Analysis of 10,000 cells per sample was done in the flow cytometer using the FL-1 channel (excitation 488 nm, 530 / 30 nm band pass filter). Non-glycated cells without *E.coli* addition (incubated in LCIS) were used for gating. Phagocytosis rate of non-glycated control cells was set to 100 % and percentage change of phagocytosis was calculated for treated cells.

2.2.1.8.2 Apoptosis assay

For the analysis of early apoptosis, allophycocyanin (APC) *annexin V apoptosis detection kit* in combination with 7-aminoactinomycin (7-AAD) staining was used. Annexin V is a marker for early apoptosis and in this assay coupled to the fluorescent dye APC, while 7-AAD only stains cells with compromised membranes, indicating dead cells. Staining was done according to the manufacturer's protocol. Approximately

0.5 x 10⁶ cells were harvested with accutase, resuspended in 200 µL annexin binding buffer (kit component) and stained with 3 µL APC annexin V and 5 µL 7-AAD for 15 min in the dark. As staining controls, cells were kept on ice, then inactivated via heat shock (75 °C, 5 min) and stained with either APC annexin V or 7-AAD or both. Analysis of 10,000 cells per sample was done in the flow cytometer, APC annexin V was measured in the FL-4 channel (excitation 633 nm, 675 / 25 nm band pass filter) and 7-AAD was measured in the FL-3 channel (excitation 488 nm, 670 nm long pass filter). Unstained control cells were used for gating. In order to determine the number of intact living cells (non-apoptotic and non-necrotic), the percentage of annexin V⁻ / 7-AAD⁻ cells was used.

2.2.1.8.3 Cell surface staining for polarization

For staining of marker proteins on the cell surface, specific antibodies labelled with fluorophores were used. In this case, special surface proteins were analysed in order to verify the polarization phenotype of macrophages. As a general marker for differentiated macrophages, an antibody against CD16 labelled with Alexa Fluor® 647 was used. M1 phenotype was verified via staining with an anti-CD68 antibody labelled with fluorescein isothiocyanate (FITC). For M2 phenotype, staining with an anti-CD209 antibody labelled with FITC and an anti-CD163 antibody labelled with Alexa Fluor® 647 were used. Approximately 0.5 x 10⁶ cells per sample were harvested with PBS-EDTA, centrifuged and washed with PBS. Cells were fixed with 200 µL fixation solution for 15 min at 4 °C. After washing with 500 µL staining buffer, cells were incubated with the respective antibodies or IgG isotype controls diluted in staining buffer for 2 h at 4 °C. Cells were centrifuged and washed with 500 µL staining buffer. Cells were finally re-suspended in 200 µL staining buffer and kept on ice. Analysis of 10,000 cells per sample was done in the flow cytometer, Alexa Fluor® 647 was measured in the FL-4 channel (excitation 633 nm, 675 / 25 nm band pass filter) and FITC was measured in the FL-1 channel (excitation 488 nm, 530 / 30 nm band pass filter). Unstained control cells were used for gating.

2.2.1.8.4 Analysis of RAGE expression via flow cytometry

For the analysis of RAGE expression, 1×10^6 cells per sample were harvested with PBS-EDA centrifuged and washed with PBS. Cells were fixed with 200 μ L fixation solution for 15 min at 4 °C. After washing with 1 mL staining buffer, cells were incubated with anti-RAGE antibody (ab3611) diluted in staining buffer for 1 h at 4 °C. After washing with 1 mL staining buffer, cells were incubated with FITC-labelled secondary antibody for 30 min at 4 °C. Cells were washed with 1 mL staining buffer and finally re-suspended in 200 μ L staining buffer. Analysis of 10,000 cells per sample was done in the flow cytometer, measured in the FL-1 channel (excitation 488 nm, 530 / 30 nm band pass filter). Unstained control cells were used for gating. Count of FITC⁺ cells and mean FITC intensities were analysed.

2.2.1.9 Preparation of cell lysates

Cell lysates had to be prepared for protein analysis. Two different methods were used for cell lysis. Cells were harvested with accutase and cell pellets were re-suspended in lysis buffer for immunoblotting and immunoprecipitation (IP). Cell suspension was homogenized by hydrodynamic shearing and rotated at low speed for at least 1 h at 4 °C. Supernatant with isolated proteins was collected after centrifugation (16,000 g, 10 min at 4 °C). For some immunoblots, cells were directly lysed in hot 2.5 x loading buffer (preheated at 95 °C) and centrifuged (16,000 g, 3 min) directly before use in order to pellet cell debris.

2.2.2 DNA analysis techniques

2.2.2.1 Total RNA isolation

Total RNA was isolated from cell pellets using *Quick-RNA™ MiniPrep* kit according to the manufacturer's protocol. This kit uses a column-based method consisting of two columns in combination with a unique buffer system including DNase I treatment in order to isolate high concentrated and DNA-free RNA. Elution of RNA was performed in 50 μ L *DNase/RNase-free water* (kit component). RNA purity and concentration was

analysed spectrophotometrically by measuring absorption at 230, 260 and 280 nm using *NanoDrop 2000*.

2.2.2.2 cDNA synthesis & quantitative real-time PCR

Complementary DNA (cDNA) was synthesized from total RNA via reverse transcription as template for analysis of gene expression in quantitative real-time PCR (qPCR). 2 µg total RNA was translated into cDNA using *SuperScript II reverse transcriptase* kit with oligo (dT)₁₂₋₁₈ as primer according to the manufacturer's instruction. For qPCR reaction, *qPCR GreenMaster* was used according to the manufacturer's instruction and composed in the following way:

1 µL	cDNA
10 µL	<i>qPCR GreenMaster</i>
1 µL	primer forward (10 pmol/µL)
1 µL	primer reverse (10 pmol/µL)
7 µL	PCR-grade H ₂ O (kit component)
<hr/>	
20 µL	total volume

Measurements were always performed in triplicates. The amount of amplified DNA was correlated with the fluorescence intensity of the *GreenMaster* and was given as CT value. Ribosomal protein L32 (RPL32) was used as reference (housekeeping gene) in order to normalize gene expression of target genes. The setup was performed as follows:

Step	Cycles	Temperature	Time
initial denaturation	1	95 °C	90 s
denaturation		95 °C	10 s
primer annealing	40	58 °C	10 s
elongation		72 °C	25 s
final elongation	1	72 °C	60 s

To validate the specificity of the PCR reaction, melt curves were generated. Temperature was increased in 1 °C steps from 55 °C to 95 °C and melt curve was recorded. $\Delta\Delta C_t$ method was used for data analysis and calculation of relative gene

expression levels (Livak and Schmittgen, 2001). Values of genes of interest were first subtracted from the values of RPL32 (ΔCt). Relative gene expression was then calculated as $2^{-(\Delta\text{Ct treated} - \Delta\text{Ct untreated})}$.

2.2.3 Protein analysis techniques

2.2.3.1 Determination of protein concentration

Protein concentrations were measured with the bicinchoninic acid (BCA) method (Smith et al., 1985). A *Pierce BCA protein assay* was performed in microplates according to the manufacturer's protocol. Absorption spectra of samples and a BSA standard curve ranging from 0 mg/mL to 1.5 mg/mL were measured at 562 nm. Concentrations were determined using quadratic equation of the standard curve. Samples were always measured in duplicates.

2.2.3.2 Immunoprecipitation

In order to analyse a special protein out of a protein solution (e.g. a cell lysate), antibody mediated immunoprecipitation (IP) was performed (Firestone and Winguth, 1990). In this work, 5 mg of cell lysate (in lysis buffer) was processed with 4 μL anti-TLR4 antibody and 75 μL *$\mu\text{MACS Protein G MicroBeads}$* , according to the manufacturer's protocol using appropriate *$\mu\text{MACS columns}$* . Final elution of precipitated protein was done using 50 μL preheated 1 x loading buffer (95 °C). Input (= cell lysate) and flow through were collected and stored.

2.2.3.3 SDS-PAGE

SDS polyacrylamide gel electrophoresis (SDS-PAGE) was used to separate proteins according to their molecular mass and charge under reducing and denaturing conditions (Laemmli, 1970). Separating and stacking gels were prepared as listed above. Equal amount of proteins (20 – 50 μg) from cell lysates were premixed with 5 x loading buffer so that finally loaded samples had a concentration of 1 x loading buffer. For samples that were directly lysed with 2.5 x loading buffer, equal volumes of

cell lysates (15 -20 μ L) were loaded. All samples were heated to 95 °C for 5 min before loading onto the gels. In order to determine the size of the separated proteins, *PageRuler Plus prestained protein ladder* was used as protein standard. Electrophoresis was performed at 120 – 150 V for 1 – 2 h in running buffer, depending on the size of protein of interest. After separation, SDS gels were used for immunoblotting.

2.2.3.4 Immunoblotting

Proteins separated by SDS-PAGE can be transferred to nitrocellulose membranes using immunoblotting (Harlow and Lane, 1988). By transferring the proteins to the membrane, they are immobilized at their specific position due to their size and charge properties after the electrophoresis. Proteins can then be visualized using specific antibodies. In this work, wet transfer technique was used, where the membrane and the gel are fully immersed in transfer buffer and a current is directed from the gel to the membrane. Transfer was carried out with 100 V for 1 h under cooling and recirculating conditions in the tank. Efficiency of protein transfer and equal loading of samples was verified via staining with reversible Ponceau S dye. Membrane blocking was followed for 1 h at room temperature in blocking solution. The blocking agent was selected according to recommendations of antibody manufacturers. After blocking, membranes were washed (3 x 10 min in TBS-T) and primary antibodies (diluted in TBS-T or blocking solution, according to the recommendations of antibody manufacturers) were incubated overnight at 4 °C. After another washing step (3 x 10 min in TBS-T), HRP-labelled secondary antibodies (diluted in TBS-T) were incubated for 1 h at room temperature. After a final washing step (3 x 10 min in TBS-T), proteins of interest were detected by addition of *Amersham ECL select* HRP substrate according to the manufacturer's instructions. Blots were visualized after exposure for 1 to 120 s.

2.2.3.5 Dot blot analysis

The dot blot analysis describes a simplified version of immunoblotting. The analysed proteins are spotted directly onto a dry nitrocellulose membrane. In this work, dot blot analysis was used to verify glycation of self-produced AGE-FCS (see 2.2.1.3). Therefore, 5 μ L of control FCS and AGE-FCS from each produced lot were spotted onto the membrane. After drying, membrane was further processed according to the immunoblot procedure, starting with the blocking step.

2.2.3.6 Cytokine quantification

Cytokine quantification was done using a multiplexed assay called cytometric bead array (CBA) assay (Morgan et al., 2004). Cell supernatants were collected 24 h post polarization and cytokine quantification was performed by *CBA Flex* detecting simultaneously IL-1 β , IL-6, IL-8, IL-10 and TNF- α according to the manufacturer's recommendation. For the detection of IL-8, samples were diluted 1:500; all other samples were not diluted. Samples were analysed by flow cytometry. Cytokine concentrations were calculated according to internal standard curves.

2.2.4 Statistical analysis

All data analyses and visualizations were performed using OriginPro 2018b software. Paired student t-test against the control group or a theoretical value of 1 (due to data normalization) was used (Student, 1908). Figures show the average mean + standard deviation (SD) and levels of significance are depicted as symbols within the figures with * $p \leq 0.05$, ** $p \leq 0.01$ and *** $p \leq 0.001$.

3 Results

3.1 Glycation of macrophages

MGO, a side product of glycolysis, is a potent glycating agent that occurs naturally in human cells. During disease development, especially in untreated diabetes patients, increased MGO concentrations can be observed and indicate a higher incidence for glycation events. In this work, MGO treatment was used in order to induce glycation of macrophages. Due to its membrane permeability, MGO is able to induce intra- and extracellular glycation.

THP-1 macrophages were incubated with different MGO concentrations (0.5 mM, 1 mM or 1.5 mM) for 24 h. Cells cultivated in normal culture medium were used as a control (Ctrl). Cells were harvested, lysed and isolated proteins were separated by SDS-PAGE. Glycation of proteins was detected by immunoblotting with an anti-AGE antibody (CML26). This antibody was originally raised against CML-modifications, but is generally able to detect several AGE-modifications (shown previously by Benmann et al., 2014). Actin served as a loading control for equal loading of the samples. In figure 9, a representative immunoblot of four independent experiments is depicted. Protein glycation could be detected for all protein samples, including the control lane, resulting in broad smear bands. Due to glucose in the culture medium, also control cells are slightly glycated over time in culture. Incubation of macrophages with MGO led to elevated glycation signals, whereas increasing MGO concentrations led to increased band intensities. This gives evidence that MGO treatment induces glycation in macrophages.

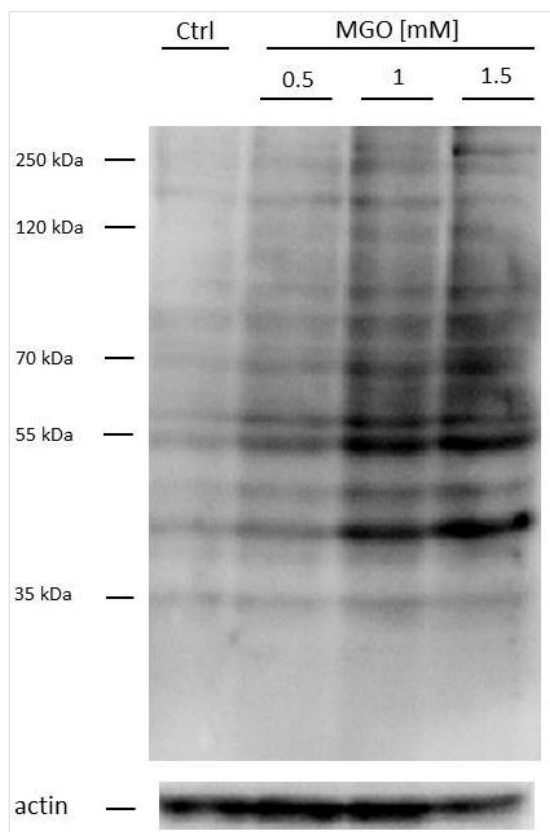


Figure 9: Immunoblot of glycated THP-1 macrophages.

THP-1 macrophages were incubated with 0.5, 1 or 1.5 mM MGO for 24 h in culture medium. Cells incubated without MGO supplementation were used as control (Ctrl). Cells were harvested and 30 μ g of each protein sample were separated by SDS-PAGE and immunoblotted using an anti-AGE antibody (CML26). Second staining with an anti-actin antibody was used as loading control. The depicted immunoblot represents four independent experiments.

In order to visualize extracellular glycation of cell surface proteins after treatment with MGO, IF staining with an anti-AGE antibody (CML26) was performed. Macrophages were incubated with 1 mM MGO for 24 h in culture medium and IF staining was performed without permeabilization of the cell membranes. Cells without MGO treatment were used as control cells (Ctrl). Figure 10 shows representative IF micrographs of four independent experiments. For nuclear staining, Hoechst was used (shown in blue). Staining with anti-AGE antibody is shown in orange. Macrophages treated with 1 mM MGO displayed a stronger AGE-dependent fluorescence signal on their surface, indicating glycation of cell surface proteins.

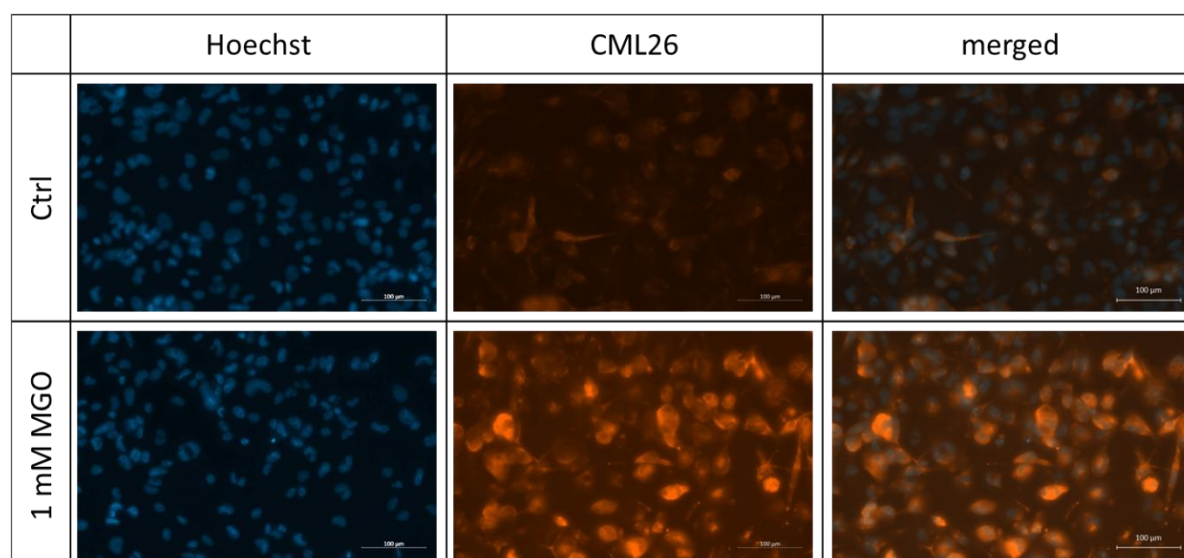


Figure 10: IF staining of surface glycation of THP-1 macrophages.

THP-1 macrophages were treated with 1 mM MGO for 24 h in culture medium (lower row). Cells cultivated without MGO addition served as control (Ctrl; upper row). IF staining of surface glycation was performed using an anti-AGE antibody (CML26; shown in orange). Hoechst was used as nuclear stain (shown in blue). Depicted micrographs are representative for four independent experiments. Scale bars indicate 100 μm .

3.1.1 Consequences of MGO treatment

Although MGO is a naturally occurring by-product of glycolysis, higher concentrations of this metabolite can be highly cytotoxic (Du et al., 2000). Therefore it is important to perform a titration of MGO for every cell type, in order to determine which concentrations are non-toxic.

Changes in cell morphology after MGO treatment were analysed by incubation of THP-1 macrophages with different MGO concentrations (0.5 mM, 1 mM or 1.5 mM). Cells cultivated in normal culture medium were used as a control (Ctrl). After 24 h, the appearance of the cells was investigated by bright-field microscopy (figure 11). Morphological changes could not be detected after treatment with any of the MGO concentrations.

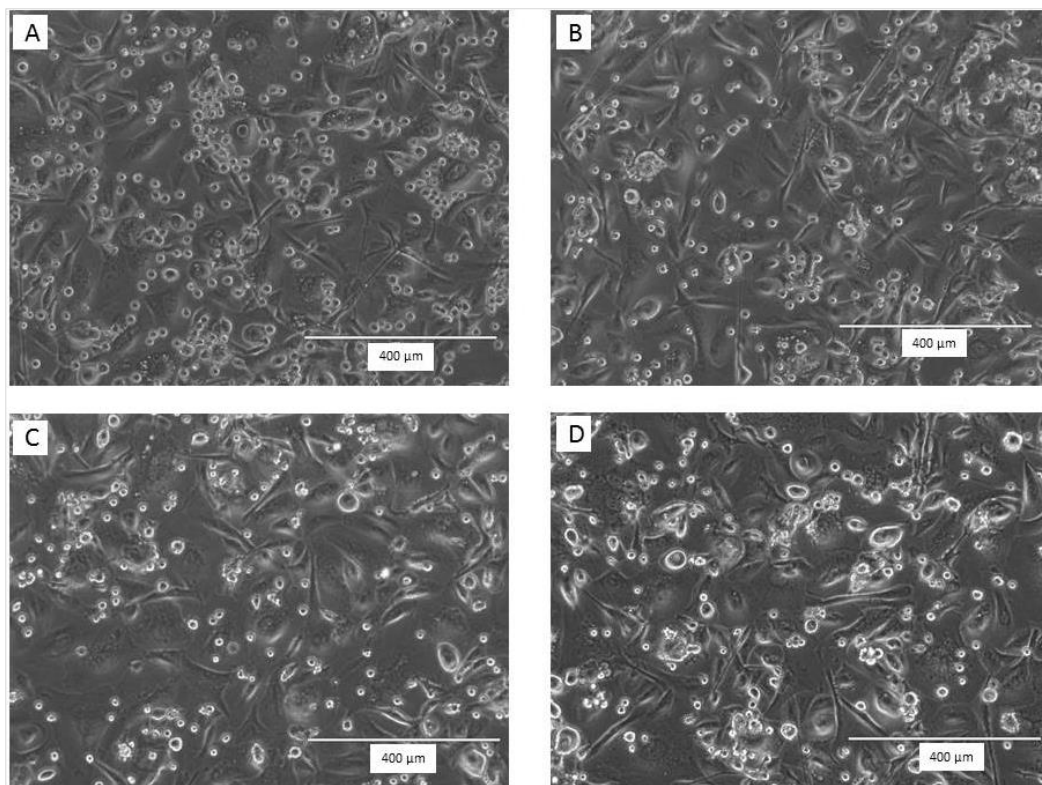


Figure 11: Micrographs of THP-1 macrophages after MGO incubation.

Bright field microscopy of THP-1 macrophages was done after incubation with different MGO concentrations for 24 h in culture medium. A) control; B) 0.5 mM; C) 1 mM; D) 1.5 mM. Scale bar indicates 400 μm . Representative micrographs of three different experiments.

3.1.1.1 Metabolic activity of macrophages after glycation

In order to analyse, whether MGO has an effect on the metabolic activity of macrophages, an MTT assay was performed. Cells were treated with 0.5 mM, 1 mM, 1.5 mM and 2 mM MGO for 24 h in culture medium. Cells cultivated without MGO addition served as a control (Ctrl) and were set to 100 % of metabolic viability. Treatment with 0.5 mM and 1 mM MGO did not lead to a significant reduction of metabolic activity (figure 12), while 1.5 mM and 2 mM MGO reduced metabolic activity by more than half.

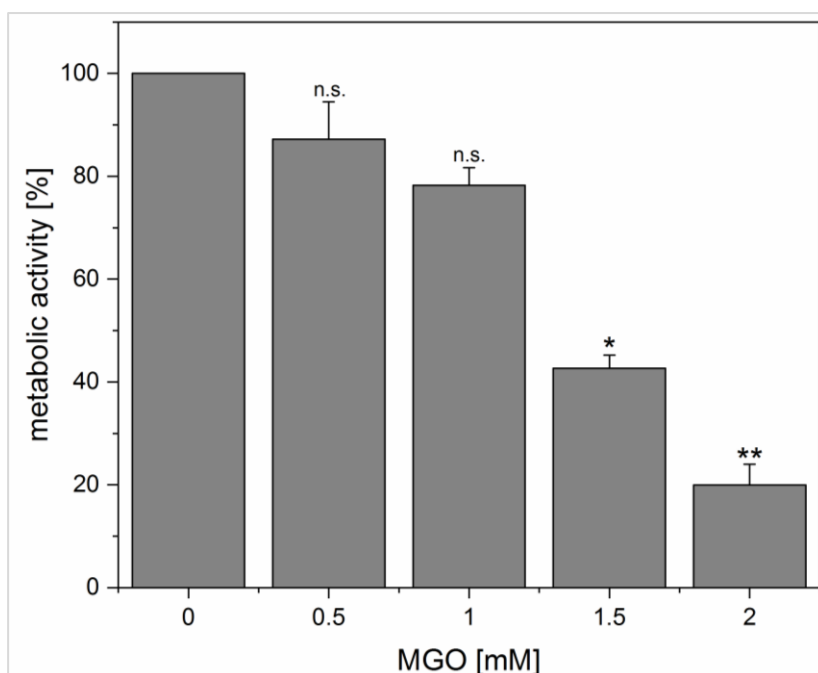


Figure 12: Metabolic activity of THP-1 macrophages after glycation.

THP-1 macrophages were treated with different concentrations of MGO for 24 h in culture medium and MTT assay was performed. Cells without MGO treatment (0 mM) were set to 100 % of metabolic activity. Data represents the mean of metabolic activity + SD of four independent experiments (* $p \leq 0.05$, ** $p \leq 0.01$).

3.1.1.2 Cell viability of macrophages after glycation

In order to determine the cell viability after MGO treatment, staining with annexin V for early apoptosis and 7-AAD for necrotic cells was performed. Cells that are stained annexin V⁺ / 7-AAD⁻ are classified as early apoptotic, cells stained annexin V⁺ / 7-AAD⁺ are dead cells and cells stained annexin V⁻ / 7-AAD⁻ mark the non-apoptotic and non-necrotic, living, intact cells. Macrophages were treated with different concentrations of MGO for 24 h in culture medium and apoptosis assay was performed. The percentage of annexin V⁻ / 7-AAD⁻ cells was used to determine the intact living cells (figure 13 A). Treatment with MGO up to 1 mM did not induce apoptosis, while 1.5 mM and 2 mM clearly reduced the percentage of living cells, indicating apoptosis and also cell death. Figure 13 B shows exemplary graphs of flow cytometric analysis for 0 mM, 0.5 mM and 2 mM MGO treatment. For 0.5 mM MGO, no differences can be seen compared to the control (0 mM). For 2 mM MGO, a clear shift of cell populations can be observed towards early apoptotic (annexin V⁺ / 7-AAD⁻, Q1-UL) and dead (annexin V⁺ / 7-AAD⁺, Q1-UR) cells.

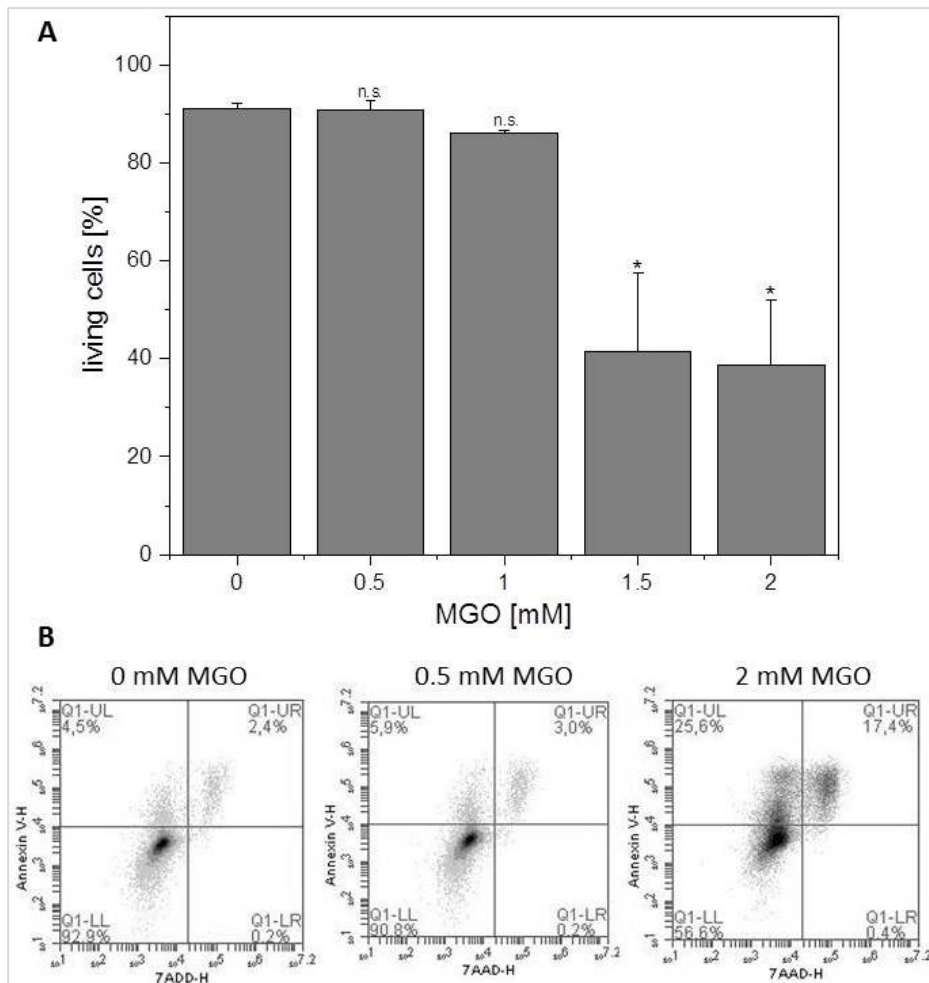


Figure 13: Cell viability of THP-1 macrophages after glycation.

THP-1 macrophages were treated with different MGO concentrations for 24 h and apoptosis assay was performed using staining with annexin V and 7-AAD.

A) The percentage of annexin V⁻ / 7-AAD⁻ cells was used to determine the intact living cells (= non-apoptotic and non-necrotic). Graph showing mean + SD of three independent experiments. (* $p \leq 0.05$)

B) Exemplary graphs of flow cytometric analyses for 0 mM, 0.5 mM and 2.0 mM MGO stained with annexin V (y-axis) and 7-AAD (x-axis). Q1-LL: living cells, Q1-UL: early apoptotic cells, Q1-UR: dead cells.

To summarise, both analysis of metabolic activity and cell viability indicate that concentrations above 1 mM MGO harm THP-1 macrophages. Therefore, 1 mM MGO should be the maximum concentration used on macrophages and is used thereafter for the induction of glycation in this experimental setup.

3.1.2 Comparison between glycation of cellular proteins and treatment with AGE-modified proteins

Glycation of THP-1 macrophages is induced by addition of MGO to the culture medium. By default, the culture medium contains 10 % FCS. Therefore, it is necessary to distinguish between effects of actual cell glycation and effects of glycated serum proteins in the medium, which could bind to receptors for AGEs and induce downstream receptor signalling. Hence, one group of cells in the experimental setup was always incubated with culture medium containing 10 % AGE-FCS, instead of the standard FCS, as a specific control. By comparing glycated cells (treated with MGO) and cells treated with AGE-FCS, the observed effects could be associated with cell glycation or activation of AGE-specific receptors. AGE-FCS was prepared as described (see 2.2.1.3) and glycation of every lot of AGE-FCS was confirmed by dot blot analysis with an anti-AGE antibody (CML26). In figure 14, one representative dot blot is shown. As a control, FCS incubated under the same conditions as AGE-FCS but without addition of MGO was used. 5 μ L per sample were spotted and staining with Ponceau S was used as a control for equal loading. AGE-FCS showed a strong signal using the anti-AGE antibody, while control FCS did not show any signal, confirming that AGE-FCS is glycated.

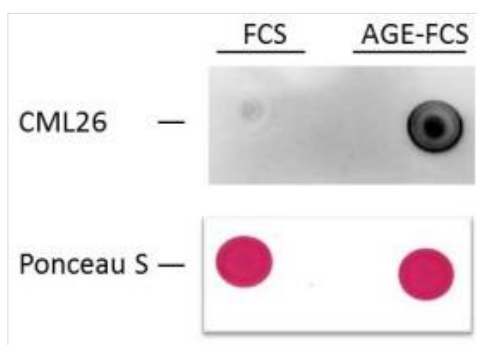


Figure 14: Dot blot analysis of AGE-FCS

Glycation of AGE-FCS was verified via dot blot analysis using an anti-AGE antibody (CML26). As a control, FCS incubated under the same conditions as AGE-FCS was used. 5 μ L per sample were spotted. Depicted blot is representative for different independent experiments.

To demonstrate that AGE-FCS has no influence on cell viability, treatment with 10 % AGE-FCS was also tested in apoptosis assays, equal to the experiments shown under chapter 3.1.1.2. There was no significant reduction of percentage of living cells (89.7 ± 2.5 %, mean \pm SD; $p = 0.337$) visible after treatment with AGE-FCS for 24 h, indicating that AGE-FCS did not interfere with cell viability.

3.1.3 Glycation does not interfere with ROS production

It has been described that glycation and AGE-signalling can increase intracellular ROS levels in some cell types. To clarify whether glycation using MGO or the treatment with AGE-FCS induce production of intracellular ROS, the fluorescent probe H₂DCFDA was used. Cells were labelled with H₂DCFDA and fluorescence intensity was measured after 10, 20, 30 and 60 min of incubation. Figure 15 shows one representative graph of three independent ROS measurements. Increasing concentrations of H₂O₂ (50, 100 and 150 μ M) were used as positive controls for ROS induction. Glycation with 0.5, 1 or 1.5 mM MGO as well as treatment with 10 % AGE-FCS did not increase intracellular ROS production compared to the untreated control (Ctrl). However, treatment with H₂O₂ raised cellular ROS levels time and concentration dependent.

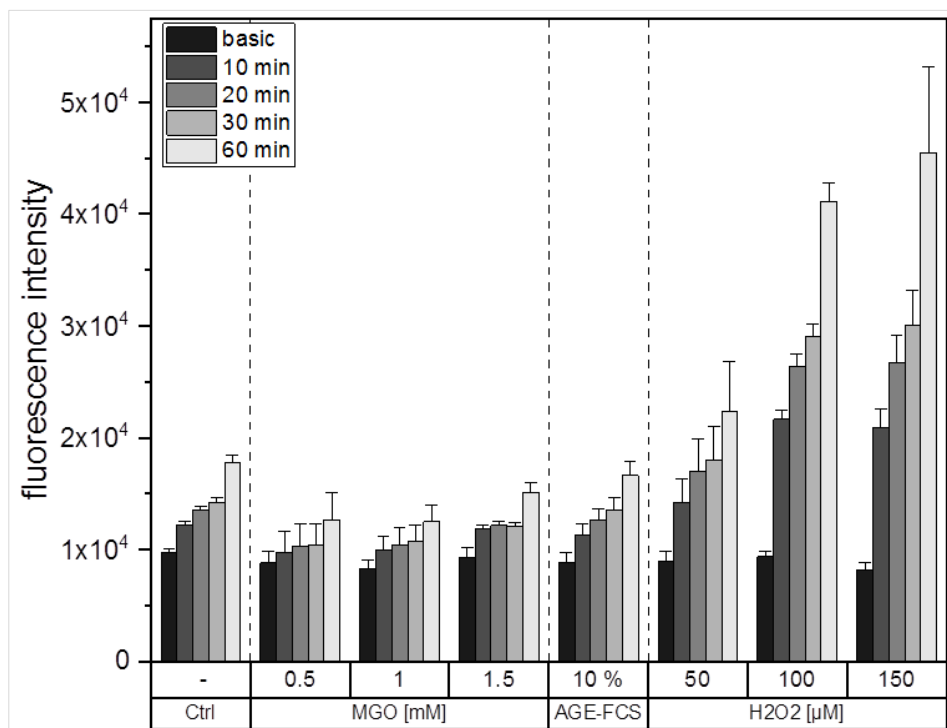


Figure 15: Intracellular ROS production after glycation.

THP-1 macrophages were treated with different MGO concentrations, 10 % AGE-FCS or different concentrations of H₂O₂ for up to 60 min. Production of intracellular ROS was determined using fluorescent probe H₂DCFDA and measurement of fluorescence intensity. The figure shows one representative graph of three independent measurements. Data represents mean + SD of five technical replicates.

3.2 Glycation and RAGE activation

RAGE is expressed on cells of the innate immune system (Kierdorf and Fritz, 2013). Macrophages are known to express RAGE on their surface, similar to blood monocytes (Neeper et al., 1992). RAGE activation finally results in activation of NF- κ B, which dislocates into the nucleus and among others stimulates expression of itself as well as expression of RAGE (Bierhaus et al., 2005). Therefore, expression of RAGE and NF- κ B after glycation or treatment with soluble AGE-FCS were analysed hereafter.

3.2.1 RAGE expression after glycation

Protein expression of RAGE was analysed for THP-1 macrophages after glycation and treatment with AGE-FCS. THP-1 macrophages were incubated with either 1 mM MGO or 10 % AGE-FCS for 24 h. After harvesting, the cells were lysed and proteins were separated by SDS-PAGE. RAGE protein expression was detected by immunoblotting with an anti-RAGE antibody (ab3611). Figure 16 A depicts one representative immunoblot, the RAGE signal can be detected as two bands at approx. 45 kDa (glycosylated and non-glycosylated form), while the band at 25 kDa shows likely a proteolytic degradation product of RAGE. Four immunoblots of RAGE protein expression were quantified in relation to actin expression against the control cells (Figure 16 B). After glycation with MGO, a slight but not significant increase of RAGE protein expression was observed. In contrast, treatment with AGE-FCS markedly increased RAGE protein expression, a more than two-fold increase compared to the control cells.

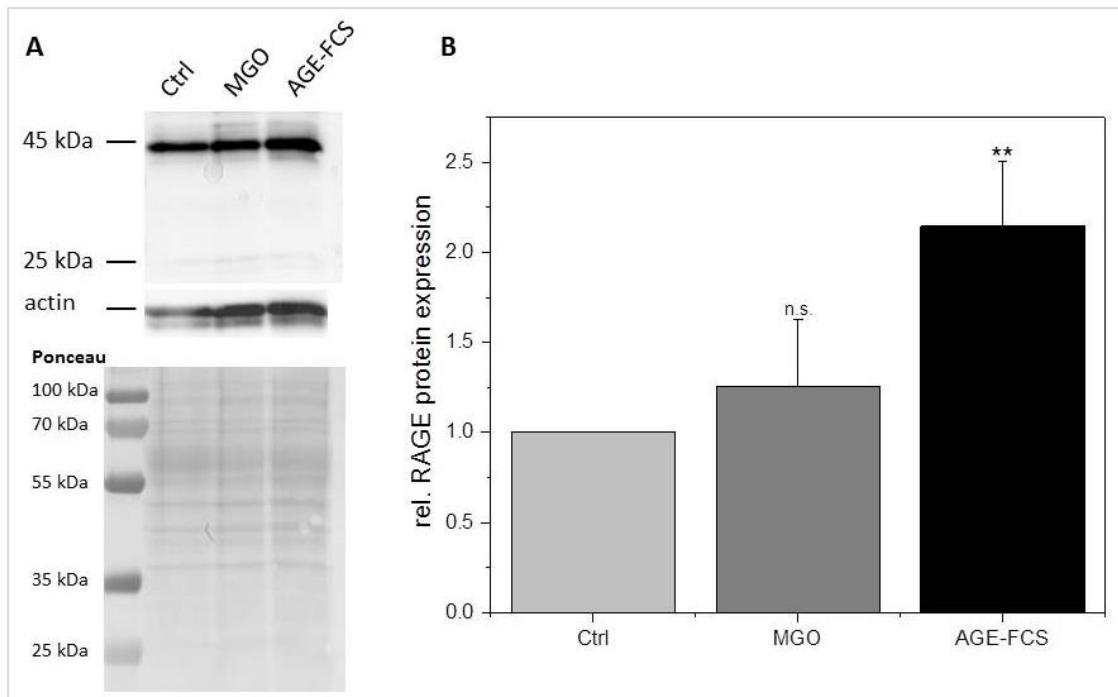


Figure 16: RAGE protein expression after glycation.

THP-1 macrophages were incubated with 1 mM MGO or 10 % AGE-FCS for 24 h. Total protein was separated by SDS-PAGE and immunoblotting. RAGE protein expression was detected using an anti-RAGE antibody (ab3611) and quantified.

A) Representative RAGE immunoblot with Ponceau S staining shown, glycosylated and non-glycosylated form at approx. 45 kDa, proteolytic degradation product at approx. 25 kDa. Second staining with anti-actin antibody was used as loading control.

B) Graph showing mean of relative RAGE protein expression + SD of four independent immunoblots. RAGE signal was quantified related to corresponding actin signal and RAGE expression of untreated control cells (Ctrl) was set to 1. (** $p \leq 0.01$)

To verify these findings, RAGE expression was also analysed using flow cytometry. THP-1 macrophages were incubated with either 1 mM MGO or 10 % AGE-FCS for 24 h, harvested and stained with an anti-RAGE antibody (ab3611). After staining with a secondary FITC-labelled antibody, cells could be analysed using flow cytometry. Figure 17 A shows a representative histogram of the RAGE-positive cells (FITC-positive stained), while figure 17 B shows the mean fluorescence intensity of RAGE-positive stained cells of three different experiments. As already shown by immunoblotting, treatment with AGE-FCS increased the expression of RAGE on macrophages compared to the untreated control cells (Ctrl), whereas glycation with MGO did not have any effect.

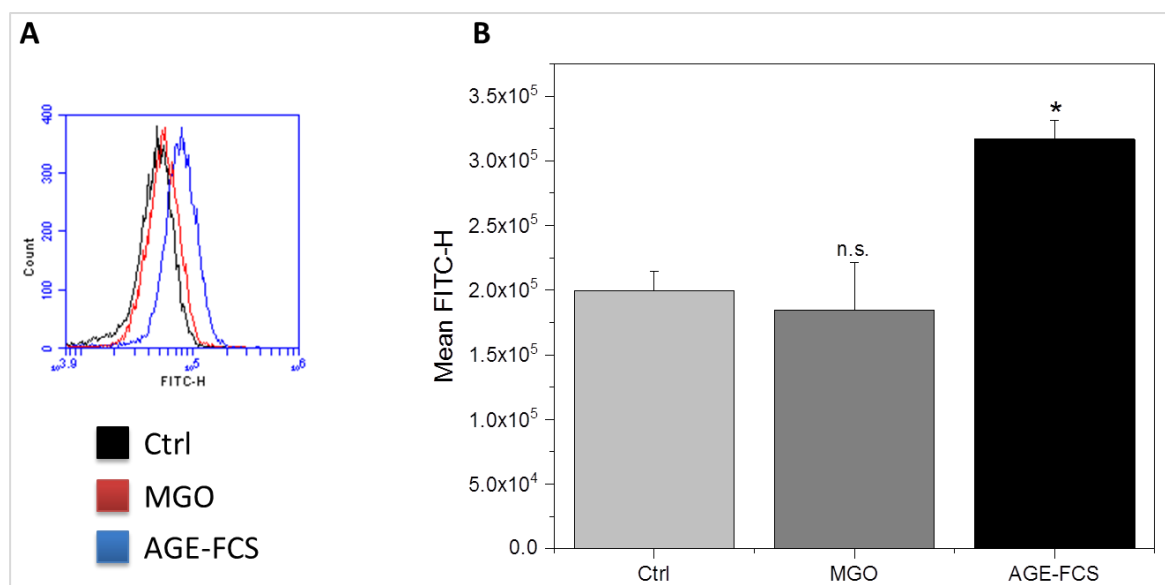


Figure 17: Detection of RAGE after glycation via flow cytometry.

THP-1 macrophages were incubated with 1 mM MGO or 10 % AGE-FCS for 24 h. Living cells were harvested and stained with an anti-RAGE antibody (ab3611) and secondary FITC labelled antibody and analysed using flow cytometry. **A)** Representative histogram of analysed FITC positive cells. **B)** Graph of mean fluorescence intensity of stained macrophages, data represents mean + SD of three independent experiments. (* $p \leq 0.05$)

3.2.2 Analysis of NF- κ B expression after glycation

Protein expression of NF- κ B p65 was analysed after glycation and treatment with AGE-FCS in order to demonstrate induction of NF- κ B expression. THP-1 macrophages were incubated with 1 mM MGO or 10 % AGE-FCS for 24 h. Cells were lysed and proteins were separated by SDS-PAGE. NF- κ B protein expression was detected by immunoblotting with an anti- NF- κ B p65 antibody. As the name indicates, the NF- κ B variant can be detected at approx. 65 kDa. Three immunoblots of NF- κ B protein expression were quantified in relation to actin expression against the control cells (Figure 18 B). After glycation with MGO, no significant induction of NF- κ B protein expression can be detected. By contrast, treatment with AGE-FCS led to a significant overexpression of NF- κ B protein, indicating that binding von AGE-FCS to RAGE induces NF- κ B signal cascade.

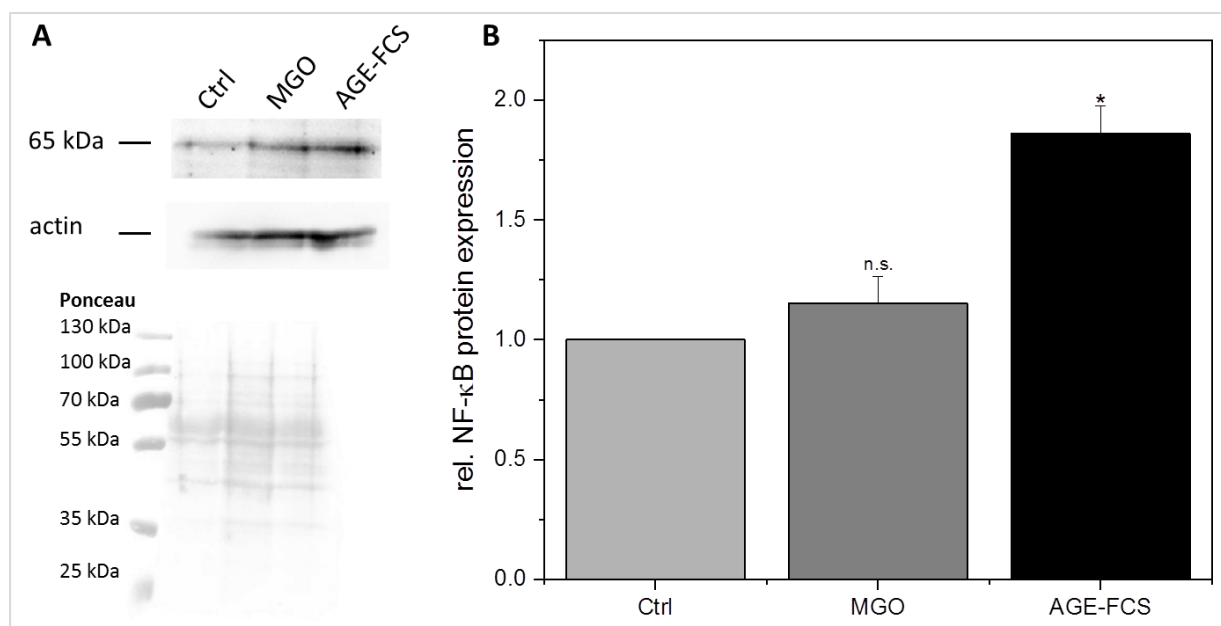


Figure 18: NF-κB protein expression after glycation

THP-1 macrophages were incubated with 1 mM MGO or 10 % AGE-FCS for 24 h. Total protein was separated by SDS-PAGE and immunoblotting. NF-κB protein expression was detected using an anti- NF-κB p65 antibody and quantified.

A) Representative NF-κB immunoblot with Ponceau S staining is depicted. Second staining with anti-actin antibody was used as loading control.

B) Graph showing mean of relative NF-κB protein expression + SD of three independent immunoblots. NF-κB signal was quantified related to corresponding actin signal and NF-κB expression of untreated control cells (Ctrl) was set to 1. (* $p \leq 0.05$)

3.3 Glycation interferes with cytokine expression

Macrophages are key players during inflammation. Besides phagocytosis, one of their major roles is the secretion of pro- and anti-inflammatory cytokines (Kloc, 2017). During acute inflammation, classically activated M1 macrophages produce mostly pro-inflammatory cytokines like IL-1 β , IL-6, IL-8 and TNF- α , while alternatively activated M2 macrophages play a more anti-inflammatory role by releasing IL-10, TGF- β and Arg1 (Gordon, 2003). In the following, some selected cytokines were analysed after glycation or treatment with AGE-FCS.

3.3.1 Expression of IL-1 β and involvement of the inflammasome

IL-1 β as pro-inflammatory cytokine is produced by activated monocytes and macrophages. It is secreted during infections, inflammatory processes, or microbial

invasion, and functions in both systemic and local response mechanisms (Dinarello, 1998). THP-1 macrophages were treated with 1 mM MGO or 10 % AGE-FCS for 24 h and polarized into M1 or M2 phenotype. Gene expression of IL-1 β mRNA was analysed using qPCR (figure 19 A) and protein secretion was measured in the cell supernatant using CBA assay (figure 19 B). M1 macrophages showed a significant increase of IL-1 β mRNA after glycation with MGO, but not after treatment with AGE-FCS. For M2 macrophages, no changes in mRNA levels could be observed, both for MGO and AGE-FCS treatment. The same effects can be seen on protein levels, MGO treatment led to an upregulation of IL-1 β in M1 macrophages while all other conditions remained unaffected.

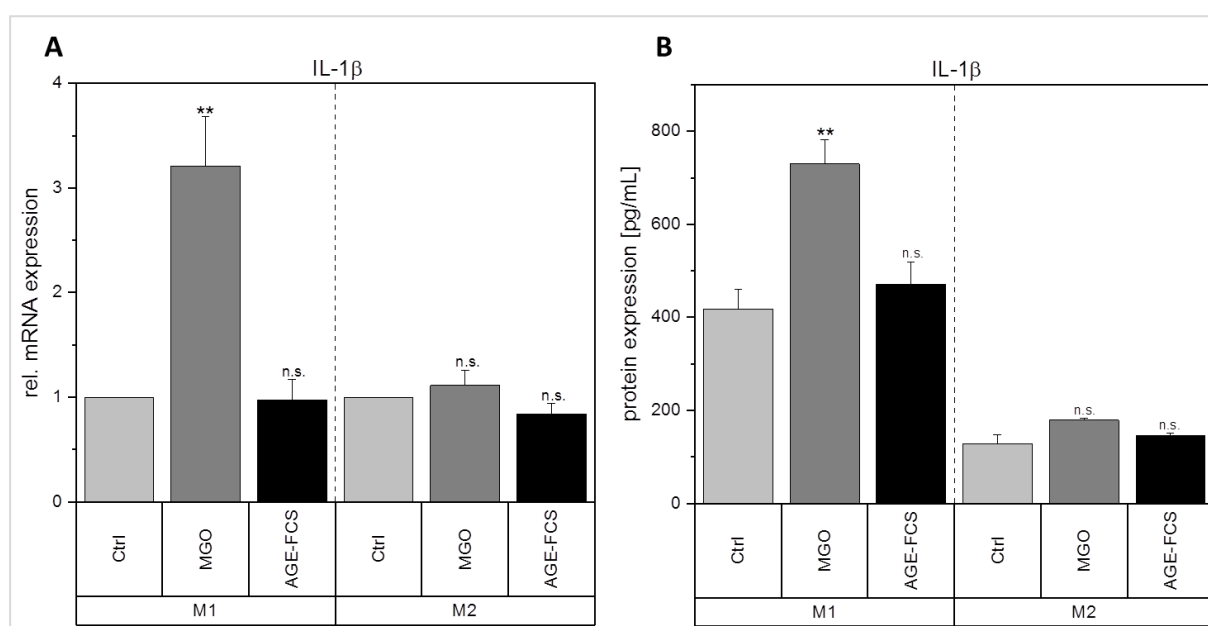


Figure 19: Expression of IL-1 β after glycation.

THP-1 macrophages were glycated with 1 mM MGO or treated with 10 % AGE-FCS and polarized in M1 or M2 phenotype. **A)** Expression of IL-1 β was quantified using qPCR. Data was normalized to untreated control cells (Ctrl). Graph showing mean of relative mRNA expression + SD of three independent experiments. **B)** Protein secretion of IL-1 β was quantified in the cell supernatant using cytometric bead array. Graph showing mean of IL-1 β concentration (in pg/mL) + SD of three independent experiments. (** $p \leq 0.01$)

Due to this increase of IL-1 β in M1 macrophages, it needs to be clarified, whether the inflammasome is also involved and upregulated. Therefore, expression of caspase-1 as activator of the inflammasome was analysed using immunoblotting. THP-1 macrophages were treated with 1 mM MGO or 10 % AGE-FCS and protein samples were collected after 4, 8 and 24 h. Caspase-1 protein expression was quantified in relation to actin expression against the control cells (figure 20). Figure 20 A shows the

relative caspase-1 expression for M1 macrophages after treatment with MGO or AGE-FCS, figure 20 B shows one representative immunoblot for caspase-1 and actin staining. Figure 20 C shows the relative caspase-1 expression for M2 macrophages after treatment with MGO or AGE-FCS, figure 20 D shows one representative immunoblot for caspase-1 and actin staining. In both phenotypes, there could not be any upregulation of caspase-1 detected over time for both treatments, indicating that the inflammasome is not influenced by glycation.

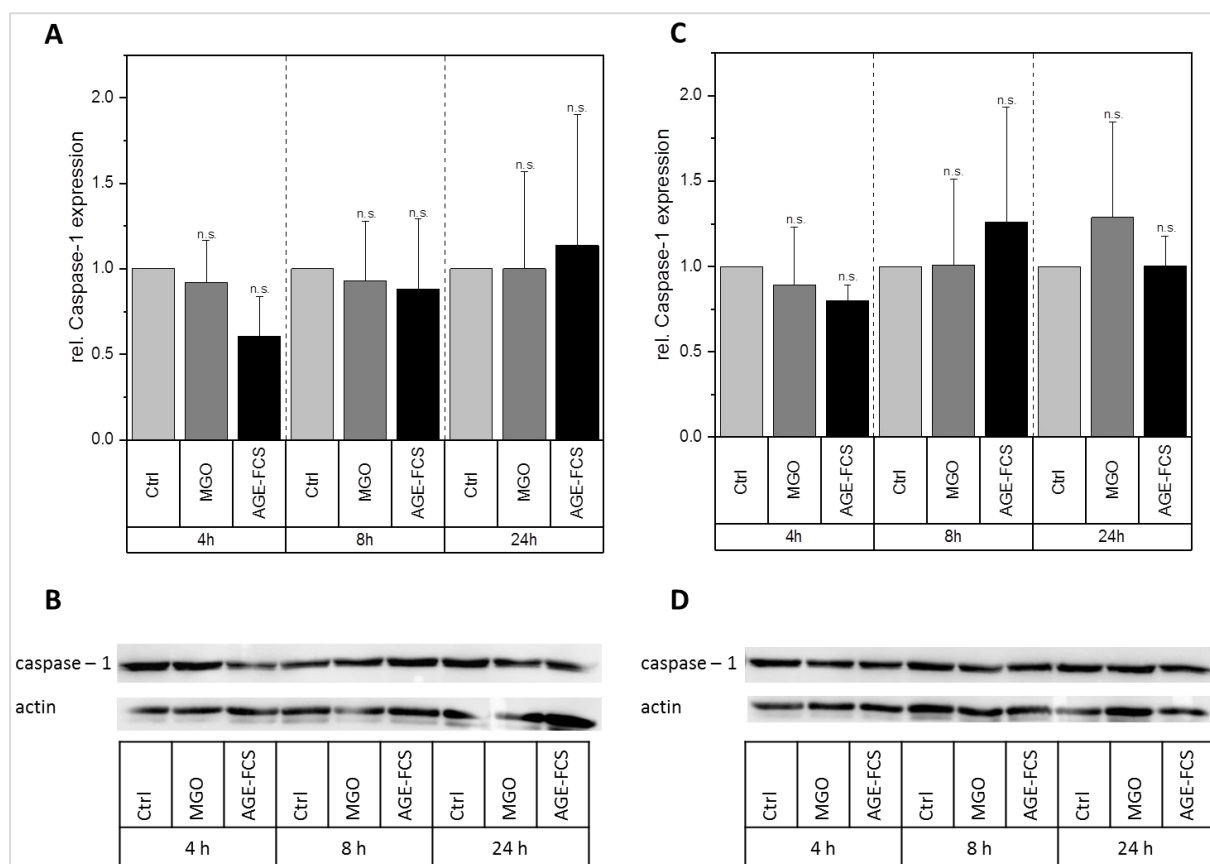


Figure 20: Expression of caspase-1 after glycation.

THP-1 macrophages were incubated with 1 mM MGO or 10 % AGE-FCS for 24 h and polarized into M1 and M2 phenotype. Total protein was isolated after 4, 8 and 24 h and separated by SDS-PAGE and immunoblotting. Caspase-1 protein expression was detected using an anti-caspase-1 antibody (2225) and quantified.

A) Graph showing mean of relative caspase-1 protein expression + SD of three independent immunoblots for M1 macrophages. The caspase-1 signal was quantified related to corresponding actin signal and caspase-1 expression of untreated control cells (Ctrl) was set to 1. **B)** Representative caspase-1 immunoblot of M1 macrophages. Second staining with anti-actin antibody was used as loading control.

C) Graph showing mean of relative caspase-1 protein expression + SD of three independent immunoblots for M2 macrophages. The caspase-1 signal was quantified related to corresponding actin signal and caspase-1 expression of untreated control cells (Ctrl) was set to 1. **D)** Representative caspase-1 immunoblot of M2 macrophages. Second staining with anti-actin antibody was used as loading control.

3.3.2 Expression of IL-6

The pro-inflammatory cytokine IL-6 is mostly produced in response to infections and contributes to the host defence by stimulating both the acute phase response and also antibody production (Tanaka et al., 2014). THP-1 macrophages were treated with 1 mM MGO or 10 % AGE-FCS for 24 h and polarized into M1 or M2 phenotype. Gene expression of IL-6 mRNA was analysed using qPCR (figure 21 A) and protein secretion was measured in the cell supernatant using CBA assay (figure 21 B). M1 macrophages showed a significant increase of IL-6 mRNA after glycation with MGO, but not after treatment with AGE-FCS. For M2 macrophages, no changes in mRNA levels could be observed, both for MGO and AGE-FCS treatment. The same effects can be seen on protein level, MGO treatment led to an upregulation of IL-6 in M1 macrophages, whereas all other conditions remained unaffected.

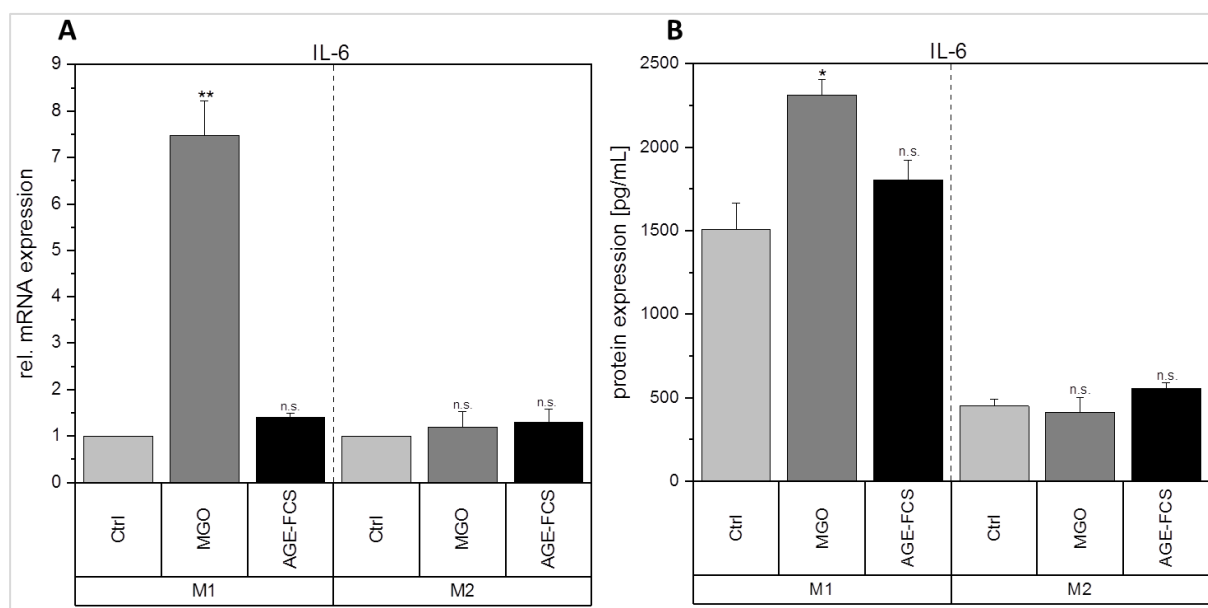


Figure 21: Expression of IL-6 after glycation.

THP-1 macrophages were glycated with 1 mM MGO or treated with 10 % AGE-FCS and polarized in M1 or M2 phenotype. A) Expression of IL-6 was quantified using qPCR. Data was normalized to untreated control cells (Ctrl). Graph showing mean of relative mRNA expression + SD of three independent experiments. B) Protein secretion of IL-6 was quantified in the cell supernatant using cytometric bead array. Graph showing mean of IL-6 concentration (in pg/mL) + SD of three independent experiments. (* $p \leq 0.05$, ** $p \leq 0.01$)

3.3.3 Expression of IL-8

IL-8 is a pro-inflammatory cytokine that has extensive functions in defensive and immune reactions as well as in inflammation (Brat et al., 2005; Harada et al., 1994). THP-1 macrophages were treated with 1 mM MGO or 10 % AGE-FCS for 24 h and polarized into M1 or M2 phenotype. Gene expression of IL-8 mRNA was analysed using qPCR (figure 22 A) and protein secretion was measured in the cell supernatant using CBA assay (figure 22 B). M1 macrophages showed a significant increase of IL-8 mRNA after glycation with MGO, but not after treatment with AGE-FCS. For M2 macrophages, an increase of IL-8 mRNA could be observed with MGO, but not with AGE-FCS treatment. The same effects could be confirmed on protein level, MGO treatment led to an upregulation of IL-8 in M1 and M2 macrophages, whereas macrophages treated with AGE-FCS remained unaffected.

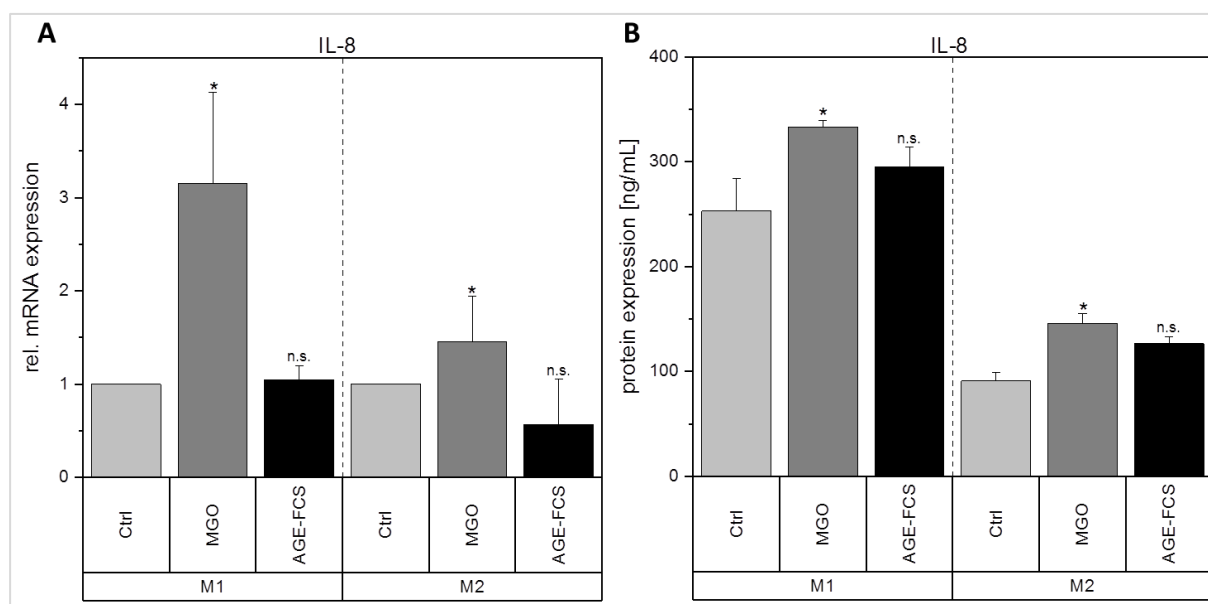


Figure 22: Expression of IL-8 after glycation.

THP-1 macrophages were glycated with 1 mM MGO or treated with 10 % AGE-FCS and polarized in M1 or M2 phenotype. A) Expression of IL-8 was quantified using qPCR. Data was normalized to untreated control cells (Ctrl). Graph showing mean of relative mRNA expression + SD of three independent experiments. B) Protein secretion of IL-8 was quantified in the cell supernatant using cytometric bead array. Graph showing mean of IL-8 concentration (in ng/mL) + SD of three independent experiments. (* $p \leq 0.05$)

3.3.4 Expression of TNF- α

TNF- α is involved in inflammation as a pleiotropic cytokine and is generated by macrophages upon cellular activation. It can be seen as a master regulator for the production and secretion of pro-inflammatory cytokines (Tracey and Cerami, 1994). THP-1 macrophages were treated with 1 mM MGO or 10 % AGE-FCS for 24 h and polarized into M1 or M2 phenotype. Gene expression of TNF- α mRNA was analysed using qPCR (figure 23 A) and protein secretion was measured in the cell supernatant using CBA assay (figure 23 B). M1 macrophages showed a significant increase of TNF- α mRNA after glycation with MGO, but not after treatment with AGE-FCS. For M2 macrophages also an increase of TNF- α mRNA could be observed with MGO but not with AGE-FCS treatment. On protein levels the same effects could be detected, MGO treatment led to an upregulation of TNF- α in M1 and M2 macrophages while macrophages treated with AGE-FCS remained unaffected.

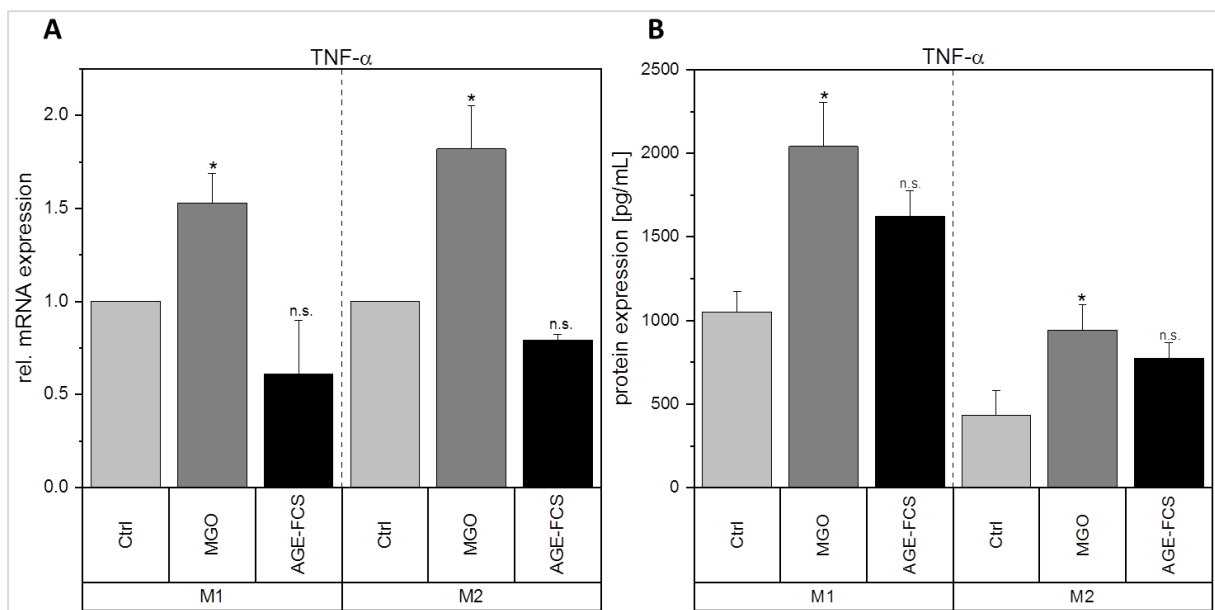


Figure 23: Expression of TNF- α after glycation.

THP-1 macrophages were glycated with 1 mM MGO or treated with 10 % AGE-FCS and polarized in M1 or M2 phenotype. A) Expression of TNF- α was quantified using qPCR. Data was normalized to untreated control cells (Ctrl). Graph showing mean of relative mRNA expression + SD of three independent experiments. B) Protein secretion of TNF- α was quantified in the cell supernatant using cytometric bead array. Graph showing mean of TNF- α concentration (in pg/mL) + SD of three independent experiments. (* $p \leq 0.05$)

3.3.5 Expression of IL-10

IL-10 is one of the most potent anti-inflammatory cytokines and inhibits the production of pro-inflammatory cytokines. It also restrains immune responses and interferes with immune cell functions, including those of macrophages (Fiorentino, 1989; Spits and Waal Malefyt, 1992). THP-1 macrophages were treated with 1 mM MGO or 10 % AGE-FCS for 24 h and polarized into M1 or M2 phenotype. Gene expression of IL-10 mRNA was analysed using qPCR (figure 24 A) and protein secretion was measured in the cell supernatant using CBA assay (figure 24 B). Interestingly, M1 macrophages did not show any effect on IL-10 mRNA after glycation with MGO or after treatment with AGE-FCS. For M2 macrophages, an increase of IL-10 mRNA could be observed with MGO but not with AGE-FCS. On protein levels the same effects could be detected, MGO treatment led to an upregulation of IL-10 secretion in M2 macrophages while all other conditions remained unaffected.

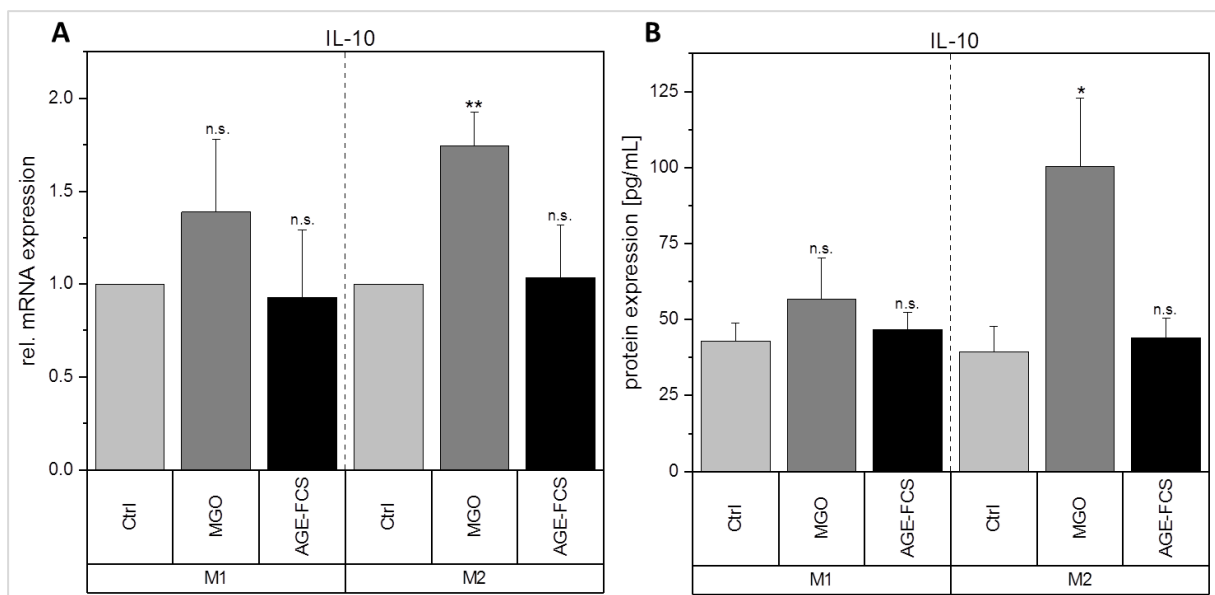


Figure 24: Expression of IL-10 after glycation.

THP-1 macrophages were glycated with 1 mM MGO or treated with 10 % AGE-FCS and polarized in M1 or M2 phenotype. A) Expression of IL-10 was quantified using qPCR. Data was normalized to untreated control cells (Ctrl). Graph showing mean of relative mRNA expression + SD of three independent experiments. B) Protein secretion of IL-10 was quantified in the cell supernatant using cytometric bead array. Graph showing mean of IL-10 concentration (in pg/mL) + SD of three independent experiments. (* $p \leq 0.05$, ** $p \leq 0.01$)

3.4 Effect of glycation on phagocytosis

One major functional role of macrophages is phagocytosis of invaded bacteria, but also of cell debris or apoptotic cells. This is important during acute infections as well as during tissue remodelling (Stuart and Ezekowitz, 2008). Dysfunction of phagocytosis leads to impaired inflammation and also interferes with wound healing processes.

3.4.1 Phagocytic efficiency

The phagocytic efficiency of THP-1 macrophages after treatment with 1 mM MGO or 10 % AGE-FCS and polarization in M1 or M2 phenotype was investigated. A phagocytosis assay with *pHrodo*[™] *Green E. coli BioParticles*[™] was performed and changes of phagocytic efficiency were calculated and compared to untreated control cells (figure 25). Both macrophage phenotypes treated with MGO showed a significant decrease of phagocytic efficiency. In comparison, treatment with AGE-FCS did not have any significant effects.

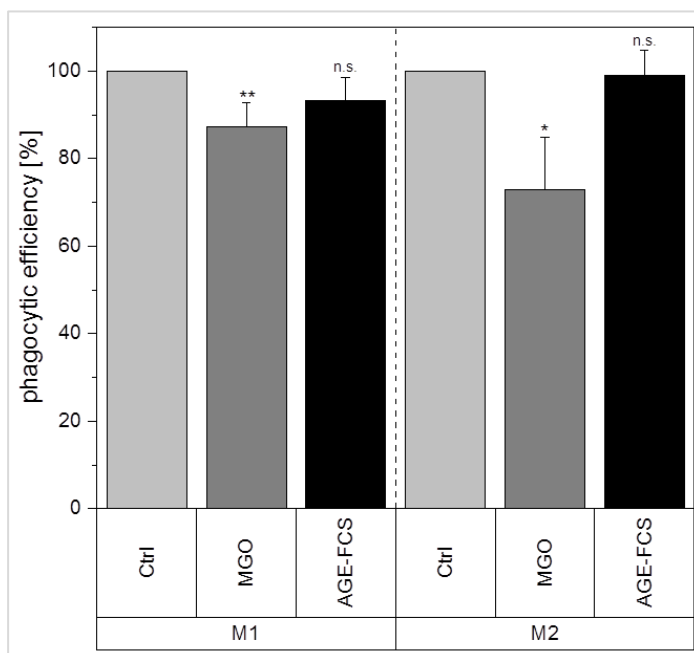


Figure 25: Phagocytic efficiency after glycation.

THP-1 macrophages were glycated with 1 mM MGO or treated with 10 % AGE-FCS for 24 h and polarized in M1 or M2 phenotype. Phagocytosis assay was performed with *pHrodo*[™] *Green E. coli BioParticles*[™]. Data was normalized to untreated control cells. Graph showing mean of phagocytic efficiency + SD of five independent experiments. (* $p \leq 0.05$, ** $p \leq 0.01$)

3.4.2 Glycation of phagocytosis associated surface receptors

In order to examine, whether the decline of phagocytic efficiency is due to glycation of phagocytosis associated surface receptors, IPs of TLR4 were performed. TLR4 is a pattern recognition receptor that mediates phagocytosis and cytokine expression in macrophages (Vaure and Liu, 2014). Cell lysate of THP-1 macrophages treated with 1 mM MGO was compared to untreated control cells. IPs were performed with an anti-TLR4 antibody. Input (= cell lysate), flow through and output were then analysed by immunoblotting with an anti-AGE antibody (CML26, figure 26 A) or with the anti-TLR4 antibody (figure 26 B). One representative immunoblot of three independent experiments is shown for both IPs. Anti-TLR4 was used as a control for the IP, while anti-AGE was used to visualize glycation of TLR4. Figure 26 B shows the control immunoblots with the anti-TLR4 antibody. TLR4 has a predicted molecular mass of approx. 95 kDa and appears in the immunoblots in the height of around 100 kDa. In the control samples as well as in the MGO treated samples, an increase of TLR4 signal after the IPs can be detected (lane 3 and lane 6). This validates the performance of the IPs with the anti-TLR4 antibody. Figure 26 A depicts the immunoblots with the anti-AGE antibody. In the control samples (lane 4 to lane 6) no distinct signal can be detected with the anti-AGE antibody. In the samples treated with MGO (lane 1 to lane 3), an AGE-signal can be detected in the IP sample (lane 3) at around 100 kDa, which correlates with the predicted molecular mass of TLR4. This confirms that TLR4 is glycated after treatment of the cells with MGO.

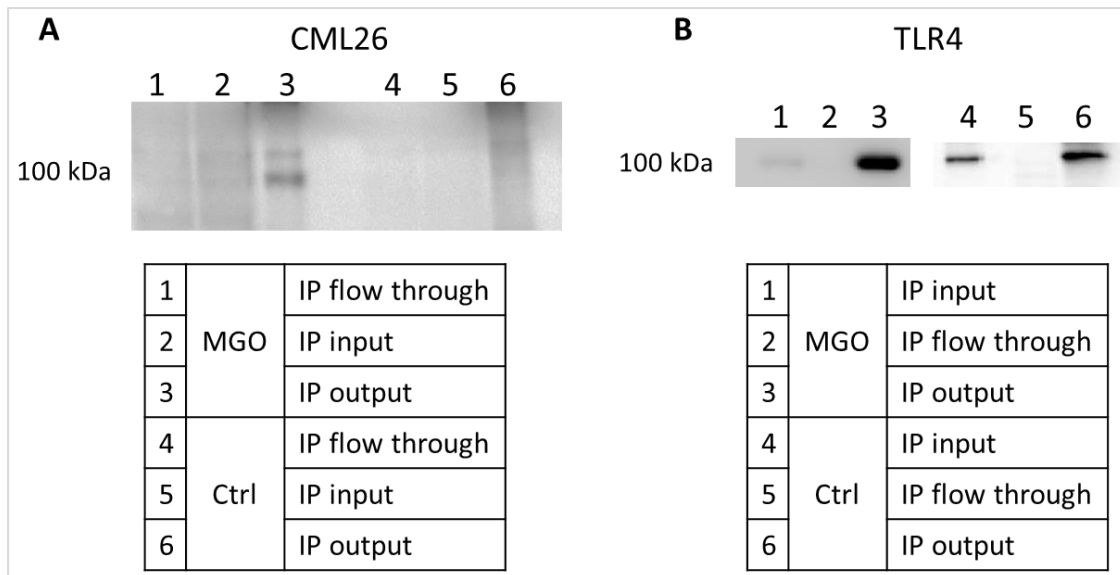


Figure 26: Detection of glycation of TLR4.

THP-1 macrophages were glycated with 1 mM MGO for 24 h. 5 mg of cell lysates of MGO treated or control cells (Ctrl) were used for IP with an anti-TLR4 antibody. Input (= cell lysate), flow through and output of the IP were separated by SDS-PAGE and immunoblotting. Anti-AGE antibody (CML26, **A**) was used for detecting glycation of TLR4 (approx. 100 kDa). Anti-TLR4 antibody was used as a control (**B**). Depicted blots are representative for three independent experiments.

3.5 Influence of glycation on macrophage polarization

Due to the changes in cytokine expression and the decline in phagocytic efficiency after glycation with MGO, the question was raised whether glycation could have an influence on macrophage polarization. Especially concerning the anti-inflammatory M2 phenotype, where the secretion of more pro-inflammatory cytokines after glycation could be shown. Therefore, the phenotype of macrophages was verified by flow cytometry based analysis with a special surface marker and by qPCR based analysis of mRNA expression level.

3.5.1 Flow cytometry analysis of surface marker

The polarization phenotype of macrophages can be verified by antibody-based staining of respective surface markers and analysis via flow cytometry. An anti-CD16 antibody was used as a general marker for differentiated macrophages and is therefore

expressed by M1 as well as M2 macrophages. As a characteristic marker for M1 phenotype, staining with an anti-CD68 antibody was used. For M2 phenotype, two surface markers were characterised, CD209 and CD163 (Duluc et al., 2007; Röszer, 2015).

THP-1 macrophages were treated with 1 mM MGO or 10 % AGE-FCS for 24 h and polarized into M1 or M2 phenotype. CD16-staining was performed as an internal control for differentiation. One representative experiment out of three is shown in figure 27. There are no visible differences in the staining of both macrophage phenotypes and treatments.

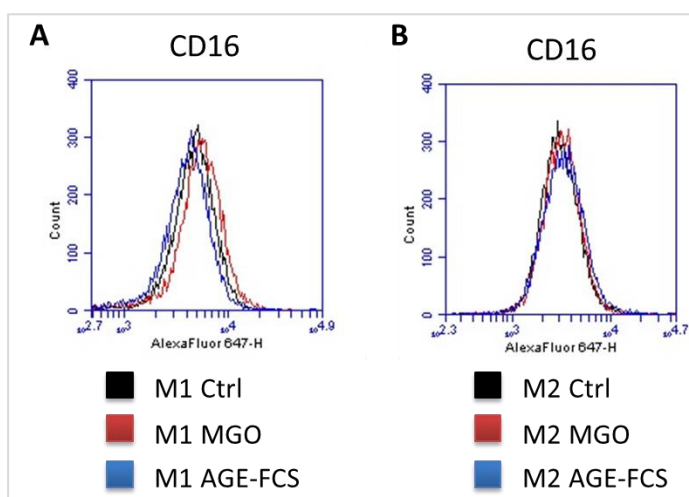


Figure 27: Analysis of CD16 in M1 and M2 macrophages.

THP-1 macrophages were glycosylated with 1 mM MGO or treated with 10 % AGE-FCS for 24 h and polarized in M1 or M2 phenotype. Living cells were harvested, stained with an anti-CD16 antibody (labelled with Alexa Fluor® 647) and analysed using flow cytometry. Representative histograms of analysed Alexa Fluor® 647 positive cells are shown for M1 (**A**) and M2 (**B**) phenotype.

In order to analyse, whether glycation triggers M2 macrophages to shift to the M1 phenotype, staining with an anti-CD68 antibody was performed. Untreated M1 macrophages served as a positive control for antibody-staining. One representative experiment out of three is depicted in figure 28 A. For all M2 macrophages (control in black, MGO treatment in red, AGE-FCS treatment in blue), no significant signal for CD68 could be observed compared to the M1 control cells (in orange). When comparing M1 macrophages treated with MGO or AGE-FCS to the control, no

significant effects could be detected (data not shown). This indicates that M2 macrophages are not triggered to the pro-inflammatory M1 phenotype by glycation. For the analysis of M2 phenotype, staining with CD209 and CD163 was performed. Figure 28 B shows one representative experiment out of three for CD209 staining and figure 28 C for CD163 staining. In both histograms a clear difference between all M1 macrophages (control in black, MGO treatment in red, AGE-FCS treatment in blue) and the untreated M2 control cells (in orange) can be seen. For M2 macrophages treated with MGO or AGE-FCS, no differences to the control cells could be observed (data not shown). These staining show that glycation does not trigger M1 macrophages to switch to the M2 phenotype.

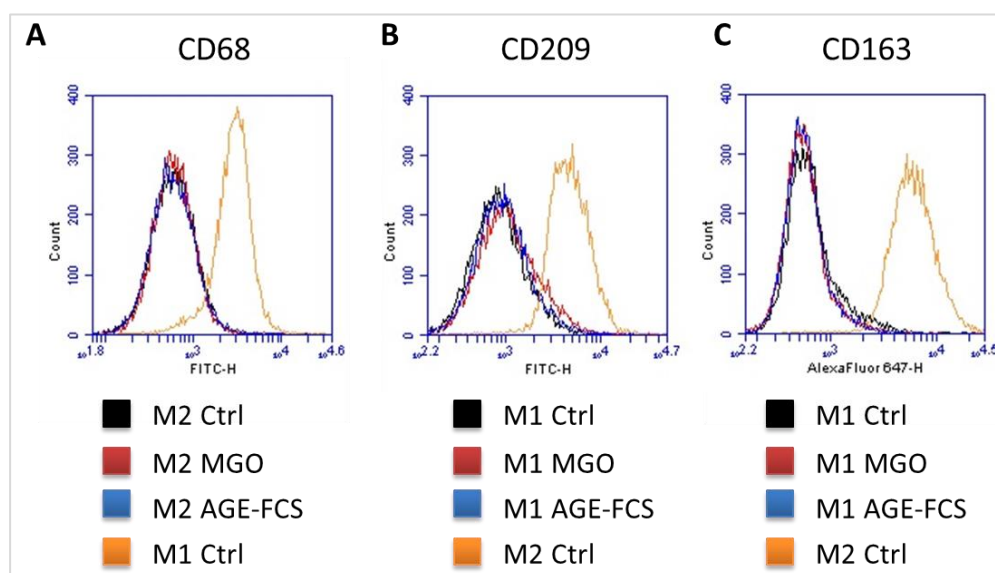


Figure 28: Analysis of polarization marker in M1 and M2 macrophages.

THP-1 macrophages were glycated with 1 mM MGO or treated with 10 % AGE-FCS for 24 h and polarized in M1 or M2 phenotype. Living cells were stained with fluorescence-labelled antibodies and analysed using flow cytometry. **A)** Representative histograms of M2 macrophages stained with M1-marker anti-CD68 (FITC). Untreated M1 macrophages serve as positive control. **B)** Representative histograms of M1 macrophages stained with M2-marker anti-CD209 (FITC). Untreated M2 macrophages serve as positive control. **C)** Representative histograms of M1 macrophages stained with M2-marker anti-CD163 (Alexa Fluor® 647). Untreated M2 macrophages serve as positive control.

3.5.2 qPCR analysis of expression marker

The polarization phenotype of macrophages can also be verified by expression of several cytokines. The M1 phenotype is characterised as IL-12^{high}, IL-23^{high}, IL-10^{low} and TGF- β ^{low}, while the M2 phenotype is described as IL-12^{low}, IL-23^{low}, IL-10^{high} and TGF- β ^{high} (Rószler, 2015). THP-1 macrophages were treated with 1 mM MGO or 10 % AGE-FCS for 24 h, polarized into M1 or M2 phenotype and mRNA expression level of the cytokines listed above were measured. Expression levels of untreated M2 macrophages (Ctrl) were always set to 1. There were no significant differences on IL-12 (figure 29 A) or IL-23 (figure 29 B) expression between M2 control cells and cells treated with either MGO or AGE-FCS. M1 control cells, however, show a significantly higher expression of both cytokines as expected. No differences of IL-12 and IL-23 expression levels of M1 cells treated with MGO or AGE-FCS could be observed (data not shown). Expression of IL-10 mRNA (figure 29 C) was significantly downregulated for all M1 macrophages in comparison to the untreated M2 cells (Ctrl). Also there was no significant effect on IL-10 secretion between M1 macrophages treated with MGO or AGE-FCS and the untreated control cells (see 3.3.5). Under 3.3.5 it has already been shown that MGO treatment led to an upregulation of IL-10 mRNA in M2 macrophages, but that AGE-FCS did not have any effect. Concerning TGF- β expression (figure 29 D), there was a downregulation of mRNA for all M1 cells compared to the untreated M2 macrophages (Ctrl). While comparing M1 cells treated with MGO or AGE-FCS to the untreated M1 control cells, no effects could be detected (data not shown). There were also no differences in TGF- β expression levels between M2 control cells and M2 cells treated with MGO or AGE-FCS (data not shown). In summary, this confirms the findings under 3.5.1 that glycation does not have an influence on the polarization phenotype of macrophages.

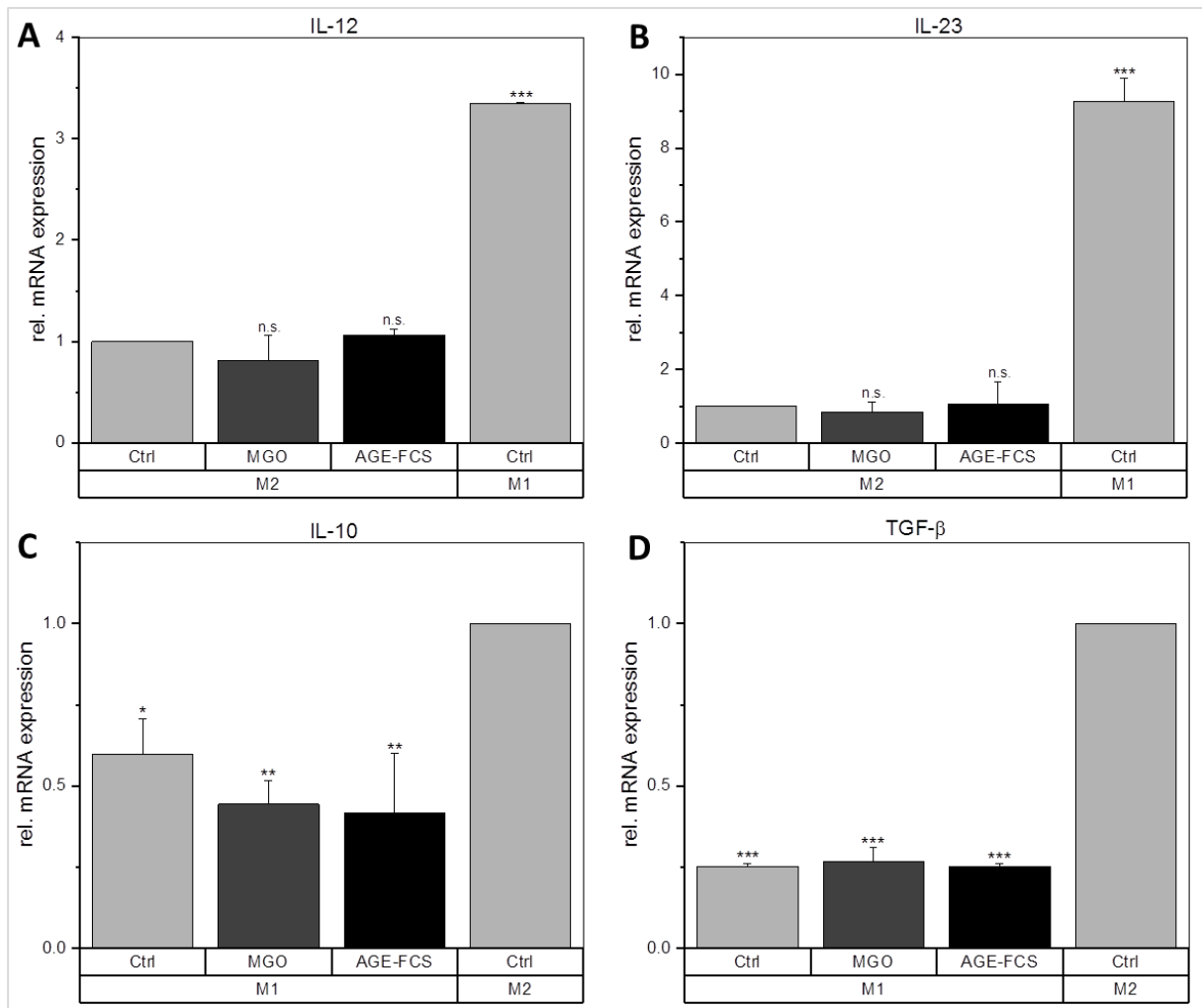


Figure 29: Analysis of polarization related cytokine expression.

THP-1 macrophages were glycated with 1 mM MGO or treated with 10 % AGE-FCS for 24 h and polarized in M1 or M2 phenotype. Expression of cytokines was quantified using qPCR and normalized to untreated M2 cells (Ctrl). **A)** Expression of IL-12. **B)** Expression of IL-23. **C)** Expression of IL-10. **D)** Expression of TGF-β.

Represented are means of relative mRNA expression + SD of three independent experiments. (* $p \leq 0.05$, ** $p \leq 0.01$, *** $p \leq 0.001$)

4 Discussion

4.1 MGO induces glycation of macrophages

Glycation is known to negatively affect protein function and maintenance of cellular homeostasis. During aging and the progression of several diseases, the accumulation of AGE-modified proteins can cause chronic complications and impairments due to modification and loss of function of specific proteins or their irreversible accumulation throughout the body. In view of the fact that not only glucose and other sugars can induce glycation, but also metabolic intermediates like highly reactive carbonyl compounds (e.g. MGO, glyoxal or 3-deoxyglucosone), the mechanisms of AGE accumulation and modification need to be further investigated. In this thesis, the influence of glycation and treatment with AGE-modified proteins of macrophages was analysed.

MGO is a natural inducer of glycation as a metabolic intermediate that is generally occurring in the human body. Due to its toxicity in higher concentrations, the body developed a special system for the detoxification of MGO, the glyoxalase system (Schmoch et al., 2017). In this work, concentrations of MGO from 0.5 up to 2 mM were tested initially. It could be shown that with increasing MGO concentrations increased band intensities could be detected in immunoblot analyses, correlating with the increased formation of AGEs. Although no morphological changes could be observed after treatment with up to 1.5 mM MGO for 24 h, metabolic activity of the macrophages declined drastically with 1.5 and 2 mM MGO. Additionally, induction of apoptosis could be observed using these MGO concentrations for glycation. In other cell lines, for example in murine alveolar macrophages, even lower concentrations of MGO (0.4 mM and 0.8 mM) were able to induce apoptosis and necrosis (Rachman et al., 2006). Even though glycation is stronger after incubation with higher concentrations, 1 mM MGO was chosen as final concentration for all following experiments. The same concentration was already used in human umbilical vein endothelial cells (Akhand et al., 2001), human retinal pigment epithelium cells (Bento et al., 2010) and human natural killer cells (Rosenstock et al., 2019). Additionally, it is known that different cells can have a different tolerance potential against MGO (Lee and Chang, 2014), so the dosage of MGO treatment needs to be investigated for every cell line. Generally, the MGO concentrations in the human body vary, depending on the tissues or organs and also the time points of measurement. The half-life time of MGO in the human blood is

estimated to be around 1 h (Brandt and Siegel, 1978). In human plasma of healthy individuals, the concentrations can differ between 330 nM and 550 nM (Han et al., 2007; Kong et al., 2014; Nemet et al., 2005). For diabetic patients, the MGO plasma concentrations vary between 840 nM for diabetes type I (Han et al., 2007) and 910 nM for diabetes type II (Kong et al., 2014). In whole blood the concentrations differ slightly, they were measured to be around 410 nM for healthy individuals and 740 nM for diabetic patients (Nemet et al., 2005). In the serum of elderly patients concentrations around 930 nM MGO were measured and could even be associated with increased mental decline (Beeri et al., 2011). Nevertheless, local concentrations of MGO can be significantly higher at the production site (Kalapos, 2008b). For instance, the MGO concentrations tend to be 20 times higher in lenses and 10 times higher in liver and kidney compared to those measured in plasma (Thornalley, 1993). In diabetic lens samples, the concentrations can even be much higher (Phillips et al., 1993). In cerebrospinal fluid samples from AD patients concentrations of around 20 μ M could be measured (Kuhla et al., 2005). The concentrations that are used for *in vitro* induction of glycation are generally higher, depending on the tissue or cell line that is glycated. For example, rat lenses or rat vascular smooth muscle cells were glycated with concentrations of around 0.5 mM MGO, while for glycation of human endothelial cells 1 mM MGO were used. For glycation of murine hepatocytes the concentrations were even higher, up to 20 mM MGO were used (summarised in Kalapos, 2008b).

Due to cultivation conditions of the THP-1 macrophages with 10 % FCS as medium supplementation, there is the possibility that MGO treatment leads to glycation of the supplemented FCS. Glycated serum proteins could bind to AGE receptors like RAGE, which in turn could induce inflammatory responses upon activation (Yan et al., 1994). In order to elucidate these effects, an adequate control for effects of glycated serum proteins needed to be established. Therefore, FCS was glycated with MGO under the same conditions as the cells. Glycation of this so called AGE-FCS was always verified prior to use via dot blot analysis with an anti-AGE antibody. Treatment with 10 % AGE-FCS instead of normal FCS in the culture medium was carried out in all experiments. Changes compared to the control cells could not be seen for macrophages treated with AGE-FCS in immunoblotting with an anti-AGE antibody (data not shown).

Binding of AGEs to RAGE is known to induce the intracellular production of ROS (Vazzana et al., 2009). For MGO treatment, these effects could be demonstrated, for example in peritoneal macrophages of tumour mice an induction of ROS levels could

be observed after incubation with MGO (Chakrabarti et al., 2014). In this work, ROS levels were also measured after treatment with MGO and AGE-FCS. Both stimuli did not enhance the intracellular production of ROS in macrophages in this setup. In diluted aqueous solutions, MGO mostly exists in its hydrated form, 56 % in the mono- and 44 % in the dihydrated form, respectively (McLellan and Thornalley, 1992). This could generally reduce the reactivity of MGO supplementation. Besides, MGO is also metabolised by the glyoxalase system which inhibits further reactions. This could explain why there was no enhanced ROS production in the macrophages after MGO treatment compared to the untreated controls. In the samples treated with AGE-FCS, no marked increase of ROS production was detectable. This could be due to the analysed time points of the ROS measurement. The macrophage samples were measured up to 90 min post-loading with the dye (data only shown up to 60 min). This should demonstrate a direct ROS induction of the substances the cells were treated with. RAGE-mediated ROS production in contrary may take longer than 60 min or 90 min due to the signal cascade. In rat mesangial cells for example, a clear induction of intracellular ROS due to AGE-dependent RAGE activation could be detected after 48 h (Coughlan et al., 2009).

4.2 RAGE is only activated upon treatment with soluble AGEs

RAGE is one of the best characterised receptors for AGEs (Ramasamy et al., 2008) and is expressed on macrophages as well as other cells of the innate immune system (Kierdorf and Fritz, 2013). As already depicted in figure 4 (see 1.1.1.2), binding of AGEs to RAGE induces diverse signalling cascades, finally resulting in the dislocation of NF- κ B into the nucleus and the induction of intracellular ROS. Activation of NF- κ B stimulates its own expression but also the expression of RAGE (Bierhaus et al., 2005). When macrophages are treated with soluble AGEs, an overexpression of RAGE is therefore expected. In the case of direct glycation of the macrophages with MGO treatment, it was not clear, whether RAGE would be activated and overexpressed. In theory, the addition of MGO to the culture medium could lead to glycation of serum proteins which then could bind to RAGE and activate signalling. It is not completely understood how much of the MGO is entering the cells and how much will remain in the medium and is able to react with serum proteins. Therefore, the expression of RAGE after glycation and treatment with AGE-FCS was assessed. An overexpression

of RAGE on protein levels and on the surface indicates activation of RAGE via its positive self-expressing feedback loop (Sun et al., 1998; Tanji et al., 2000). After treatment of macrophages with AGE-FCS, a significant upregulation of RAGE on protein level was measured and could be confirmed in flow cytometry via antibody staining of living cells. After treatment with MGO, no effects on RAGE expression could be detected either in immunoblotting or with flow cytometry. This is an indicator that if there is glycation of serum proteins after addition of MGO to the culture medium, the influence on RAGE activation is not given. Still, the activation of NF- κ B needs to be examined in order to verify these findings. NF- κ B is also a downstream target of LOX-1, another receptor for AGEs, but it has already been demonstrated that it rather binds oxidised low-density lipoproteins than AGE-modified proteins, e.g. AGE-modified BSA (Shiu et al., 2012). Therefore, expression of NF- κ B can be correlated to RAGE activation in this experimental setup. The expression of NF- κ B on protein levels was analysed after glycation or treatment with AGEs. While incubation with AGEs led to an increased expression of NF- κ B, indicating its activation feedback loop (Bierhaus et al., 2005), treatment with MGO did not have any effects on NF- κ B protein levels. This leads to the conclusion that only treatment with AGEs but not glycation itself leads to RAGE activation and overexpression. These experiments were needed in order to distinguish between effects caused by binding of AGEs to specific receptors on the cell surface or by direct glycation of cellular proteins. It has already been demonstrated that some specific AGE-structures are able to induce RAGE activation and signalling in human peripheral blood monocytes (Takahashi et al., 2009). Although these AGE-structures were derived from incubation of BSA with glyceraldehyde-3-phosphate or glycolaldehyde, it cannot be excluded that MGO derived AGE-structures are not recognised by RAGE and activate signalling. At least for macrophages activation of RAGE with MGO derived AGEs could be demonstrated in this work.

4.3 Glycation has an influence on cytokine expression

Macrophages, in their function as key players during inflammation, are responsible for the secretion of pro- and anti-inflammatory cytokines, depending on their polarization phenotype or tissue specificity (Gordon, 2003; Kloc, 2017). The following table (figure 30) summarises the findings on cytokine expression after glycation or AGE-treatment for M1 and M2 macrophages. The summarised findings represent data from mRNA and protein analyses, because the same effects could be observed in both experimental setups. The cytokines that are upregulated are highlighted in green colour.

	M1 macrophages		M2 macrophages	
	glycation	AGE-treatment	glycation	AGE-treatment
IL-1β	↑	no effect	no effect	no effect
IL-6	↑	no effect	no effect	no effect
IL-8	↑	no effect	↑	no effect
TNF-α	↑	no effect	↑	no effect
IL-10	no effect	no effect	↑	no effect

Figure 30: Table of analysed cytokines.

In M1 macrophages, all analysed pro-inflammatory cytokines (IL-1 β , IL-6, IL-8 and TNF- α) are upregulated after glycation, while there is no visible effect after treatment with AGE-FCS. The expression of anti-inflammatory cytokine IL-10 is not affected in both conditions. Regarding M2 macrophages, only pro-inflammatory cytokines IL-8 and TNF- α are upregulated after glycation, while AGE-FCS also has no effect on these cytokines. Although M2 macrophages already express high amounts of this anti-inflammatory cytokine, a further upregulation of IL-10 could be detected after glycation, but not after treatment with AGEs.

IL-1 β is produced by activated monocytes and macrophages and is secreted during infections, inflammatory processes or microbial invasion. It functions in both systemic and local response mechanisms (Dinarello, 1998). For maturation of pro-IL-1 β into the mature protein, secretion and activation of caspase-1 is needed (Martinon et al., 2002; Tschopp et al., 2003). This involves the activation of the inflammasome. IL-1 β is further suggested to block the induction of M2 phenotype during normal healing processes. Increased concentrations of IL-1 β were already demonstrated in diabetic wounds and were correlated with a positive feedback loop that sustains the pro-inflammatory macrophage phenotype observed in poorly healing wounds (Mirza et al., 2013). Other studies also showed increased IL-1 β expression in murine tumour macrophages after MGO treatment (Chakrabarti et al., 2014; Pal et al., 2009). Here, an overexpression of IL-1 β was detected in M1 macrophages, which corroborates these studies. Although increased concentrations of IL-1 β were measured, an involvement of the inflammasome could not be confirmed. Expression of caspase-1 was investigated via immunoblotting after glycation or treatment with AGE-FCS. In either M1 or M2 phenotype no differences were detected between the different conditions. During infections it is known that activation of caspase-1 increases its expression due to a positive feedback loop (Kumaresan et al., 2016). Since caspase-1 is directly activated by the inflammasome, a higher expression of caspase-1 would indicate an increased activation of the inflammasome pathway (Blander, 2014), which could not be detected in this experimental setup.

IL-6 is produced as response to infections, immune reactions and host defence mechanisms (Kishimoto, 1989; Tanaka et al., 2014). It was first described as B-cell stimulatory factor 2 due to its ability to activate the differentiation of B-cells into antibody producing cells (Kishimoto, 1985). Although its expression is strictly regulated via transcriptional and posttranscriptional pathways, continual overproduction of IL-6 can be found in the pathology of chronic inflammation and also autoimmunity (Tanaka et al., 2014). After glycation, an increase of IL-6 could be detected in M1 macrophages, but not after incubation with AGE-FCS. This could be an indicator for excessive and uncontrolled inflammation reactions after glycation of cellular proteins. It correlates with the observed overexpression of other pro-inflammatory cytokines, like IL-1 β , IL-8 and TNF- α . M2 macrophages in contrary remained unaffected after glycation as well as after treatment with soluble AGEs.

IL-8 has extensive functions in immune and defensive reactions as well as in inflammation (Brat et al., 2005; Harada et al., 1994). It is highly expressed by activated M1 macrophages and turned off during resolution (Italiani and Boraschi, 2014; Tarique et al., 2015). The increased IL-8 concentrations, which were shown in M1 macrophages after glycation, could therefore indicate a prolonged inflammation phase. Also, an upregulation of IL-8 in M2 macrophages could be detected upon glycation. M2 macrophages should only produce low levels of IL-8, though (Duluc et al., 2007; Röszer, 2015). This could give a hint that glycation of macrophages triggers the anti-inflammatory phenotype to a more pro-inflammatory, which impairs proper function of these macrophages.

TNF- α is a pleiotropic cytokine and can be seen as a master regulator for the production and secretion of pro-inflammatory cytokines (Tracey and Cerami, 1994) and is mostly produced by activated macrophages (Olszewski et al., 2007). It is able to induce inflammation, sepsis and fever and can inhibit virus replication and tumorigenesis. On the other hand, TNF- α is also able to induce apoptosis via activation of caspases and needs to be regulated strictly (Rath and Aggarwal, 1999). In M1 macrophages, overexpression of TNF- α contributes to the pro-inflammatory activation of glycation that was already observed by the overexpression of IL-1 β , IL-6 and IL-8. In M2 macrophages, it indicates a severe change in their anti-inflammatory phenotype. Secretion of TNF- α during remodelling phase of wound healing can promote tissue damage and induce apoptosis of the renewed cells.

IL-10 is one of the most potent anti-inflammatory cytokines. It is able to inhibit pro-inflammatory cytokine production, restrain immune response and interfere with immune cell functions, including those of macrophages (Fiorentino, 1989; Spits and Waal Malefyt, 1992). Expression of IL-10 is known to reduce M1 macrophage activation and also increases M2 activation (Villalta et al., 2011). Even though no changes of IL-10 secretion could be seen in M1 macrophages, the overexpression of pro-inflammatory cytokines like IL-1 β , IL-6, IL-8 and TNF- α could mask the effects of IL-10 on the polarization-switch *in vivo*. If these pro-inflammatory cytokines remain in the wounds during remodelling phase, basal expression levels of IL-10 could not be sufficient to trigger the switch to the anti-inflammatory M2 phenotype. Regarding the data for the M2 phenotype, IL-10 expression was upregulated after glycation. This could be the effect of upregulation of pro-inflammatory cytokines IL-8 and TNF- α , which possibly trigger M2 macrophages to shift to a more pro-inflammatory phenotype. IL-10

overexpression could therefore indicate a self-regulating reaction of the cells to stay in their anti-inflammatory phenotype.

To summarise, it is obvious that glycation has an influence on cytokine secretion of both macrophage phenotypes. Mostly, pro-inflammatory cytokines are overexpressed and can contribute to disturbed wound healing processes that can be seen in diabetic and elderly patients. Although incubation with AGE-FCS leads to the activation of RAGE and NF- κ B, no changes in cytokine secretion could be demonstrated in this work. In contrary, it has been shown by others that activation of RAGE and its signalling cascade can upregulate the production of pro-inflammatory cytokines and chemokines in monocytes and macrophages, for instance such as IL-1 β (Kierdorf and Fritz, 2013). This indicates that the different expression levels after treatment with MGO are due to glycation of the cells and no results of RAGE signalling.

4.4 Phagocytic efficiency is reduced upon glycation

As professional phagocytes, one of the major roles of macrophages is phagocytosis. Besides removal of microbes and invading bacteria during acute infections, they also engage and clear up cell debris and apoptotic cells during tissue remodelling (Stuart and Ezekowitz, 2008). Even though the overexpression of pro-inflammatory cytokines indicates prolonged inflammation reactions, a reduction of phagocytic efficiency was detected for M1 as well as M2 macrophages after glycation. This finding could have an impact on impaired wound healing as well. On the one hand, this can be an important factor regarding impaired clearance rates of invading microbes during the inflammation phase (Gundra et al., 2014). If clearance of microbes is delayed or disturbed, the inflammation phase will be prolonged and infections can be more severe when microbes reproduce in the wounds. On the other hand, reduced phagocytosis can interfere with tissue remodelling, when cell debris and apoptotic cells are not removed properly (Kotwal and Chien, 2017). In general, dysfunction of wound healing processes is also known to increase the formation of scar tissue (Wynn and Vannella, 2016). In contrary, treatment with AGE-FCS did not have any influence on phagocytic efficiency. Therefore the question arises whether glycation of surface proteins could be the reason for reduced phagocytosis after treatment with MGO. In order to analyse this, IPs of TLR4 were performed. TLR4 is one of the most characterised TLR (Vaure

and Liu, 2014) and is known to regulate phagocytosis in macrophages (Anand et al., 2007). Glycation of TLR4 could be confirmed in macrophages treated with MGO. This result, as well as the surface staining with anti-AGE antibody (figure 10), proves that surface glycation could be the reason for reduced phagocytosis. If surface receptors are glycated, the binding affinity of the ligands can be influenced. For the high affinity tyrosine kinase receptor, it has already been demonstrated that glycation reduces its binding ability to the nerve growth factor by the factor of three (Bennmann et al., 2015). It has also been shown that glycation of substrates, for example the low-density lipoprotein, can lead to impaired recognition of the corresponding receptor (Steinbrecher and Witztum, 1984). In the case analysed in this work, reduced phagocytic efficiency can only be correlated with receptor glycation. The *E.coli* particles used in the phagocytosis experiments were not exposed to MGO and were therefore not glycated.

On the contrary, TLRs are important for the secretion of IL-6 and a loss of their binding affinity due to glycation could negatively influence the expression of IL-6. Especially TLR4 is known to recognise LPS and induce the production of IL-6 mRNA by activation of its transcription factors (Tanaka et al., 2014). Nevertheless, an increased expression of IL-6 mRNA could be demonstrated after glycation (see 3.3.2), at least in the M1 phenotype. However, it is known that IL-1 β and TNF- α are also able to activate transcription factors that induce the production of IL-6 (Tanaka et al., 2014). Therefore, an overexpression of IL-6 mRNA after glycation can be associated to the overexpression of IL-1 β and TNF- α that has been demonstrated (see 3.3.1 and 3.3.4) and does not directly exclude the dysfunction of TLRs after glycation.

4.5 Glycation has no influence on macrophage polarization

The polarization switch of macrophages from the pro- to the anti-inflammatory phenotype plays an important role in wound healing (Mantovani et al., 2004; Martinez et al., 2009). In diabetic wounds it has already been shown that the phenotype switch of macrophages seems to be affected (Yan et al., 2018). The resident macrophages also tend to remain predominantly in the pro-inflammatory M1 phenotype (Baltzis et al., 2014; Falanga, 2005; Loots et al., 1998). In order to analyse whether glycation has an influence on the polarization phenotype, the phenotypes of M1 and M2

macrophages were characterised after glycation or treatment with AGE-FCS. Two different methods were applied; the phenotype was first verified with staining of specific cell surface marker in flow cytometry, like CD68 for M1 phenotype and CD163 and CD209 for M2 phenotype (Duluc et al., 2007; Rószler, 2015). Next, expression analyses of specific phenotype-related cytokines by qPCR were carried out, like IL-12, IL-23, IL-10 and TGF- β . Normalised to the expression of the M0 macrophages, the M1 phenotype is characterised as IL-12^{high}, IL-23^{high}, IL-10^{low} and TGF- β ^{low}, while the M2 phenotype is described as IL-12^{low}, IL-23^{low}, IL-10^{high} and TGF- β ^{high} (Rószler, 2015). However, with both methods, the same results were obtained. Neither glycation nor treatment with soluble AGEs led to a phenotype switch of macrophages from M1 to M2 or from M2 to M1 phenotype. For the switch from M1 to M2 phenotype, this can apparently be correlated with the overexpression of pro-inflammatory cytokines. The macrophages are intensified in their pro-inflammatory expression profile. For M2 macrophages, a glycation-triggered switch from M2 to M1 would be expected due to the untypical high expression of pro-inflammatory cytokines (IL-8 and TNF- α). The enhanced secretion of IL-10 seems to be beneficial for keeping the macrophages in their anti-inflammatory phenotype. It is known that IL-10 is able to inhibit M1 macrophage activation and promote M2 activation (Villalta et al., 2011). Even if glycation itself does not induce a phenotype switch in the M2 macrophages, it could still explain the pro-inflammatory environment of the diabetic wounds. Nevertheless, the exposure time of the macrophage phenotypes to the glycating agent is limited in this setup. Therefore, it cannot be excluded completely, whether longer incubation times with MGO, for example over years or decades in diabetic patients, could be able to induce a polarization switch of macrophages in wounds.

5 Summary

Glycation and the accumulation of AGEs are known to have negative effects during aging as well as in several disease models. Especially in diabetes, high concentrations of MGO and elevated glycolysis rates lead to their accumulation. Regarding impaired wound healing in diabetic and elderly patients, it is known that macrophages play a pivotal role, but the concrete mechanisms underlying their dysfunction are still not completely elucidated. Based on the findings, that wound healing is impaired in diabetes as well as during the aging process as such, the influence of glycation and AGEs on macrophages should be investigated in this thesis. For first investigations, THP-1 macrophages were treated with different concentrations of MGO in order to induce glycation. A positive correlation between MGO concentrations and intensity of glycation could be detected. It could also be verified that surface proteins were glycated as well as intracellular proteins. Next, the metabolic activity and the induction of apoptosis by MGO treatment were investigated. It could be shown that only concentrations above 1 mM MGO (e.g. 1.5 mM and 2 mM MGO) were able to reduce metabolic activity of the macrophages and induce apoptosis. In order to differentiate between effects of glycation and effects of soluble AGEs that bind to their receptors and induce signalling (e.g. RAGE), macrophages were also treated with AGE-FCS in the experimental setups. It could be shown that AGE-FCS activated RAGE, which resulted in overexpression of RAGE as a positive feedback loop. An overexpression of NF- κ B could also be seen after RAGE activation and indicates activation of NF- κ B. Treatment with MGO instead did not result in RAGE or NF- κ B activation. These experiments were crucial in order to exclude if the effects of glycation come from AGE-formation in the medium or can be directly related to glycation of cellular proteins. For activation analyses of macrophages, the expression of pro- and anti-inflammatory cytokines was investigated on mRNA as well as on protein level after glycation or treatment with AGE-FCS. An overexpression of pro-inflammatory cytokines IL-1 β , IL-6, IL-8 and TNF- α was detected after glycation of M1 macrophages, indicating prolonged inflammation phases. In M2 macrophages, pro-inflammatory cytokine IL-8 and TNF- α were overexpressed as well as anti-inflammatory cytokine IL-10. In both phenotypes, AGE-FCS did not have an influence on cytokine expression. These data demonstrate that glycation triggers even anti-inflammatory macrophages to secrete more pro-inflammatory cytokines. Next, also functional abilities of macrophages were analysed. Their phagocytic efficiency was measured after glycation or treatment with

AGEs. In M1 and M2 macrophages, phagocytosis was reduced after glycation while AGEs did not have any influence. This demonstrates that even though the cells are pro-inflammatory active, their ability to remove microbes or cell debris is decreased. This can also lead to prolonged inflammation phases. It could be verified that receptors important for phagocytosis, like TLR4, are glycated after treatment with MGO. This could explain why phagocytosis is reduced, because glycated receptors are known to have lower binding affinities to their substrates. As another point, the polarization phenotype of macrophages was verified after glycation and treatment with AGEs. Although both macrophage phenotypes seem to be pro-inflammatory stimulated by glycation, a switch in their polarization state could not be demonstrated. Taken all this together, this thesis shows that glycation indeed has an influence on macrophage activation and triggers them to a more pro-inflammatory behaviour. These findings could therefore contribute to the understanding of disturbed wound healing during diabetes as well as during normal aging.

References

- Akhand**, A.A; Hossain, K; Mitsui, H; Kato, M; Miyata, T; Inagi, R; Du, J; Takeda, K; Kawamoto, Y; Suzuki, H; Kurokawa, K; Nakashima, I., 2001. Glyoxal and methylglyoxal trigger distinct signals for map family kinases and caspase activation in human endothelial cells. *Free radical biology & medicine* 31, 20–30.
- Akirav**, E.M; Preston-Hurlburt, P; Garyu, J; Henegariu, O; Clynes, R; Schmidt, A. M; Herold, K. C., 2012. RAGE expression in human T cells: A link between environmental factors and adaptive immune responses. *PloS one* 7, e34698. 10.1371/journal.pone.0034698.
- Ali**, M.F; Driscoll, C. B; Walters, P. R; Limper, A. H; Carmona, E. M., 2015. β -Glucan-Activated Human B Lymphocytes Participate in Innate Immune Responses by Releasing Proinflammatory Cytokines and Stimulating Neutrophil Chemotaxis. *Journal of immunology* (Baltimore, Md. : 1950) 195, 5318–5326. 10.4049/jimmunol.1500559.
- Anand**, R.J; Kohler, J. W; Cavallo, J. A; Li, J; Dubowski, T; Hackam, D. J., 2007. Toll-like receptor 4 plays a role in macrophage phagocytosis during peritoneal sepsis. *Journal of pediatric surgery* 42, 927-32; discussion 933. 10.1016/j.jpedsurg.2007.01.023.
- Angeloni**, C; Zambonin, L; Hrelia, S., 2014. Role of methylglyoxal in Alzheimer's disease. *BioMed research international* 2014, 238485. 10.1155/2014/238485.
- Araki**, N; Higashi, T; Mori, T; Shibayama, R; Kawabe, Y; Kodama, T; Takahashi, K; Shichiri, M; Horiuchi, S., 1995. Macrophage Scavenger Receptor Mediates the Endocytic Uptake and Degradation of Advanced Glycation End Products of the Maillard Reaction. *European journal of biochemistry* 230, 408–415. 10.1111/j.1432-1033.1995.0408h.x.
- Baltzis**, D; Eleftheriadou, I; Veves, A., 2014. Pathogenesis and Treatment of Impaired Wound Healing in Diabetes Mellitus: New Insights. *Advances in Therapy* 31, 817–836. 10.1007/s12325-014-0140-x.
- Barros**, M.H.M; Hauck, F; Dreyer, J. H; Kempkes, B; Niedobitek, G., 2013. Macrophage polarisation: An immunohistochemical approach for identifying M1 and M2 macrophages. *PloS one* 8, e80908. 10.1371/journal.pone.0080908.
- Basu Mallik**, S; Jayashree, B. S; Shenoy, R. R., 2018. Epigenetic modulation of macrophage polarization- perspectives in diabetic wounds. *Journal of diabetes and its complications* 32, 524–530. 10.1016/j.jdiacomp.2018.01.015.
- Baynes**, J.W., 1991. Role of oxidative stress in development of complications in diabetes. *Diabetes* 40, 405–412. 10.2337/diab.40.4.405.
- Beeri**, M.S; Moshier, E; Schmeidler, J; Godbold, J; Uribarri, J; Reddy, S; Sano, M; Grossman, H. T; Cai, W; Vlassara, H; Silverman, J. M., 2011. Serum concentration of an inflammatory glycotoxin, methylglyoxal, is associated with increased cognitive decline in elderly individuals. *Mechanisms of ageing and development* 132, 583–587. 10.1016/j.mad.2011.10.007.
- Beisswenger**, P.J., 2014. Methylglyoxal in diabetes: Link to treatment, glycaemic control and biomarkers of complications. *Biochemical Society transactions* 42, 450–456. 10.1042/BST20130275.
- Beisswenger**, P.J; Drummond, K. S; Nelson, R. G; Howell, S. K; Szwergold, B. S; Mauer, M., 2005. Susceptibility to diabetic nephropathy is related to dicarbonyl and oxidative stress. *Diabetes* 54, 3274–3281. 10.2337/diabetes.54.11.3274.
- Bennmann**, D; Horstkorte, R; Hofmann, B; Jacobs, K; Navarrete-Santos, A; Simm, A; Bork, K; Gnanapragassam, V. S., 2014. Advanced glycation endproducts interfere with adhesion and neurite outgrowth. *PloS one* 9, e112115. 10.1371/journal.pone.0112115.
- Bennmann**, D; Kannicht, C; Fisseau, C; Jacobs, K; Navarrete-Santos, A; Hofmann, B; Horstkorte, R., 2015. Glycation of the high affinity NGF-receptor and RAGE leads to reduced ligand affinity. *Mechanisms of ageing and development* 150, 1–11. 10.1016/j.mad.2015.07.003.
- Bento**, C.F; Marques, F; Fernandes, R; Pereira, P., 2010. Methylglyoxal alters the function and stability of critical components of the protein quality control. *PloS one* 5, e13007. 10.1371/journal.pone.0013007.

- Bezold, V;** Rosenstock, P; Scheffler, J; Geyer, H; Horstkorte, R; Bork, K., 2019. Glycation of macrophages induces expression of pro-inflammatory cytokines and reduces phagocytic efficiency. *aging* 11, 5258–5275. 10.18632/aging.102123.
- Bierhaus, A;** Humpert, P. M; Morcos, M; Wendt, T; Chavakis, T; Arnold, B; Stern, D. M; Nawroth, P. P., 2005. Understanding RAGE, the receptor for advanced glycation end products. *Journal of molecular medicine (Berlin, Germany)* 83, 876–886. 10.1007/s00109-005-0688-7.
- Blander, J.M.,** 2014. A long-awaited merger of the pathways mediating host defence and programmed cell death. *Nature Reviews Immunology* 14, 601 EP -. 10.1038/nri3720.
- Boniakowski, A.E;** Kimball, A. S; Jacobs, B. N; Kunkel, S. L; Gallagher, K. A., 2017. Macrophage-Mediated Inflammation in Normal and Diabetic Wound Healing. *Journal of immunology (Baltimore, Md. : 1950)* 199, 17–24. 10.4049/jimmunol.1700223.
- Boyer, F;** Vidot, J. B; Dubourg, A. G; Rondeau, P; Essop, M. F; Bourdon, E., 2015. Oxidative stress and adipocyte biology: Focus on the role of AGEs. *Oxidative medicine and cellular longevity* 2015, 534873. 10.1155/2015/534873.
- Brandt, R.B;** Siegel, S. A., 1978. Methylglyoxal production in human blood. *Ciba Foundation symposium*, 211–223.
- Brat, D.J;** Bellail, A. C; van Meir, E. G., 2005. The role of interleukin-8 and its receptors in gliomagenesis and tumoral angiogenesis. *Neuro-oncology* 7, 122–133. 10.1215/S1152851704001061.
- Brett, J;** Schmidt, A. M; Yan, S. D; Zou, Y. S; Weidman, E; Pinsky, D; Nowygrod, R; Neeper, M; Przysecki, C; Shaw, A., 1993. Survey of the distribution of a newly characterized receptor for advanced glycation end products in tissues. *The American journal of pathology* 143, 1699–1712.
- Bulteau, A.L;** Verbeke, P; Petropoulos, I; Chaffotte, A. F; Friguet, B., 2001. Proteasome inhibition in glyoxal-treated fibroblasts and resistance of glycated glucose-6-phosphate dehydrogenase to 20 S proteasome degradation in vitro. *The Journal of biological chemistry* 276, 45662–45668. 10.1074/jbc.M105374200.
- Cerami, A.,** 1985. Hypothesis. Glucose as a mediator of aging. *Journal of the American Geriatrics Society* 33, 626–634.
- Cerami, C;** Founds, H; Nicholl, I; Mitsuhashi, T; Giordano, D; Vanpatten, S; Lee, A; Al-Abed, Y; Vlassara, H; Bucala, R; Cerami, A., 1997. Tobacco smoke is a source of toxic reactive glycation products. *Proceedings of the National Academy of Sciences of the United States of America* 94, 13915–13920.
- Cerretti, D.P;** Kozlosky, C. J; Mosley, B; Nelson, N; van Ness, K; Greenstreet, T. A; March, C. J; Kronheim, S. R; Druck, T; Cannizzaro, L. A., 1992. Molecular cloning of the interleukin-1 beta converting enzyme. *Science (New York, N.Y.)* 256, 97–100. 10.1126/science.1373520.
- Chakrabarti, A;** Talukdar, D; Pal, A; Ray, M., 2014. Immunomodulation of macrophages by methylglyoxal conjugated with chitosan nanoparticles against Sarcoma-180 tumor in mice. *Cellular immunology* 287, 27–35. 10.1016/j.cellimm.2013.11.006.
- Chanput, W;** Mes, J; Vreeburg, R. A. M; Savelkoul, H. F. J; Wichers, H. J., 2010. Transcription profiles of LPS-stimulated THP-1 monocytes and macrophages: A tool to study inflammation modulating effects of food-derived compounds. *Food & function* 1, 254–261. 10.1039/c0fo00113a.
- Chistiakov, D.A;** Killingsworth, M. C; Myasoedova, V. A; Orekhov, A. N; Bobryshev, Y. V., 2017. CD68/macrosialin: Not just a histochemical marker. *Laboratory investigation; a journal of technical methods and pathology* 97, 4–13. 10.1038/labinvest.2016.116.
- Chuah, Y.K;** Basir, R; Talib, H; Tie, T. H; Nordin, N., 2013. Receptor for advanced glycation end products and its involvement in inflammatory diseases. *International journal of inflammation* 2013, 403460. 10.1155/2013/403460.
- Coughlan, M.T;** Thorburn, D. R; Penfold, S. A; Laskowski, A; Harcourt, B. E; Sourris, K. C; Tan, A. L. Y; Fukami, K; Thallas-Bonke, V; Nawroth, P. P; Brownlee, M; Bierhaus, A; Cooper, M. E; Forbes, J. M., 2009. RAGE-induced cytosolic ROS promote mitochondrial superoxide generation in diabetes. *Journal of the American Society of Nephrology : JASN* 20, 742–752. 10.1681/ASN.2008050514.

- Diez**, R.L; Shekhtman, A; Ramasamy, R; Schmidt, A. M., 2016. Cellular Mechanisms and Consequences of Glycation in Atherosclerosis and Obesity. *Biochimica et biophysica acta* 1862, 2244–2252. 10.1016/j.bbadis.2016.05.005.
- Dinarello**, C.A., 1998. Interleukin-1 beta, interleukin-18, and the interleukin-1 beta converting enzyme. *Annals of the New York Academy of Sciences* 856, 1–11.
- Du**, J; Suzuki, H; Nagase, F; Akhand, A. A; Yokoyama, T; Miyata, T; Kurokawa, K; Nakashima, I., 2000. Methylglyoxal induces apoptosis in Jurkat leukemia T cells by activating c-Jun N-Terminal kinase. *J. Cell. Biochem.* 77, 333–344. 10.1002/(SICI)1097-4644(20000501)77:2<333:AID-JCB15>3.0.CO;2-Q.
- Duluc**, D; Delneste, Y; Tan, F; Moles, M.-P; Grimaud, L; Lenoir, J; Preisser, L; Anegon, I; Catala, L; Ifrah, N; Descamps, P; Gamelin, E; Gascan, H; Hebbar, M; Jeannin, P., 2007. Tumor-associated leukemia inhibitory factor and IL-6 skew monocyte differentiation into tumor-associated macrophage-like cells. *Blood* 110, 4319–4330. 10.1182/blood-2007-02-072587.
- Dunn**, J.A; Patrick, J. S; Thorpe, S. R; Baynes, J. W., 1989. Oxidation of glycated proteins: Age-dependent accumulation of N epsilon-(carboxymethyl)lysine in lens proteins. *Biochemistry* 28, 9464–9468. 10.1021/bi00450a033.
- Falanga**, V., 2005. Wound healing and its impairment in the diabetic foot. *Lancet (London, England)* 366, 1736–1743. 10.1016/S0140-6736(05)67700-8.
- Falcone**, C; Bozzini, S; D'Angelo, A; Matrone, B; Colonna, A; Benzi, A; Paganini, E. M; Falcone, R; Pelissero, G., 2013. Plasma levels of soluble receptor for advanced glycation end products and coronary atherosclerosis: Possible correlation with clinical presentation. *Disease markers* 35, 135–140. 10.1155/2013/129360.
- Fiorentino**, D.F., 1989. Two types of mouse T helper cell. IV. Th2 clones secrete a factor that inhibits cytokine production by Th1 clones. *Journal of Experimental Medicine* 170, 2081–2095. 10.1084/jem.170.6.2081.
- Firestone**, G.L; Winguth, S. D., 1990. Immunoprecipitation of proteins. *Methods in enzymology* 182, 688–700.
- Fitzgerald**, K.A; Rowe, D. C; Golenbock, D. T., 2004. Endotoxin recognition and signal transduction by the TLR4/MD2-complex. *Microbes and infection* 6, 1361–1367. 10.1016/j.micinf.2004.08.015.
- Forero**, A; Moore, P. S; Sarkar, S. N., 2013. Role of IRF4 in IFN-stimulated gene induction and maintenance of Kaposi sarcoma-associated herpesvirus latency in primary effusion lymphoma cells. *Journal of immunology (Baltimore, Md. : 1950)* 191, 1476–1485. 10.4049/jimmunol.1202514.
- Franklin**, B.S; Bossaller, L; Nardo, D. de; Ratter, J. M; Stutz, A; Engels, G; Brenker, C; Nordhoff, M; Mirandola, S. R; Al-Amoudi, A; Mangan, M. S; Zimmer, S; Monks, B. G; Fricke, M; Schmidt, R. E; Espevik, T; Jones, B; Jarnicki, A. G; Hansbro, P. M; Busto, P; Marshak-Rothstein, A; Hornemann, S; Aguzzi, A; Kastentmüller, W; Latz, E., 2014. The adaptor ASC has extracellular and 'prionoid' activities that propagate inflammation. *Nature immunology* 15, 727–737. 10.1038/ni.2913.
- Goerd**, S; Orfanos, C. E., 1999. Other functions, other genes: Alternative activation of antigen-presenting cells. *Immunity* 10, 137–142.
- Gordon**, S., 2003. Alternative activation of macrophages. *Nature reviews. Immunology* 3, 23–35. 10.1038/nri978.
- Gordon**, S., 2007. The macrophage: Past, present and future. *European journal of immunology* 37 Suppl 1, S9-17. 10.1002/eji.200737638.
- Grimm**, S; Ernst, L; Grötzinger, N; Höhn, A; Breusing, N; Reinheckel, T; Grune, T., 2010. Cathepsin D is one of the major enzymes involved in intracellular degradation of AGE-modified proteins. *Free Radical Research* 44, 1013–1026. 10.3109/10715762.2010.495127.
- Grimm**, S; Ott, C; Hörlacher, M; Weber, D; Höhn, A; Grune, T., 2012. Advanced-glycation-end-product-induced formation of immunoproteasomes: Involvement of RAGE and Jak2/STAT1. *The Biochemical journal* 448, 127–139. 10.1042/BJ20120298.
- Gugliucci**, A; Bendayan, M., 1996. Renal fate of circulating advanced glycated end products (AGE): Evidence for reabsorption and catabolism of AGE-peptides by renal proximal tubular cells. *Diabetologia* 39, 149–160. 10.1007/BF00403957.

- Gundra**, U.M; Girgis, N. M; Ruckerl, D; Jenkins, S; Ward, L. N; Kurtz, Z. D; Wiens, K. E; Tang, M. S; Basu-Roy, U; Mansukhani, A; Allen, J. E; Loke, P.n., 2014. Alternatively activated macrophages derived from monocytes and tissue macrophages are phenotypically and functionally distinct. *Blood* 123, e110-22. 10.1182/blood-2013-08-520619.
- Hamilton**, J.A; Achuthan, A., 2013. Colony stimulating factors and myeloid cell biology in health and disease. *Trends in immunology* 34, 81–89. 10.1016/j.it.2012.08.006.
- Han**, Y; Randell, E; Vasdev, S; Gill, V; Gadag, V; Newhook, L. A; Grant, M; Hagerty, D., 2007. Plasma methylglyoxal and glyoxal are elevated and related to early membrane alteration in young, complication-free patients with Type 1 diabetes. *Molecular and cellular biochemistry* 305, 123–131. 10.1007/s11010-007-9535-1.
- Harada**, A; Sekido, N; Akahoshi, T; Wada, T; Mukaida, N; Matsushima, K., 1994. Essential involvement of interleukin-8 (IL-8) in acute inflammation. *Journal of leukocyte biology* 56, 559–564.
- Harlow**, E; Lane, David, 1988. *Antibodies: A laboratory manual*. Cold Spring Harbor Laboratory, New York, XIII, 726.
- Henle**, T., 2003. AGEs in foods: Do they play a role in uremia? *Kidney international*. Supplement, S145-7. 10.1046/j.1523-1755.63.s84.16.x.
- Henle**, T., 2005. Protein-bound advanced glycation endproducts (AGEs) as bioactive amino acid derivatives in foods. *Amino Acids* 29, 313–322. 10.1007/s00726-005-0200-2.
- Henning**, C; Glomb, M. A., 2016. Pathways of the Maillard reaction under physiological conditions. *Glycoconjugate journal* 33, 499–512. 10.1007/s10719-016-9694-y.
- Herold**, K; Moser, B; Chen, Y; Zeng, S; Yan, S. F; Ramasamy, R; Emond, J; Clynes, R; Schmidt, A. M., 2007. Receptor for advanced glycation end products (RAGE) in a dash to the rescue: Inflammatory signals gone awry in the primal response to stress. *Journal of leukocyte biology* 82, 204–212. 10.1189/jlb.1206751.
- Hori**, O; Brett, J; Slattery, T; Cao, R; Zhang, J; Chen, J. X; Nagashima, M; Lundh, E. R; Vijay, S; Nitecki, D., 1995. The receptor for advanced glycation end products (RAGE) is a cellular binding site for amphoterin. Mediation of neurite outgrowth and co-expression of rage and amphoterin in the developing nervous system. *The Journal of biological chemistry* 270, 25752–25761. 10.1074/jbc.270.43.25752.
- Horiuchi**, S; Sakamoto, Y; Sakai, M., 2003. Scavenger receptors for oxidized and glycated proteins. *Amino Acids* 25, 283–292. 10.1007/s00726-003-0029-5.
- Italiani**, P; Boraschi, D., 2014. From Monocytes to M1/M2 Macrophages: Phenotypical vs. Functional Differentiation. *Frontiers in immunology* 5, 514. 10.3389/fimmu.2014.00514.
- Jakus**, V; Rietbrock, N., 2004. Advanced glycation end-products and the progress of diabetic vascular complications. *Physiological research* 53, 131–142.
- Jones**, E.Y; Fugger, L; Strominger, J. L; Siebold, C., 2006. MHC class II proteins and disease: A structural perspective. *Nature reviews. Immunology* 6, 271–282. 10.1038/nri1805.
- Jono**, T; Miyazaki, A; Nagai, R; Sawamura, T; Kitamura, T; Horiuchi, S., 2002. Lectin-like oxidized low density lipoprotein receptor-1 (LOX-1) serves as an endothelial receptor for advanced glycation end products (AGE). *FEBS Letters* 511, 170–174. 10.1016/S0014-5793(01)03325-7.
- Kalapos**, M.P., 2008a. Methylglyoxal and glucose metabolism: A historical perspective and future avenues for research. *Drug Metabolism and Drug Interactions* 23, 69–91.
- Kalapos**, M.P., 2008b. The tandem of free radicals and methylglyoxal. *Chemico-biological interactions* 171, 251–271. 10.1016/j.cbi.2007.11.009.
- Kang**, Y; Edwards, L. G; Thornalley, P. J., 1996. Effect of methylglyoxal on human leukaemia 60 cell growth: Modification of DNA G1 growth arrest and induction of apoptosis. *Leukemia research* 20, 397–405.
- Kanneganti**, T.-D., 2015. The inflammasome: Firing up innate immunity. *Immunological reviews* 265, 1–5. 10.1111/imr.12297.
- Kierdorf**, K; Fritz, G., 2013. RAGE regulation and signaling in inflammation and beyond. *Journal of leukocyte biology* 94, 55–68. 10.1189/jlb.1012519.
- Kim**, S.Y; Nair, M. G., 2019. Macrophages in wound healing: Activation and plasticity. *Immunology and cell biology* 97, 258–267. 10.1111/imcb.12236.
- Kishimoto**, T., 1985. Factors affecting B-cell growth and differentiation. *Annual review of immunology* 3, 133–157. 10.1146/annurev.iy.03.040185.001025.

- Kishimoto**, T., 1989. The biology of interleukin-6. *Blood* 74, 1–10.
- Kloc**, M. (Ed.), 2017. *Macrophages: Origin, Functions and Biointervention*. Springer International Publishing, Cham, s.l., 27 pp.
- Knecht**, K.J; Dunn, J. A; McFarland, K. F; McCance, D. R; Lyons, T. J; Thorpe, S. R; Baynes, J. W., 1991. Effect of diabetes and aging on carboxymethyllysine levels in human urine. *Diabetes* 40, 190–196. 10.2337/diab.40.2.190.
- Kong**, X; Ma, M.-z; Huang, K; Qin, L; Zhang, H.-m; Yang, Z; Li, X.-y; Su, Q., 2014. Increased plasma levels of the methylglyoxal in patients with newly diagnosed type 2 diabetes 2. *Journal of diabetes* 6, 535–540. 10.1111/1753-0407.12160.
- Kotwal**, G.J; Chien, S., 2017. Macrophage Differentiation in Normal and Accelerated Wound Healing. Results and problems in cell differentiation 62, 353–364. 10.1007/978-3-319-54090-0_14.
- Kristiansen**, M; Graversen, J. H; Jacobsen, C; Sonne, O; Hoffman, H. J; Law, S. K; Moestrup, S. K., 2001. Identification of the haemoglobin scavenger receptor. *Nature* 409, 198–201. 10.1038/35051594.
- Kröger**, K; Berg, C; Santosa, F; Malyar, N; Reinecke, H., 2017. Lower Limb Amputation in Germany. *Deutsches Arzteblatt international* 114, 130–136. 10.3238/arztebl.2017.0130.
- Kueper**, T; Grune, T; Prah, S; Lenz, H; Welge, V; Biernoth, T; Vogt, Y; Muhr, G.-M; Gaemlich, A; Jung, T; Boemke, G; Elsässer, H.-P; Wittern, K.-P; Wenck, H; Stäb, F; Blatt, T., 2007. Vimentin is the specific target in skin glycation. Structural prerequisites, functional consequences, and role in skin aging. *The Journal of biological chemistry* 282, 23427–23436. 10.1074/jbc.M701586200.
- Kuhla**, B; Lüth, H.-J; Haferburg, D; Boeck, K; Arendt, T; Münch, G., 2005. Methylglyoxal, glyoxal, and their detoxification in Alzheimer's disease. *Annals of the New York Academy of Sciences* 1043, 211–216. 10.1196/annals.1333.026.
- Kumaresan**, V; Ravichandran, G; Nizam, F; Dhayanithi, N. B; Arasu, M. V; Al-Dhabi, N. A; Harikrishnan, R; Arockiaraj, J., 2016. Multifunctional murrel caspase 1, 2, 3, 8 and 9: Conservation, uniqueness and their pathogen-induced expression pattern. *Fish & shellfish immunology* 49, 493–504. 10.1016/j.fsi.2016.01.008.
- Laemmli**, U.K., 1970. Cleavage of Structural Proteins during the Assembly of the Head of Bacteriophage T4. *Nature* 227, 680–685. 10.1038/227680a0.
- Lamkanfi**, M; Dixit, V. M., 2014. Mechanisms and functions of inflammasomes. *Cell* 157, 1013–1022. 10.1016/j.cell.2014.04.007.
- Lavery**, L.A; Armstrong, D. G; Wunderlich, R. P; Tredwell, J; Boulton, A. J. M., 2003. Diabetic foot syndrome: Evaluating the prevalence and incidence of foot pathology in Mexican Americans and non-Hispanic whites from a diabetes disease management cohort. *Diabetes care* 26, 1435–1438. 10.2337/diacare.26.5.1435.
- Lavin**, Y; Mortha, A; Rahman, A; Merad, M., 2015. Regulation of macrophage development and function in peripheral tissues. *Nature reviews. Immunology* 15, 731–744. 10.1038/nri3920.
- Lee**, D.-Y; Chang, G.-D., 2014. Methylglyoxal in cells elicits a negative feedback loop entailing transglutaminase 2 and glyoxalase 1. *Redox biology* 2, 196–205. 10.1016/j.redox.2013.12.024.
- Lee**, E.J; Park, J. H., 2013. Receptor for Advanced Glycation Endproducts (RAGE), Its Ligands, and Soluble RAGE: Potential Biomarkers for Diagnosis and Therapeutic Targets for Human Renal Diseases. *Genomics & informatics* 11, 224–229. 10.5808/GI.2013.11.4.224.
- Lewis**, C.E; McGee, J. O'D, 1992. *The Macrophage*. IRL Press at Oxford University Press, Oxford, New York, xxii, 423.
- Li**, Y.M; Mitsuhashi, T; Wojciechowicz, D; Shimizu, N; Li, J; Stitt, A; He, C; Banerjee, D; Vlassara, H., 1996. Molecular identity and cellular distribution of advanced glycation endproduct receptors: Relationship of p60 to OST-48 and p90 to 80K-H membrane proteins. *Proceedings of the National Academy of Sciences of the United States of America* 93, 11047–11052. 10.1073/pnas.93.20.11047.
- Lin**, J; Zhou, Z; Huo, R; Xiao, L; Ouyang, G; Wang, L; Sun, Y; Shen, B; Li, D; Li, N., 2012. Cyr61 induces IL-6 production by fibroblast-like synoviocytes promoting Th17

- differentiation in rheumatoid arthritis. *Journal of immunology* (Baltimore, Md. : 1950) 188, 5776–5784. 10.4049/jimmunol.1103201.
- Lindley**, L.E; Stojadinovic, O; Pastar, I; Tomic-Canic, M., 2016. Biology and Biomarkers for Wound Healing. *Plastic and reconstructive surgery* 138, 18S-28S. 10.1097/PRS.0000000000002682.
- Liu**, Y; Liang, C; Liu, X; Liao, B; Pan, X; Ren, Y; Fan, M; Li, M; He, Z; Wu, J; Wu, Z., 2010. AGEs increased migration and inflammatory responses of adventitial fibroblasts via RAGE, MAPK and NF-kappaB pathways. *Atherosclerosis* 208, 34–42. 10.1016/j.atherosclerosis.2009.06.007.
- Livak**, K.J; Schmittgen, T. D., 2001. Analysis of relative gene expression data using real-time quantitative PCR and the 2(-Delta Delta C(T)) Method. *Methods* (San Diego, Calif.) 25, 402–408. 10.1006/meth.2001.1262.
- Loots**, M.A; Lamme, E. N; Zeegelaar, J; Mekkes, J. R; Bos, J. D; Middelkoop, E., 1998. Differences in cellular infiltrate and extracellular matrix of chronic diabetic and venous ulcers versus acute wounds. *The Journal of investigative dermatology* 111, 850–857. 10.1046/j.1523-1747.1998.00381.x.
- Madsen**, D.H; Leonard, D; Masedunskas, A; Moyer, A; Jürgensen, H. J; Peters, D. E; Amornphimoltham, P; Selvaraj, A; Yamada, S. S; Brenner, D. A; Burgdorf, S; Engelholm, L. H; Behrendt, N; Holmbeck, K; Weigert, R; Bugge, T. H., 2013. M2-like macrophages are responsible for collagen degradation through a mannose receptor-mediated pathway. *The Journal of cell biology* 202, 951–966. 10.1083/jcb.201301081.
- Maillard**, L.C., 1912. Action des acides aminés sur les sucres; formation des mélanoides par voie méthodique. *C. R. Acad. Sci. III*, 66–68.
- Mantovani**, A; Sica, A; Sozzani, S; Allavena, P; Vecchi, A; Locati, M., 2004. The chemokine system in diverse forms of macrophage activation and polarization. *Trends in immunology* 25, 677–686. 10.1016/j.it.2004.09.015.
- Mariathasan**, S; Newton, K; Monack, D. M; Vucic, D; French, D. M; Lee, W. P; Roose-Girma, M; Erickson, S; Dixit, V. M., 2004. Differential activation of the inflammasome by caspase-1 adaptors ASC and Ipaf. *Nature* 430, 213–218. 10.1038/nature02664.
- Martin**, P; Leibovich, S. J., 2005. Inflammatory cells during wound repair: The good, the bad and the ugly. *Trends in cell biology* 15, 599–607. 10.1016/j.tcb.2005.09.002.
- Martinez**, F.O; Helming, L; Gordon, S., 2009. Alternative activation of macrophages: An immunologic functional perspective. *Annual review of immunology* 27, 451–483. 10.1146/annurev.immunol.021908.132532.
- Martinon**, F; Burns, K; Tschopp, J., 2002. The Inflammasome: A Molecular Platform Triggering Activation of Inflammatory Caspases and Processing of proIL- β . *Molecular Cell* 10, 417–426. 10.1016/S1097-2765(02)00599-3.
- McLellan**, A.C; Thornalley, P. J., 1992. Synthesis and chromatography of 1,2-diamino-4,5-dimethoxybenzene, 6,7-dimethoxy-2-methylquinoxaline and 6,7-dimethoxy-2,3-dimethylquinoxaline for use in a liquid chromatographic fluorimetric assay of methylglyoxal. *Analytica Chimica Acta* 263, 137–142. 10.1016/0003-2670(92)85435-9.
- McLellan**, A.C; Thornalley, P. J; Benn, J; Sonksen, P. H., 1994. Glyoxalase System in Clinical Diabetes Mellitus and Correlation with Diabetic Complications. *Clin. Sci.* 87, 21–29. 10.1042/cs0870021.
- Mills**, C.D; Kincaid, K; Alt, J. M; Heilman, M. J; Hill, A. M., 2000. M-1/M-2 macrophages and the Th1/Th2 paradigm. *Journal of immunology* (Baltimore, Md. : 1950) 164, 6166–6173. 10.4049/jimmunol.164.12.6166.
- Minutti**, C.M; Knipper, J. A; Allen, J. E; Zaiss, D. M. W., 2017. Tissue-specific contribution of macrophages to wound healing. *Seminars in cell & developmental biology* 61, 3–11. 10.1016/j.semcdb.2016.08.006.
- Mirza**, R.E; Fang, M. M; Ennis, W. J; Koh, T. J., 2013. Blocking interleukin-1 β induces a healing-associated wound macrophage phenotype and improves healing in type 2 diabetes. *Diabetes* 62, 2579–2587. 10.2337/db12-1450.
- Miyata**, S; Liu, B. F; Shoda, H; Ohara, T; Yamada, H; Suzuki, K; Kasuga, M., 1997. Accumulation of pyrraline-modified albumin in phagocytes due to reduced degradation by

- lysosomal enzymes. *The Journal of biological chemistry* 272, 4037–4042. 10.1074/jbc.272.7.4037.
- Morgan, E;** Varro, R; Sepulveda, H; Ember, J. A; Apgar, J; Wilson, J; Lowe, L; Chen, R; Shivraj, L; Agadir, A; Campos, R; Ernst, D; Gaur, A., 2004. Cytometric bead array: A multiplexed assay platform with applications in various areas of biology. *Clinical immunology (Orlando, Fla.)* 110, 252–266. 10.1016/j.clim.2003.11.017.
- Mosser, D.M;** Edwards, J. P., 2008. Exploring the full spectrum of macrophage activation. *Nature reviews. Immunology* 8, 958–969. 10.1038/nri2448.
- Murray, P.J.,** 2017. Macrophage Polarization. *Annual review of physiology* 79, 541–566. 10.1146/annurev-physiol-022516-034339.
- Nathan, C.F;** Murray, H. W; Wiebe, M. E; Rubin, B. Y., 1983. Identification of interferon-gamma as the lymphokine that activates human macrophage oxidative metabolism and antimicrobial activity. *Journal of Experimental Medicine* 158, 670–689. 10.1084/jem.158.3.670.
- Neepser, M;** Schmidt, A. M; Brett, J; Yan, S. D; Wang, F; Pan, Y. C; Elliston, K; Stern, D; Shaw, A., 1992. Cloning and expression of a cell surface receptor for advanced glycosylation end products of proteins. *The Journal of biological chemistry* 267, 14998–15004.
- Negre-Salvayre, A;** Salvayre, R; Augé, N; Pamplona, R; Portero-Otín, M., 2009. Hyperglycemia and glycation in diabetic complications. *Antioxidants & redox signaling* 11, 3071–3109. 10.1089/ars.2009.2484.
- Nemet, I;** Turk, Z; Duvnjak, L; Car, N; Varga-Defterdarović, L., 2005. Humoral methylglyoxal level reflects glycemic fluctuation. *Clinical biochemistry* 38, 379–383. 10.1016/j.clinbiochem.2004.12.008.
- Novak, M.L;** Koh, T. J., 2013. Macrophage phenotypes during tissue repair. *Journal of leukocyte biology* 93, 875–881. 10.1189/jlb.1012512.
- Ohashi, K;** Takahashi, H. K; Mori, S; Liu, K; Wake, H; Sadamori, H; Matsuda, H; Yagi, T; Yoshino, T; Nishibori, M; Tanaka, N., 2010. Advanced glycation end products enhance monocyte activation during human mixed lymphocyte reaction. *Clinical immunology (Orlando, Fla.)* 134, 345–353. 10.1016/j.clim.2009.10.008.
- Ohgami, N;** Nagai, R; Ikemoto, M; Arai, H; Kuniyasu, A; Horiuchi, S; Nakayama, H., 2001a. CD36, a member of class B scavenger receptor family, is a receptor for advanced glycation end products. *Annals of the New York Academy of Sciences* 947, 350–355. 10.1111/j.1749-6632.2001.tb03961.x.
- Ohgami, N;** Nagai, R; Miyazaki, A; Ikemoto, M; Arai, H; Horiuchi, S; Nakayama, H., 2001b. Scavenger receptor class B type I-mediated reverse cholesterol transport is inhibited by advanced glycation end products. *The Journal of biological chemistry* 276, 13348–13355. 10.1074/jbc.M011613200.
- Olszewski, M.B;** Groot, A. J; Dastyh, J; Knol, E. F., 2007. TNF trafficking to human mast cell granules: Mature chain-dependent endocytosis. *Journal of immunology (Baltimore, Md. : 1950)* 178, 5701–5709. 10.4049/jimmunol.178.9.5701.
- Onofre, G;** Koláčková, M; Jankovicová, K; Krejsek, J., 2009. Scavenger receptor CD163 and its biological functions. *Acta medica (Hradec Kralove)* 52, 57–61.
- Ott, C;** Jacobs, K; Haucke, E; Navarrete Santos, A; Grune, T; Simm, A., 2014. Role of advanced glycation end products in cellular signaling. *Redox biology* 2, 411–429. 10.1016/j.redox.2013.12.016.
- Pal, A;** Bhattacharya, I; Bhattacharya, K; Mandal, C; Ray, M., 2009. Methylglyoxal induced activation of murine peritoneal macrophages and surface markers of T lymphocytes in sarcoma-180 bearing mice: Involvement of MAP kinase, NF-kappa beta signal transduction pathway. *Molecular immunology* 46, 2039–2044. 10.1016/j.molimm.2009.03.014.
- Pålsson-McDermott, E.M;** O'Neill, L. A. J., 2004. Signal transduction by the lipopolysaccharide receptor, Toll-like receptor-4. *Immunology* 113, 153–162. 10.1111/j.1365-2567.2004.01976.x.
- Peach, R.J;** Bajorath, J; Naemura, J; Leytze, G; Greene, J; Aruffo, A; Linsley, P. S., 1995. Both extracellular immunoglobulin-like domains of CD80 contain residues critical for binding T cell surface receptors CTLA-4 and CD28. *The Journal of biological chemistry* 270, 21181–21187. 10.1074/jbc.270.36.21181.

- Phillips, S.A;** Mirrlees, D; THORNALLEY, P. J., 1993. Modification of the glyoxalase system in streptozotocin-induced diabetic rats. *Biochemical Pharmacology* 46, 805–811. 10.1016/0006-2952(93)90488-I.
- Phillips, S.A;** Thornalley, P. J., 1993a. Formation of methylglyoxal and D-lactate in human red blood cells in vitro. *Biochemical Society transactions* 21, 163S.
- Phillips, S.A;** Thornalley, P. J., 1993b. The formation of methylglyoxal from triose phosphates. Investigation using a specific assay for methylglyoxal. *European journal of biochemistry* 212, 101–105.
- Pollreis, A;** Hudson, B. I; Chang, J. S; Qu, W; Cheng, B; Papapanou, P. N; Schmidt, A. M; Lalla, E., 2010. Receptor for advanced glycation endproducts mediates pro-atherogenic responses to periodontal infection in vascular endothelial cells. *Atherosclerosis* 212, 451–456. 10.1016/j.atherosclerosis.2010.07.011.
- Porcheray, F;** Viaud, S; Rimaniol, A.-C; Léone, C; Samah, B; Dereuddre-Bosquet, N; Dormont, D; Gras, G., 2005. Macrophage activation switching: An asset for the resolution of inflammation. *Clinical and experimental immunology* 142, 481–489. 10.1111/j.1365-2249.2005.02934.x.
- Qureshi, S.T;** Medzhitov, R., 2003. Toll-like receptors and their role in experimental models of microbial infection. *Genes and immunity* 4, 87–94. 10.1038/sj.gene.6363937.
- Rabbani, N;** Thornalley, P. J., 2012. Methylglyoxal, glyoxalase 1 and the dicarbonyl proteome. *Amino Acids* 42, 1133–1142. 10.1007/s00726-010-0783-0.
- Rabbani, N;** Thornalley, P. J., 2015. Dicarbonyl stress in cell and tissue dysfunction contributing to ageing and disease. *Biochemical and biophysical research communications* 458, 221–226. 10.1016/j.bbrc.2015.01.140.
- Rabbani, N;** Xue, M; THORNALLEY, P. J., 2014. Activity, regulation, copy number and function in the glyoxalase system. *Biochemical Society transactions* 42, 419–424. 10.1042/BST20140008.
- Rachman, H;** Kim, N; Ulrichs, T; Baumann, S; Pradl, L; Nasser Eddine, A; Bild, M; Rother, M; Kuban, R.-J; Lee, J. S; Hurwitz, R; Brinkmann, V; Kosmiadi, G. A; Kaufmann, S. H. E., 2006. Critical role of methylglyoxal and AGE in mycobacteria-induced macrophage apoptosis and activation. *PloS one* 1, e29. 10.1371/journal.pone.0000029.
- Rai, V;** Touré, F; Chitayat, S; Pei, R; Song, F; Li, Q; Zhang, J; Rosario, R; Ramasamy, R; Chazin, W. J; Schmidt, A. M., 2012. Lysophosphatidic acid targets vascular and oncogenic pathways via RAGE signaling. *The Journal of experimental medicine* 209, 2339–2350. 10.1084/jem.20120873.
- Ramachandra Bhat, L;** Vedantham, S; Krishnan, U. M; Rayappan, J. B. B., 2019. Methylglyoxal - An emerging biomarker for diabetes mellitus diagnosis and its detection methods. *Biosensors & bioelectronics* 133, 107–124. 10.1016/j.bios.2019.03.010.
- Ramasamy, R;** Yan, S. F; Herold, K; Clynes, R; Schmidt, A. M., 2008. Receptor for advanced glycation end products: Fundamental roles in the inflammatory response: winding the way to the pathogenesis of endothelial dysfunction and atherosclerosis. *Annals of the New York Academy of Sciences* 1126, 7–13. 10.1196/annals.1433.056.
- Ramasamy, R;** Yan, S. F; Schmidt, A. M., 2012. The diverse ligand repertoire of the receptor for advanced glycation endproducts and pathways to the complications of diabetes. *Vascular pharmacology* 57, 160–167. 10.1016/j.vph.2012.06.004.
- Rath, P.C;** Aggarwal, B. B., 1999. TNF-induced signaling in apoptosis. *Journal of clinical immunology* 19, 350–364.
- Reddy, S;** Bichler, J; Wells-Knecht, K. J; Thorpe, S. R; Baynes, J. W., 1995. N epsilon-(carboxymethyl)lysine is a dominant advanced glycation end product (AGE) antigen in tissue proteins. *Biochemistry* 34, 10872–10878.
- Richard, J.P.**, 1993. Mechanism for the formation of methylglyoxal from triosephosphates. *Biochemical Society transactions* 21, 549–553.
- Rosenstock, P;** Bezold, V; Bork, K; Scheffler, J; Horstkorte, R., 2019. Glycation interferes with natural killer cell function. *Mechanisms of ageing and development* 178, 64–71. 10.1016/j.mad.2019.01.006.
- Röszer, T.**, 2015. Understanding the Mysterious M2 Macrophage through Activation Markers and Effector Mechanisms. *Mediators of inflammation* 2015, 816460. 10.1155/2015/816460.

- Royall**, J.A; Ischiropoulos, H., 1993. Evaluation of 2',7'-dichlorofluorescein and dihydrorhodamine 123 as fluorescent probes for intracellular H₂O₂ in cultured endothelial cells. *Archives of biochemistry and biophysics* 302, 348–355. 10.1006/abbi.1993.1222.
- Saftig**, P; Klumperman, J., 2009. Lysosome biogenesis and lysosomal membrane proteins: Trafficking meets function. *Nature reviews. Molecular cell biology* 10, 623–635. 10.1038/nrm2745.
- Salahuddin**, P; Rabbani, G; Khan, R. H., 2014. The role of advanced glycation end products in various types of neurodegenerative disease: A therapeutic approach. *Cellular & molecular biology letters* 19, 407–437. 10.2478/s11658-014-0205-5.
- Schmoch**, T; Uhle, F; Siegler, B. H; Fleming, T; Morgenstern, J; Nawroth, P. P; Weigand, M. A; Brenner, T., 2017. The Glyoxalase System and Methylglyoxal-Derived Carbonyl Stress in Sepsis: Glycotoxic Aspects of Sepsis Pathophysiology. *International Journal of Molecular Sciences* 18. 10.3390/ijms18030657.
- Shinohara**, M; Thornalley, P. J; Giardino, I; Beisswenger, P; Thorpe, S. R; Onorato, J; Brownlee, M., 1998. Overexpression of glyoxalase-I in bovine endothelial cells inhibits intracellular advanced glycation endproduct formation and prevents hyperglycemia-induced increases in macromolecular endocytosis. *The Journal of clinical investigation* 101, 1142–1147. 10.1172/JCI119885.
- Shiu**, S.W.M; Wong, Y; Tan, K. C. B., 2012. Effect of advanced glycation end products on lectin-like oxidized low density lipoprotein receptor-1 expression in endothelial cells. *Journal of atherosclerosis and thrombosis* 19, 1083–1092. 10.5551/jat.11742.
- Singh**, N; Armstrong, D. G; Lipsky, B. A., 2005. Preventing foot ulcers in patients with diabetes. *JAMA* 293, 217–228. 10.1001/jama.293.2.217.
- Smith**, P.K; Krohn, R. I; Hermanson, G. T; Mallia, A. K; Gartner, F. H; Provenzano, M. D; Fujimoto, E. K; Goeke, N. M; Olson, B. J; Klenk, D. C., 1985. Measurement of protein using bicinchoninic acid. *Analytical Biochemistry* 150, 76–85. 10.1016/0003-2697(85)90442-7.
- Sousa Silva**, M; Gomes, R. A; Ferreira, A. E. N; Ponces Freire, A; Cordeiro, C., 2013. The glyoxalase pathway: The first hundred years... and beyond. *The Biochemical journal* 453, 1–15. 10.1042/BJ20121743.
- Spits**, H; Waal Malefyt, R. de, 1992. Functional characterization of human IL-10. *International archives of allergy and immunology* 99, 8–15. 10.1159/000236329.
- Stein**, M; Keshav, S; Harris, N; Gordon, S., 1992. Interleukin 4 potently enhances murine macrophage mannose receptor activity: A marker of alternative immunologic macrophage activation. *Journal of Experimental Medicine* 176, 287–292. 10.1084/jem.176.1.287.
- Steinbrecher**, U.P; Witztum, J. L., 1984. Glucosylation of low-density lipoproteins to an extent comparable to that seen in diabetes slows their catabolism. *Diabetes* 33, 130–134. 10.2337/diab.33.2.130.
- Stolzing**, A; Widmer, R; Jung, T; Voss, P; Grune, T., 2006. Degradation of glycated bovine serum albumin in microglial cells. *Free radical biology & medicine* 40, 1017–1027. 10.1016/j.freeradbiomed.2005.10.061.
- Stuart**, L.M; Ezekowitz, R. A., 2008. Phagocytosis and comparative innate immunity: Learning on the fly. *Nature reviews. Immunology* 8, 131–141. 10.1038/nri2240.
- Student**, 1908. The Probable Error of a Mean. *Biometrika* 6, 1. 10.2307/2331554.
- Sun**, M; Yokoyama, M; Ishiwata, T; Asano, G., 1998. Deposition of advanced glycation end products (AGE) and expression of the receptor for AGE in cardiovascular tissue of the diabetic rat. *International journal of experimental pathology* 79, 207–222.
- Takahashi**, H.K; Mori, S; Wake, H; Liu, K; Yoshino, T; Ohashi, K; Tanaka, N; Shikata, K; Makino, H; Nishibori, M., 2009. Advanced glycation end products subspecies-selectively induce adhesion molecule expression and cytokine production in human peripheral blood mononuclear cells. *The Journal of pharmacology and experimental therapeutics* 330, 89–98. 10.1124/jpet.109.150581.
- Tamura**, Y; Adachi, H; Osuga, J.-i; Ohashi, K; Yahagi, N; Sekiya, M; Okazaki, H; Tomita, S; Iizuka, Y; Shimano, H; Nagai, R; Kimura, S; Tsujimoto, M; Ishibashi, S., 2003. FEEL-1 and

- FEEL-2 are endocytic receptors for advanced glycation end products. *The Journal of biological chemistry* 278, 12613–12617. 10.1074/jbc.M210211200.
- Tanaka, T;** Narazaki, M; Kishimoto, T., 2014. IL-6 in inflammation, immunity, and disease. *Cold Spring Harbor perspectives in biology* 6, a016295. 10.1101/cshperspect.a016295.
- Tanji, N;** Markowitz, G. S; Fu, C; Kislinger, T; Taguchi, A; Pischetsrieder, M; Stern, D; Schmidt, A. M; D'Agati, V. D., 2000. Expression of advanced glycation end products and their cellular receptor RAGE in diabetic nephropathy and nondiabetic renal disease. *Journal of the American Society of Nephrology* : JASN 11, 1656–1666.
- Tarique, A.A;** Logan, J; Thomas, E; Holt, P. G; Sly, P. D; Fantino, E., 2015. Phenotypic, functional, and plasticity features of classical and alternatively activated human macrophages. *American journal of respiratory cell and molecular biology* 53, 676–688. 10.1165/rcmb.2015-0012OC.
- Tassaneeritthep, B;** Burgess, T. H; Granelli-Piperno, A; Trumfheller, C; Finke, J; Sun, W; Eller, M. A; Pattanapanyasat, K; Sarasombath, S; Birx, D. L; Steinman, R. M; Schlesinger, S; Marovich, M. A., 2003. DC-SIGN (CD209) mediates dengue virus infection of human dendritic cells. *Journal of Experimental Medicine* 197, 823–829. 10.1084/jem.20021840.
- Thornalley, P.J.,** 1988. Modification of the glyoxalase system in human red blood cells by glucose in vitro. *Biochem. J.* 254, 751–755. 10.1042/bj2540751.
- Thornalley, P.J.,** 1990. The glyoxalase system: New developments towards functional characterization of a metabolic pathway fundamental to biological life. *Biochem. J.* 269, 1–11. 10.1042/bj2690001.
- Thornalley, P.J.,** 1993. The glyoxalase system in health and disease. *Molecular aspects of medicine* 14, 287–371.
- Thornalley, P.J.,** 2003. Glyoxalase I-structure, function and a critical role in the enzymatic defence against glycation. *Biochemical Society transactions* 31, 1343–1348.
- Thornalley, P.J;** Langborg, A; Minhas, H. S., 1999. Formation of glyoxal, methylglyoxal and 3-deoxyglucosone in the glycation of proteins by glucose. *Biochem. J.* 344 Pt 1, 109–116.
- Thornberry, N.A;** Bull, H. G; Calaycay, J. R; Chapman, K. T; Howard, A. D; Kostura, M. J; Miller, D. K; Molineaux, S. M; Weidner, J. R; Aunins, J., 1992. A novel heterodimeric cysteine protease is required for interleukin-1 beta processing in monocytes. *Nature* 356, 768–774. 10.1038/356768a0.
- Thuraisingam, T;** Xu, Y. Z; Eadie, K; Heravi, M; Guiot, M.-C; Greemberg, R; Gaestel, M; Radzioch, D., 2010. MAPKAPK-2 signaling is critical for cutaneous wound healing. *The Journal of investigative dermatology* 130, 278–286. 10.1038/jid.2009.209.
- Tomko, R.J;** Hochstrasser, M., 2013. Molecular architecture and assembly of the eukaryotic proteasome. *Annual review of biochemistry* 82, 415–445. 10.1146/annurev-biochem-060410-150257.
- Toshchakov, V;** Jones, B. W; Perera, P.-Y; Thomas, K; Cody, M. J; Zhang, S; Williams, B. R. G; Major, J; Hamilton, T. A; Fenton, M. J; Vogel, S. N., 2002. TLR4, but not TLR2, mediates IFN-beta-induced STAT1alpha/beta-dependent gene expression in macrophages. *Nature immunology* 3, 392–398. 10.1038/ni774.
- Tracey, K.J;** Cerami, A., 1994. Tumor necrosis factor: A pleiotropic cytokine and therapeutic target. *Annual review of medicine* 45, 491–503. 10.1146/annurev.med.45.1.491.
- Tschopp, J;** Martinon, F; Burns, K., 2003. NALPs: A novel protein family involved in inflammation. *Nature reviews. Molecular cell biology* 4, 95–104. 10.1038/nrm1019.
- Tsuchiya, S;** Yamabe, M; Yamaguchi, Y; Kobayashi, Y; Konno, T; Tada, K., 1980. Establishment and characterization of a human acute monocytic leukemia cell line (THP-1). *International journal of cancer* 26, 171–176.
- Ulrich, P;** Cerami, A., 2001. Protein glycation, diabetes, and aging. *Recent progress in hormone research* 56, 1–21.
- Uribarri, J;** del Castillo, M. D; La Maza, M. P. de; Filip, R; Gugliucci, A; Luevano-Contreras, C; Macías-Cervantes, M. H; Markowicz Bastos, D. H; Medrano, A; Menini, T; Portero-Otin, M; Rojas, A; Sampaio, G. R; Wrobel, K; Wrobel, K; Garay-Sevilla, M. E., 2015. Dietary advanced glycation end products and their role in health and disease. *Advances in nutrition (Bethesda, Md.)* 6, 461–473. 10.3945/an.115.008433.

- Vaca**, C.E; Fang, J. L; Conradi, M; Hou, S. M., 1994. Development of a 32P-postlabelling method for the analysis of 2'-deoxyguanosine-3'-monophosphate and DNA adducts of methylglyoxal. *Carcinogenesis* 15, 1887–1894. 10.1093/carcin/15.9.1887.
- van Furth**, R; Cohn, Z. A; Hirsch, J. G; Humphrey, J. H; Spector, W. G; Langevoort, H. L., 1972. The mononuclear phagocyte system: A new classification of macrophages, monocytes, and their precursor cells. *Bulletin of the World Health Organization* 46, 845–852.
- van Heijst**, J.W.J; Niessen, H. W.M; Musters, R. J; van Hinsbergh, V. W.M; Hoekman, K; Schalkwijk, C. G., 2006. Argpyrimidine-modified Heat Shock Protein 27 in human non-small cell lung cancer: A possible mechanism for evasion of apoptosis. *Cancer Letters* 241, 309–319. 10.1016/j.canlet.2005.10.042.
- Vaure**, C; Liu, Y., 2014. A comparative review of toll-like receptor 4 expression and functionality in different animal species. *Frontiers in immunology* 5, 316. 10.3389/fimmu.2014.00316.
- Vazzana**, N; Santilli, F; Cuccurullo, C; Davì, G., 2009. Soluble forms of RAGE in internal medicine. *Internal and emergency medicine* 4, 389–401. 10.1007/s11739-009-0300-1.
- Vicente Miranda**, H; El-Agnaf, O. M. A; Outeiro, T. F., 2016. Glycation in Parkinson's disease and Alzheimer's disease. *Movement disorders : official journal of the Movement Disorder Society* 31, 782–790. 10.1002/mds.26566.
- Villalta**, S.A; Rinaldi, C; Deng, B; Liu, G; Fedor, B; Tidball, J. G., 2011. Interleukin-10 reduces the pathology of mdx muscular dystrophy by deactivating M1 macrophages and modulating macrophage phenotype. *Human molecular genetics* 20, 790–805. 10.1093/hmg/ddq523.
- Vistoli**, G; Maddis, D. de; Cipak, A; Zarkovic, N; Carini, M; Aldini, G., 2013. Advanced glycoxidation and lipoxidation end products (AGEs and ALEs): an overview of their mechanisms of formation. *Free Radical Research* 47, 3–27. 10.3109/10715762.2013.815348.
- Vlassara**, H; Brownlee, M; Cerami, A., 1984. Accumulation of diabetic rat peripheral nerve myelin by macrophages increases with the presence of advanced glycosylation endproducts. *The Journal of experimental medicine* 160, 197–207.
- Vlassara**, H; Li, Y. M; Imani, F; Wojciechowicz, D; Yang, Z; Liu, F.-T; Cerami, A., 1995. Identification of Galectin-3 As a High-Affinity Binding Protein for Advanced Glycation End Products (AGE): A New Member of the AGE-Receptor Complex. *Mol Med* 1, 634–646. 10.1007/BF03401604.
- Walsh**, J.G; Muruve, D. A; Power, C., 2014. Inflammasomes in the CNS. *Nature reviews. Neuroscience* 15, 84–97. 10.1038/nrn3638.
- Wang**, P.-H; Huang, B.-S; Horng, H.-C; Yeh, C.-C; Chen, Y.-J., 2018. Wound healing. *Journal of the Chinese Medical Association : JCMA* 81, 94–101. 10.1016/j.jcma.2017.11.002.
- Wang**, Q; Ni, H; Lan, L; Wei, X; Xiang, R; Wang, Y., 2010a. Fra-1 protooncogene regulates IL-6 expression in macrophages and promotes the generation of M2d macrophages. *Cell research* 20, 701–712. 10.1038/cr.2010.52.
- Wang**, Y; Wang, H; Piper, M. G; McMaken, S; Mo, X; Opalek, J; Schmidt, A. M; Marsh, C. B., 2010b. sRAGE induces human monocyte survival and differentiation. *Journal of immunology (Baltimore, Md. : 1950)* 185, 1822–1835. 10.4049/jimmunol.0903398.
- Wetzels**, S; Wouters, K; Schalkwijk, C. G; Vanmierlo, T; Hendriks, J. J. A; Kleinschnitz, C., 2017. Methylglyoxal-Derived Advanced Glycation Endproducts in Multiple Sclerosis. *International Journal of Molecular Sciences* 18, 421. 10.3390/ijms18020421.
- Wu**, J.T., 1993. Advanced glycosylation end products: A new disease marker for diabetes and aging. *Journal of clinical laboratory analysis* 7, 252–255. 10.1002/jcla.1860070503.
- Wynn**, T.A; Vannella, K. M., 2016. Macrophages in Tissue Repair, Regeneration, and Fibrosis. *Immunity* 44, 450–462. 10.1016/j.immuni.2016.02.015.
- Yamagishi**, S.-i., 2011. Role of advanced glycation end products (AGEs) and receptor for AGEs (RAGE) in vascular damage in diabetes. *Experimental Gerontology* 46, 217–224. 10.1016/j.exger.2010.11.007.
- Yamamoto**, A; Simonsen, A., 2011. The elimination of accumulated and aggregated proteins: A role for aggrephagy in neurodegeneration. *Neurobiology of disease* 43, 17–28. 10.1016/j.nbd.2010.08.015.

- Yamamoto**, Y; Harashima, A; Saito, H; Tsuneyama, K; Munesue, S; Motoyoshi, S; Han, D; Watanabe, T; Asano, M; Takasawa, S; Okamoto, H; Shimura, S; Karasawa, T; Yonekura, H; Yamamoto, H., 2011. Septic shock is associated with receptor for advanced glycation end products ligation of LPS. *Journal of immunology (Baltimore, Md. : 1950)* 186, 3248–3257. 10.4049/jimmunol.1002253.
- Yan**, J; Tie, G; Wang, S; Tutto, A; DeMarco, N; Khair, L; Fazio, T. G; Messina, L. M., 2018. Diabetes impairs wound healing by Dnmt1-dependent dysregulation of hematopoietic stem cells differentiation towards macrophages. *Nature communications* 9, 33. 10.1038/s41467-017-02425-z.
- Yan**, S.D; Schmidt, A. M; Anderson, G. M; Zhang, J; Brett, J; Zou, Y. S; Pinsky, D; Stern, D., 1994. Enhanced cellular oxidant stress by the interaction of advanced glycation end products with their receptors/binding proteins. *The Journal of biological chemistry* 269, 9889–9897.
- Yonekura**, H; Yamamoto, Y; Sakurai, S; Petrova, R. G; Abedin, M. J; Li, H; Yasui, K; Takeuchi, M; Makita, Z; Takasawa, S; Okamoto, H; Watanabe, T; Yamamoto, H., 2003. Novel splice variants of the receptor for advanced glycation end-products expressed in human vascular endothelial cells and pericytes, and their putative roles in diabetes-induced vascular injury. *Biochem. J.* 370, 1097–1109. 10.1042/BJ20021371.
- Zhu**, Y; Snooks, H; Sang, S., 2018. Complexity of Advanced Glycation End Products in Foods: Where Are We Now? *Journal of agricultural and food chemistry* 66, 1325–1329. 10.1021/acs.jafc.7b05955.

Acknowledgements

First, I would like to thank Prof. Dr. Rüdiger Horstkorte and Dr. Kaya Bork for giving me the opportunity to work on this interesting project in their laboratory. I want to thank both of you for the support, the scientific input and mentoring, as well as their never-ending patience. It was always a pleasure to discuss my results critically with you. I want to thank Rüdiger for being my second supervisor for this dissertation and all the efforts that were included in doing this. Eminently, I need to thank Kaya for his believe in my skills and the chance to start working in this group, even though we could not manage to continue with our initial project.

I want to thank PD Dr. Ralph Golbik who kindly accepted to be my first supervisor for this dissertation and gave me the opportunity to graduate in the Faculty I of Natural Science - Biological Science. I would like to express my gratitude for the supportive discussions and all your efforts.

I also thank Prof. Dr. Otmar Huber from the Friedrich-Schiller-University Jena who kindly accepted to be my third supervisor for this dissertation. Thank you for being a member of my thesis advisory committee and also my third supervisor in our graduate school ProMoAge (GRK 2155). I really enjoyed your helpful comments and advise.

Next, I truly need to thank all former and current members of the Horstkorte group, among them especially Philip Rosenstock, Jonas Scheffler, Annett Thate, Franziska Frank, Philipp Selke, Heidi Olzscha, Vinayaga Srinivasan Gnanapragassam and Manimozhi Nagasundaram. Thank you so much for the familiar and always joyful atmosphere, all your help and understanding. I guess there could have been no better working group for my PhD thesis, I really enjoyed every second with you crazy lab mates!

I also want to thank the whole Institute for Physiological Chemistry for the support and scientific input. I cannot mention all of you, but I especially want to thank Dagobert and Gabi, Fabi, Robert, Ingo and Sara for the good times.

I need to express my thanks to Guido, Jette, Ilona and Conny from Octapharma Biopharmaceuticals GmbH in Berlin for helping me with some of the experiments I could not realize in our lab. I always enjoyed my times in Berlin with you.

I thank the whole graduate school ProMoAge (GRK 2155) for the guidance during my PhD thesis and the scientific knowledge I could gain.

Last but not least I want to thank my family and friends for all the love and support during these challenging times. My mom and my elder brother Michi, you don't understand my work but you always stayed opportunistic when I didn't see the end of the road. Also I want to thank my best friend Jul, as well as Alex and Ingrid. Thank you all for being there for me.

This work was partly financially supported by the Deutsche Forschungsgemeinschaft (DFG).

List of Publications

Bezold, Veronika; Rosenstock, Philip; Scheffler, Jonas; Geyer, Henriette; Horstkorte, Rüdiger; Bork, Kaya (2019): Glycation of macrophages induces expression of pro-inflammatory cytokines and reduces phagocytic efficiency.

In: *Aging* 11 (14), S. 5258-5275.

DOI: 10.18632/aging.102123.

Frank, Franziska; **Bezold, Veronika;** Bork, Kaya; Rosenstock, Philip; Scheffler, Jonas; Horstkorte, Rüdiger (2019): Advanced glycation endproducts and polysialylation affect the turnover of the neural cell adhesion molecule (NCAM) and the receptor for advanced glycation endproducts (RAGE).

In: *Biological chemistry* 400 (2), S. 219–226.

DOI: 10.1515/hsz-2018-0291.

Rosenstock, Philip; **Bezold, Veronika;** Bork, Kaya; Scheffler, Jonas; Horstkorte, Rüdiger (2019): Glycation interferes with natural killer cell function.

In: *Mechanisms of ageing and development* 178, S. 64–71.

DOI: 10.1016/j.mad.2019.01.006.

Scheffler, Jonas; Bork, Kaya; **Bezold, Veronika;** Rosenstock, Philip; Gnanapragassam, Vinayaga S.; Horstkorte, Rüdiger (2018): Ascorbic acid leads to glycation and interferes with neurite outgrowth.

In: *Experimental gerontology*.

DOI: 10.1016/j.exger.2018.08.005.

Curriculum vitae

personal information

name: Veronika Bezold
residence: D-04299 Leipzig
birth date: 04/06/1991
birth place: D-92224 Amberg
nationality: German

academic education

since 06/2016 Martin-Luther-University Halle-Wittenberg, D-06114
graduation as Dr. rer. nat. in biochemistry

10/2013 – 09/2015 Anhalt University of Applied Sciences, D-06366 Köthen
M.Sc. Biotechnology
title: Development and optimization of an enzyme
immunoassay for the detection of secretory
component in bovine milk
degree: 1,3

10/2010 – 10/2013 Anhalt University of Applied Sciences, D-06366 Köthen
B.Sc. molecular Biotechnology
dual studies in coop. with Probiodrug AG, D-06120 Halle
title: Development of a bioinformatics-based method for
the isolation of microsatellite motives from the
genome of *Trichoderma* spp.
degree: 1,9

work experience

- | | |
|-------------------|---|
| since 06/2016 | Martin-Luther-University Halle Wittenberg, D-06114
research associate/ PhD student
project: Impact of glycation and advanced glycation
end products on macrophage activation |
| 03/2016 – 05/2016 | Fraunhofer IZI, D-04103 Leipzig
research assistant
project: detection of biomarkers in bovine serum and
milk via in-house developed ELISAs |
| 01/2014 – 04/2014 | LAGOTEC GmbH, D-39106 Magdeburg
research assistant
project: analysis of fungal and algae resistance of
in-house developed timber coatings |

internships

- | | |
|-------------------|--|
| 02/2015 – 03/2015 | Fraunhofer IZI, D-04103 Leipzig,
preliminary internship for graduation as M.Sc. |
| 02/2013 – 05/2013 | Anhalt University of Applied Sciences, D-06406 Bernburg
obligatory internship for graduation as B.Sc. |
| 02/2012 – 09/2012 | Probiodrug AG, D-06120 Halle
internships during dual studies |

place, date

signature

Eidesstattliche Erklärung

Hiermit erkläre ich an Eides statt, dass die vorliegende Arbeit selbstständig und nur unter Zuhilfenahme der angegebenen Quellen und Hilfsmittel angefertigt wurde. Die aus den verwendeten Quellen wörtlich oder inhaltlich übernommenen Stellen wurden durch Verwendung einer Quellenangabe solche gekennzeichnet.

Des Weiteren versichere ich, dass die Arbeit in dieser oder ähnliche Form nur in diesem und keinem weiteren Promotionsverfahren vorgelegt wurde. Zudem versichere ich, dass diesem Promotionsverfahren keine endgültig gescheiterten Promotionsverfahren vorausgegangen sind.

Ort, Datum

Unterschrift